Sex-Specific Disruption of the Gut-Liver-Brain Axis

Developmental Programming and Behavioral Outcomes Following PCB Exposure

Youjun Park Suh

A dissertation

submitted in partial fulfillment of the

requirements for the degree of

Doctor of Philosophy

University of Washington

2025

Reading Committee:

Julia Yue Cui, Co-Chair

Elaine M. Faustman, Co-Chair

Judit Marsillach

Program Authorized to Offer Degree:

Environmental & Occupational Health Sciences

University of Washington

Abstract

Sex-Specific Disruption of the Gut-Liver-Brain Axis
Developmental Programming and Behavioral Outcomes Following PCB Exposure

Youjun Park Suh

Chairs of the Supervisory Committee:
Julia Yue Cui
Elaine M. Faustman
Department of Environmental & Occupational Health Sciences

Polychlorinated biphenyls (PCBs) are persistent environmental contaminants that continue to pose health risks despite being banned decades ago. Developmental exposure to PCBs has been associated with neurodevelopmental disorders that exhibit pronounced sex-specific patterns. However, previous research has focused on individual organ systems, limiting understanding of how PCBs affect integrated physiological networks during development.

We investigated whether maternal PCB exposure causes sex-specific alterations across the gut-liver-brain axis using the Fox River Mixture, an environmentally relevant PCB mixture reflecting contemporary human exposure patterns. Pregnant C57BL/6J mouse dams were exposed to vehicle or PCB mixture (0.1, 1.0, or 6.0 mg/kg/day) throughout gestation and

lactation, with offspring assessed at multiple developmental timepoints for behavioral, microbiome, metabolomic, and hepatic transcriptomic outcomes.

Maternal PCB exposure induced dose-dependent gut microbiome disruption, enhanced hepatic xenobiotic processing, and sex-specific alterations in hepatic type 1 deiodinase (DIO1) expression. Males showed dose-dependent DIO1 upregulation while females exhibited non-monotonic responses. By PND28, distinct sex-specific patterns at the transcriptomic(?) level emerged: males exhibited extensive gut-liver molecular connectivity (>7,000 significant correlations) with enhanced hepatic detoxification responses and dose-dependent DIO1 upregulation, while females showed focused connectivity patterns in molecular networks connectivity (<3,000 correlations) with inflammatory liver activation and non-monotonic DIO1 responses. At PND35, a reversal of vulnerability was observed: males showed behavioral resilience despite continued molecular alterations, while females developed significant social memory deficits at low and medium doses with concurrent thyroid hormone suppression.

Integration of microbiome, metabolomic, and transcriptomic data revealed fundamentally different network architectures between sexes. Males developed redundant, highly interconnected networks with balanced hub distribution across bacterial species, metabolites, and hepatic genes, providing system robustness. Females showed hierarchical networks dominated by specific bacterial super-hubs, creating efficiency but increased vulnerability to disruption. These architectural differences correlated with behavioral outcomes, with network topology metrics predicting functional resilience versus vulnerability.

This work provides comprehensive evidence that maternal PCB exposure causes persistent, sex-specific alterations across the gut-liver-brain axis through fundamentally different biological strategies. The identification of sex-specific DIO1 regulation as a mechanism

underlying differential thyroid hormone disruption, combined with distinct microbiome-metabolite-transcriptome network architectures, reveals how the same environmental exposure leads to divergent developmental outcomes. These findings emphasize the critical importance of considering sex as a biological variable in environmental health risk assessment and suggest that current regulatory frameworks based on single-sex studies may inadequately protect vulnerable populations.

Table of Contents

Chapter 1: Introduction

1.1 Polychlorinated Biphenyls: A Persistent Environmental Challenge

1.1.1 Historical Context and Current Exposure

Polychlorinated biphenyls (PCBs) represent one of the most persistent environmental challenges of the modern era. These synthetic organic compounds, comprising 209 distinct congeners with varying degrees of chlorination, were manufactured extensively from 1929 to 1979 for diverse industrial applications including electrical equipment, hydraulic fluids, plasticizers, and paints (Klocke et al., 2020). The United States alone produced approximately 680,000 tons of PCBs before their ban under the Toxic Substances Control Act in 1979, following mounting evidence of their environmental persistence and adverse health effects (Kostyniak et al., 2005).

Despite cessation of production over four decades ago, PCBs remain ubiquitous environmental contaminants due to their exceptional chemical stability and lipophilic nature. These properties enable PCBs to resist degradation, bioaccumulate through food chains, and persist in environmental matrices for decades. Environmental half-lives range from 2-10 years in soil and sediment, while biological half-lives in humans vary from 6 months for lower-chlorinated congeners to over 15 years for highly chlorinated congeners like PCB-153 and PCB-180. Contemporary human exposure continues through multiple pathways, with diet representing the primary route, particularly through consumption of contaminated fish, meat, and dairy products (Marek et al., 2014). PCBs are still routinely detected in human blood, adipose tissue, and breast milk across global populations, with serum levels ranging from 0.5 to 4.0 ng/mL in non-occupationally exposed adults (Li et al., 2022).

The health implications of ongoing PCB exposure are substantial. PCBs are classified as probable human carcinogens by the International Agency for Research on Cancer and have been associated with diverse adverse health outcomes including hepatotoxicity, endocrine disruption, immunotoxicity, and neurodevelopmental deficits (Klocke and Lein, 2020). Of particular concern is the vulnerability of developing organisms, as PCBs readily cross the placental barrier and are transferred through breast milk, with cord blood PCB levels reaching 30-70% of maternal serum concentrations (Grandjean et al., 2001; Soechitram et al., 2004).

1.1.2 Fox River Contamination and Human Relevance

The Fox River in Wisconsin exemplifies the ongoing public health challenge posed by historical PCB contamination. Between 1954 and 1971, paper manufacturing facilities along the lower Fox River discharged an estimated 700,000 pounds of PCBs into the river system while using Aroclor mixtures in carbonless copy paper production (Imamoglu & Christensen, 2002). Despite extensive remediation efforts including dredging and natural attenuation processes (EPA, 2023; Wisconsin DNR, 2024), PCB concentrations in Fox River sediments remain elevated, ranging from 1 to over 10,000 mg/kg in hotspot areas (Kaya et al., 2018).

The Fox River serves as a major tributary to Lake Michigan and provides habitat for substantial populations of game fish that constitute primary protein sources for surrounding communities, particularly among subsistence fishing populations (Christensen et al., 2016; Steenport et al., 2000). Consumption of Fox River fish has been directly correlated with elevated serum PCB levels in residents, with fish consumers showing 2-3-fold higher PCB body burdens compared to non-consumers (Schantz et al., 2010). Contemporary human serum samples show PCB levels ranging from 0.5 to 4.0 ng/mL in non-occupationally exposed adults, with higher levels in fish-consuming populations (CDC, 2023; Marek et al., 2014). More concerning, adolescents from fish-consuming families in the Green Bay area demonstrate measurable cognitive deficits, including reduced IQ scores and impaired executive function, associated with prenatal PCB exposure (Sprowles et al., 2022).

1.1.3 Contemporary PCB Mixtures versus Legacy Aroclors

A critical consideration in PCB toxicology is that the congener profile in contemporary human samples differs substantially from the original commercial Aroclor mixtures used in most toxicological studies. While Aroclors contained specific congener distributions determined by manufacturing conditions, environmental weathering, metabolism, and differential bioaccumulation have altered the PCB profiles found in human tissues today (Koh et al., 2016). Contemporary human serum samples show enrichment of more persistent, higher-chlorinated congeners and their hydroxylated metabolites, particularly PCBs 138, 153, and 180, which comprise up to 60% of the total PCB burden (Marek et al., 2014).

This shift in congener profiles has important toxicological implications. The Fox River Mixture (FRM) was specifically formulated to mimic the PCB congener profile found in contaminated fish from the Fox River, representing current human exposure patterns rather than historical Aroclor compositions (Kostyniak et al., 2005). The FRM consists of 35% Aroclor 1242, 35% Aroclor 1248, 15% Aroclor 1254, and 15% Aroclor 1260 by weight, creating a mixture that reflects the environmental weathering and bioaccumulation processes that have occurred over decades. Importantly, the FRM demonstrates greater potency than individual Aroclors in sensitizing ryanodine receptors (RyR), a molecular initiating event in PCB developmental neurotoxicity (Bal-Price et al., 2015). This enhanced potency of environmentally relevant mixtures compared to legacy Aroclors raises critical questions about whether current risk assessments based on single congeners or commercial mixtures adequately protect human health.

1.1.4 PCB Absorption, Distribution, Metabolism, and Excretion

PCBs are efficiently absorbed through the gastrointestinal tract with bioavailability exceeding 90% for most congeners. Following absorption, PCBs rapidly distribute to lipid-rich tissues, with adipose tissue serving as the primary reservoir. The liver accumulates substantial PCB concentrations due to both lipid content and first-pass metabolism. PCBs readily cross the placental barrier and blood-brain barrier, with brain : blood partition coefficients ranging from 5:1 to 20:1 depending on chlorination pattern.

Metabolism occurs primarily in the liver through cytochrome P450-mediated reactions. Phase I metabolism produces hydroxylated PCBs (OH-PCBs) that may retain biological activity. Lower-chlorinated congeners are metabolized more readily, with half-lives ranging from weeks to months, while higher-chlorinated congeners persist for years. In humans, PCB-153 has an estimated half-life of 14 years. Phase II conjugation with glucuronic acid or sulfate facilitates elimination through bile and urine. Lactation represents a significant elimination route, with nursing infants receiving 10-20% of the maternal body burden during breastfeeding.

1.2 Developmental Neurotoxicity and Sex Differences

1.2.1 Epidemiological Evidence Linking PCBs to Neurodevelopmental Outcomes

Extensive epidemiological evidence has established PCBs as developmental neurotoxicants with impact on cognitive and behavioral outcomes. Longitudinal cohort studies

spanning multiple decades have consistently demonstrated associations between prenatal PCB exposure and adverse neurodevelopmental outcomes in children. The Michigan fish-eater cohort, one of the earliest prospective studies, found that children born to mothers who consumed PCB-contaminated Lake Michigan fish showed reduced birth weight, smaller head circumference, and poorer performance on infant behavioral assessments (Jacobson and Jacobson, 1996). Follow-up assessments revealed persistent deficits in IQ, reading comprehension, and executive function that extended into adolescence.

Similar findings have emerged from diverse populations worldwide. The Dutch cohort study reported dose-dependent relationships between prenatal PCB exposure and reduced cognitive abilities, with effects most pronounced in verbal and memory domains (Patandin et al., 1999). The Faroe Islands study, examining a population with high seafood consumption, demonstrated that prenatal PCB exposure was associated with deficits in language, attention, and memory functions at 7 and 14 years of age (Grandjean et al., 2001). Meta-analyses of these and other studies estimate that each doubling of prenatal PCB exposure is associated with a 2–3-point reduction in Full Scale IQ (Schantz et al., 2003).

Beyond cognitive impacts, prenatal PCB exposure has been increasingly linked to neurodevelopmental disorders (NDDs). Multiple studies have reported associations between maternal PCB levels and increased risk of attention-deficit/hyperactivity disorder (ADHD) symptoms in offspring (Sagiv et al., 2010). The MARBLES (Markers of Autism Risk in Babies-Learning Early Signs) study at UC Davis, a longitudinal study that followed pregnant women with a child previously diagnosed with autism spectrum disorder (ASD), found that younger siblings later diagnosed with ASD had significantly higher prenatal exposure to specific PCB congeners compared to neurotypical children, with PCBs 138, 153, and 170 showing the strongest associations (Lyall et al., 2017). A recent meta-analysis encompassing 11 studies reported that children in the highest quartile of prenatal PCB exposure had 1.8-fold increased odds of ASD diagnosis compared to those in the lowest quartile (Mehri et al., 2021).

1.2.2 Sex-Specific Vulnerabilities in Neurodevelopmental Disorders

Sex differences in neurodevelopmental outcomes following environmental exposures represent a critical but understudied aspect of developmental toxicology. Males consistently show higher prevalence of NDDs, with male-to-female ratios of approximately 4:1 for ASD and 2:1 for

ADHD (Lord et al., 2000). This sex bias extends to environmental risk factors, where males often demonstrate greater vulnerability to prenatal toxicant exposures, though the mechanisms underlying this differential susceptibility remain incompletely understood.

Several biological factors contribute to sex-specific developmental vulnerabilities. Gonadal hormones, particularly testosterone and estradiol, influence neurodevelopmental trajectories through both organizational effects during critical periods and activational effects throughout life (McCarthy et al., 2018). Sex chromosome complement contributes additional variation, with X-linked genes showing sex-specific expression patterns in the developing brain independent of hormonal influences. Males' hemizygous state for X-linked genes may increase vulnerability to mutations or environmental perturbations affecting X-linked neurodevelopmental pathways.

Epigenetic mechanisms also demonstrate sexual dimorphism, with sex-specific patterns of DNA methylation, histone modifications, and microRNA expression observed in developing brain tissue (Nugent et al., 2015). These sex-specific epigenetic landscapes may differentially respond to environmental exposures, creating distinct vulnerabilities. Additionally, sex differences in xenobiotic metabolism, with females generally showing higher expression of certain cytochrome P450 enzymes and phase II conjugation enzymes, may influence the internal dose and metabolite profiles following toxicant exposure (Keil et al., 2019).

1.2.3 Critical Developmental Windows

Figure 1.2 Overview of Brain Development

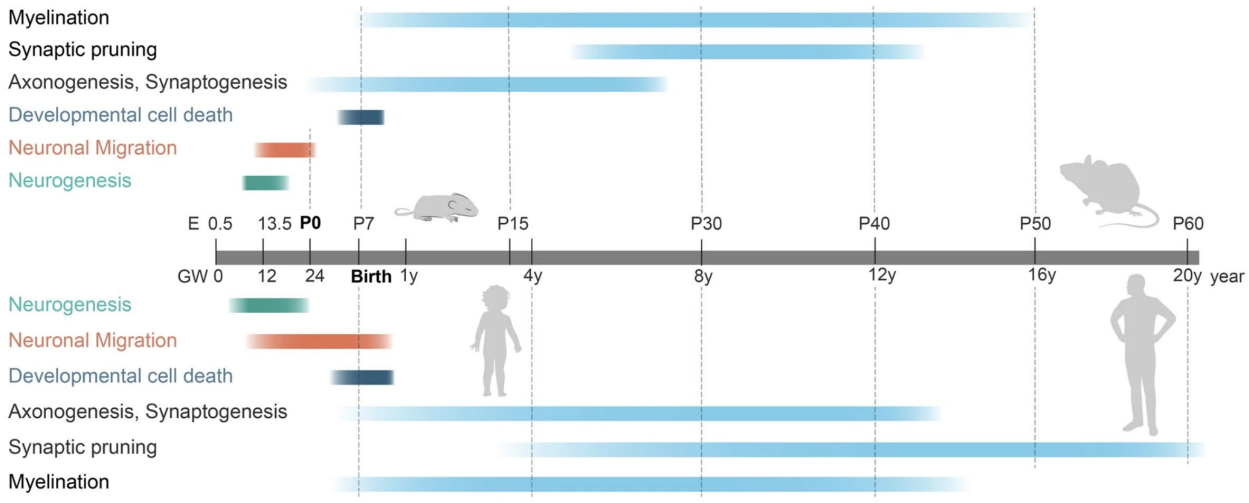

The concept of critical developmental windows emphasizes that the developing nervous system exhibits heightened vulnerability to environmental insults during specific temporal periods characterized by rapid cellular proliferation, differentiation, migration, and synaptogenesis. These windows vary across brain regions and neural processes, creating a complex landscape of vulnerability that extends from early gestation through adolescence. During the prenatal period, neurogenesis peaks between gestational weeks 8-16 in humans, followed by extensive neuronal migration that establishes the basic architecture of the brain. The perinatal period witnesses explosive synaptogenesis and the initiation of myelination, processes that continue through early childhood with region-specific timing.

PCB exposure during these critical windows can produce distinct phenotypic outcomes depending on the timing of exposure. Early gestational exposure primarily affects neuronal proliferation and migration, potentially leading to structural brain abnormalities and severe cognitive impairment. Perinatal exposure, coinciding with synaptogenesis and early myelination, more commonly results in subtle functional deficits in cognitive flexibility, social behavior, and executive function (Klocke and Lein, 2020). The extended developmental timeline of the prefrontal cortex, which continues maturing through adolescence, creates a particularly prolonged window of vulnerability for executive function and social cognition.

1.3 The Gut-Liver-Brain Axis

1.3.1 System Components and Bidirectional Communication

The gut-liver-brain axis represents an integrated physiological network through which the intestinal microbiome, hepatic metabolism, and central nervous system engage in continuous bidirectional communication. This complex system employs multiple signaling pathways including neural connections via the vagus nerve and enteric nervous system, endocrine signaling through gut hormones and hepatic factors, immune-mediated communication via cytokines and pattern recognition receptors, and metabolic signaling through microbial metabolites and bile acids (Cryan et al., 2019).

The gut microbiome, comprising trillions of microorganisms with collective genetic material exceeding the human genome by 150-fold, serves as a metabolic organ that profoundly influences host physiology. Commensal bacteria produce numerous neuroactive compounds

including neurotransmitters (GABA, serotonin, dopamine), short-chain fatty acids (SCFAs; acetate, propionate, butyrate), and other bioactive metabolites that can influence brain function through direct and indirect mechanisms (Mayer et al., 2022). These microbial products can signal locally to the enteric nervous system, enter systemic circulation to affect distant organs, or modulate intestinal barrier function and immune responses.

The liver serves as a critical metabolic hub in this axis, receiving approximately 70% of its blood supply from the portal vein, which delivers gut-derived metabolites, microbial products, and xenobiotics absorbed from the intestinal lumen. Hepatic metabolism transforms these compounds through phase I and II biotransformation reactions, producing metabolites that may have distinct biological activities compared to parent compounds. The liver also synthesizes numerous factors that influence both gut and brain function, including bile acids that shape microbiome composition, acute phase proteins that modulate neuroinflammation, and metabolic hormones that affect appetite and behavior (Tripathi et al., 2018).

1.3.2 Role in Neurodevelopment and Behavior

The gut-liver-brain axis plays crucial roles in neurodevelopment, with disruptions during critical periods potentially leading to lasting behavioral alterations. During early life, the developing microbiome participates in essential neurodevelopmental processes including microglial maturation, blood-brain barrier formation, myelination, and neurogenesis (Sharon et al., 2016). Germ-free mice, which lack a microbiome, exhibit altered brain structure and function, including increased hippocampal neurogenesis, altered microglial morphology, deficient myelination, and abnormal neurotransmitter levels, demonstrating the microbiome's necessity for normal brain development.

Microbial metabolites serve as key mediators of gut-brain communication during development. Short-chain fatty acids, particularly butyrate, cross the blood-brain barrier and influence microglial maturation, with deficiency during critical windows leading to persistent alterations in microglial function and increased neuroinflammation (Erny et al., 2015). Microbial production of neurotransmitter precursors, such as tryptophan metabolites that serve as serotonin precursors, can influence neurotransmitter synthesis in the developing brain. Bacterial production of metabolites that resemble host signaling molecules, termed molecular mimicry, may also influence neurodevelopmental processes through activation of host receptors.

Clinical evidence increasingly supports the importance of the gut-liver-brain axis in neurodevelopmental disorders. Children with ASD frequently exhibit gastrointestinal dysfunction and altered microbiome composition, with specific bacterial taxa showing consistent associations with symptom severity (Hsiao et al., 2013). Microbiome transfer therapy in children with ASD has shown promising results in improving both gastrointestinal and behavioral symptoms, suggesting causal relationships between gut dysbiosis and neurodevelopmental outcomes (Kang et al., 2017). Similarly, alterations in hepatic metabolism, particularly in detoxification pathways, have been observed in individuals with NDDs, potentially contributing to increased vulnerability to environmental toxicants.

1.3.3 Environmental Toxicant Impacts on Axis Function

Environmental toxicants can disrupt the gut-liver-brain axis through multiple mechanisms, with effects potentially amplified during developmental periods. Direct toxicant effects on the gut microbiome include alterations in community composition, reduced diversity, and shifts in metabolic capacity. PCBs and other persistent organic pollutants have been shown to alter gut microbiome composition in both human cohorts and animal models, with specific taxa showing differential sensitivity to toxicant exposure (Lim et al., 2020). These microbiome alterations can secondarily affect xenobiotic metabolism, as certain bacterial species participate in toxicant biotransformation, potentially generating toxic metabolites.

Toxicant-induced disruption of intestinal barrier function represents another critical mechanism affecting axis function. PCB exposure has been associated with increased intestinal permeability, allowing bacterial products such as lipopolysaccharide to enter systemic circulation and trigger inflammatory responses in the liver and brain (Choi et al., 2010). This "leaky gut" phenomenon may amplify the neurological effects of environmental toxicants by promoting neuroinflammation and microglial activation.

The liver's central role in xenobiotic metabolism creates complex interactions between toxicant exposure and axis function. PCBs induce hepatic cytochrome P450 enzymes and phase II conjugation pathways, altering the metabolism not only of PCBs themselves but also of endogenous compounds and other xenobiotics (Lim et al., 2020). These metabolic alterations can affect the production and circulation of neuroactive metabolites, bile acids, and hormones that

influence brain function. Additionally, toxicant-induced hepatic inflammation can generate systemic inflammatory mediators that affect neuroinflammation and behavior.

1.4 Thyroid Hormones in Development

1.4.1 Hypothalamus-Pituitary-Thyroid Axis Overview

The hypothalamus-pituitary-thyroid (HPT) axis represents a critical endocrine system regulating metabolism, growth, and neurodevelopment through the production and circulation of thyroid hormones. The hypothalamus secretes thyrotropin-releasing hormone (TRH), which stimulates the anterior pituitary to release thyroid-stimulating hormone (TSH). TSH acts on the thyroid gland to promote synthesis and secretion of thyroxine (T4) and, to a lesser extent, triiodothyronine (T3). This system operates under negative feedback control, with circulating thyroid hormones suppressing TRH and TSH production to maintain homeostasis (Bernal, 2000).

Thyroid hormones exert their biological effects primarily through nuclear thyroid hormone receptors (TRα and TRβ), which function as ligand-activated transcription factors. T3, the more biologically active form, binds to these receptors with approximately 10-fold higher affinity than T4. Upon hormone binding, thyroid hormone receptors regulate expression of target genes involved in cellular metabolism, differentiation, and proliferation. The developing brain expresses high levels of thyroid hormone receptors, particularly TRα1, which is essential for neuronal differentiation, migration, and myelination (O'Shaughnessy et al., 2018).

The regulation of thyroid hormone signaling occurs not only through HPT axis control of hormone production but also through tissue-specific metabolism by deiodinase enzymes. This local control mechanism allows tissues to fine-tune thyroid hormone signaling independent of circulating hormone levels, providing precise temporal and spatial regulation during development.

1.4.2 Hepatic Metabolism and Deiodinase Enzymes

The liver plays a central role in thyroid hormone metabolism through expression of deiodinase enzymes that catalyze the removal of iodine atoms from thyroid hormones. Three deiodinase isoforms (DIO1, DIO2, DIO3) exhibit distinct tissue distributions, substrate preferences, and regulatory mechanisms. DIO1, predominantly expressed in liver, kidney, and thyroid, catalyzes both outer-ring deiodination (activation of T4 to T3) and inner-ring deiodination

(inactivation to reverse T3 and T2). The liver contributes approximately 30-40% of circulating T3 through DIO1-mediated conversion of T4, making hepatic DIO1 activity a critical determinant of systemic thyroid hormone status (Bianco et al., 2002).

DIO2, primarily expressed in brain, pituitary, and brown adipose tissue, specifically catalyzes outer ring deiodination to generate T3 locally within these tissues. In the developing brain, DIO2 activity in astrocytes provides T3 to neighboring neurons, creating a cellular relay system for thyroid hormone signaling. DIO3, highly expressed in fetal tissues and placenta, catalyzes only inner ring deiodination, serving to protect developing tissues from excessive thyroid hormone exposure. The coordinated expression and activity of these deiodinases creates tissue-specific thyroid hormone environments that change dynamically during development.

Regulation of deiodinase expression and activity occurs through multiple mechanisms including thyroid hormone status, nutritional factors, inflammatory mediators, and xenobiotic exposure. PCBs and their metabolites have been shown to inhibit deiodinase activities, particularly DIO1, through competitive inhibition and transcriptional downregulation (Martin and Klaassen, 2010). Certain PCB metabolites structurally resemble thyroid hormones and can bind to thyroid hormone transport proteins, receptors, and metabolizing enzymes, creating complex disruptions of thyroid hormone signaling.

Of particular importance to the gut-liver-brain axis is the regulation of type 1 deiodinase (DIO1), which serves as a critical metabolic hub linking gut microbiome activity, hepatic metabolism, and systemic thyroid hormone status. DIO1 expression and activity are regulated by microbial metabolites, particularly secondary bile acids produced through bacterial 7α-dehydroxylation of primary bile acids (Sinha et al., 2019). Deoxycholic acid and lithocholic acid, the major secondary bile acids, can modulate DIO1 expression through activation of nuclear receptors including the farnesoid X receptor (FXR) and G-protein coupled bile acid receptor (TGR5). This creates a regulatory circuit where gut dysbiosis can alter bile acid profiles, subsequently affecting hepatic DIO1 activity and systemic T3 availability. While the brain produces most of its T3 locally through DIO2 activity in astrocytes, systemic T3 generated by hepatic DIO1 remains physiologically important. Circulating T3 contributes approximately 20-30% of total brain T3, with this proportion varying by brain region and developmental stage. Moreover, systemic thyroid status affects the expression of thyroid hormone transporters at the blood-brain

barrier, influencing T4 uptake into the brain. Thus, disruption of hepatic DIO1 activity can indirectly affect brain thyroid hormone status even when local DIO2 function remains intact. Furthermore, certain PCB congeners and their hydroxylated metabolites can directly inhibit DIO1 activity through competitive binding at the active site, creating potential for synergistic disruption when combined with microbiome alterations (Martin and Klaassen, 2010). This multilevel regulation of DIO1 – by direct PCB effects, microbiome metabolites, and inflammatory mediators – positions it as a critical node in understanding how environmental toxicants disrupt the gut-liver-brain axis during development.

1.4.3 Microbiome Interactions with Thyroid Function

Emerging evidence reveals significant interactions between the gut microbiome and thyroid hormone metabolism, adding another layer of complexity to the regulation of thyroid status (Knezevic et al., 2020). The gut microbiome influences thyroid function through multiple mechanisms including modulation of iodine uptake, enterohepatic recycling of thyroid hormones, and production of metabolites that affect deiodinase activity (Sinha et al., 2019; Virili et al., 2018).

Intestinal bacteria express enzymes capable of deconjugating thyroid hormones that have been sulfated or glucuronidated in the liver and excreted in bile (Hazenberg et al., 1988). This bacterial deconjugation allows reabsorption of thyroid hormones, contributing to their enterohepatic recycling and extending their biological half-life. Alterations in gut microbiome composition can affect this recycling process, potentially influencing systemic thyroid hormone levels (de Herder et al., 1989). Additionally, certain bacterial species can directly metabolize thyroid hormones through deiodination reactions, though the quantitative contribution to overall thyroid hormone metabolism remains unclear.

The gut microbiome influences thyroid hormone metabolism through multiple interconnected mechanisms (Sinha et al., 2019). Intestinal bacteria express sulfatase and glucuronidase enzymes that deconjugate thyroid hormones excreted in bile, enabling reabsorption and extending their biological half-life. Specific bacterial metabolites, particularly secondary bile acids produced by bacterial 7α-dehydroxylation, regulate hepatic DIO1 expression through nuclear receptor signaling pathways including FXR and TGR5 (Ridlon et al., 2014; Wahlström et al., 2016). This creates a microbiome-bile acid-thyroid axis whereby gut dysbiosis can alter systemic thyroid hormone availability (Knezevic et al., 2020; Virili et al., 2018). The disruption of these bacterial

populations by PCBs may therefore affect thyroid homeostasis through both direct effects on hormone recycling and indirect effects on DIO1 regulation.

1.5 Knowledge Gaps and Dissertation Objectives

1.5.1 Current Limitations in Understanding PCB Developmental Toxicity

Despite decades of research establishing PCBs as developmental neurotoxicants, significant knowledge gaps remain in our understanding of the mechanisms underlying PCB-induced neurodevelopmental deficits. Most mechanistic studies have focused on single organ systems in isolation, typically examining either direct neurotoxic effects, hepatic metabolism, or more recently, microbiome alterations. This reductionist approach, while providing valuable insights into specific pathways, fails to capture the integrated nature of physiological responses to toxicant exposure. The gut-liver-brain axis operates as an interconnected network where perturbations in one component can cascade through the system, yet few studies have examined these multi-organ interactions comprehensively.

The relevance of legacy Aroclor studies to contemporary human health risks remains uncertain given the substantial differences in congener profiles between commercial mixtures and current environmental samples. While the Fox River Mixture was developed to address this limitation, its effects on integrated physiological systems, particularly during development, have not been thoroughly characterized. Furthermore, most studies have utilized single, often high doses that may not reflect the complex dose-response relationships observed with endocrine-disrupting compounds, which often exhibit non-monotonic dose responses.

Sex differences in PCB developmental toxicity remain poorly understood despite clear sex biases in neurodevelopmental disorder prevalence. While some studies have reported sex-specific effects, most have either studied only one sex or failed to adequately power studies to detect sex-by-exposure interactions. The mechanisms underlying differential vulnerability, whether related to sex-specific differences in xenobiotic metabolism, hormone interactions, or developmental trajectories, require systematic investigation. Additionally, the temporal dynamics of sex-specific vulnerabilities across development have not been well characterized.

1.5.2 Research Questions and Hypotheses

This dissertation addresses these knowledge gaps through systematic investigation of how maternal PCB exposure affects offspring development through integrated disruption of the gut-liver-brain axis. The overarching research question asks: How does developmental exposure to an environmentally relevant PCB mixture alter the gut-liver axis in a sex-specific manner, and how do these molecular changes manifest as measurable neurobehavioral outcomes?

Specific research questions include: First, does maternal PCB exposure alter maternal physiology in ways that could influence offspring development? Second, are there sex-specific differences in early behavioral development following maternal PCB exposure? Third, how does PCB exposure affect the developing gut microbiome in male versus female offspring? Fourth, what are the sex-specific hepatic transcriptomic responses to developmental PCB exposure? Fifth, do behavioral phenotypes differ between male and female offspring, and do these differences correlate with molecular alterations?

Based on existing literature and preliminary observations, we hypothesized that maternal PCB exposure would disrupt the gut-liver axis through coordinated effects on microbiome composition, hepatic metabolism, and thyroid hormone regulation, with these molecular alterations manifesting as sex-specific neurobehavioral outcomes in offspring. We predicted that the timing and nature of these effects would differ between sexes due to differential developmental trajectories and sex-specific vulnerabilities to endocrine disruption.

1.5.3 Dissertation Aims and Scope

This dissertation comprises three specific aims designed to systematically characterize the effects of developmental PCB exposure on the gut-liver-axis with behavioral outcomes.

Aim 1: Characterize maternal responses to PCB exposure and early behavioral offspring effects. This aim examined how PCB exposure affects maternal physiology during pregnancy and lactation, including changes in gut microbiome composition, hepatic gene expression, and thyroid hormone status. Additionally, this aim assessed early neurodevelopmental effects in offspring through analysis of ultrasonic vocalizations at postnatal day (PND) 7, which represents peak ultrasonic vocalization emission in C57BL/6J mice (Branchi et al., 2001). This timepoint precedes the reversal of sex differences in call duration that occurs after PND8, allowing assessment of early communication before major sex hormone influences.

Aim 2: Determine sex-specific molecular alterations in developing offspring. This aim characterized sex-specific changes in gut microbiome composition, intestinal metabolomics, and hepatic transcriptomics at critical developmental timepoints (PND28 and PND35). Comprehensive multi-omics profiling enabled identification of sex-specific molecular signatures and their temporal dynamics during development.

Aim 3: Evaluate behavioral outcomes and integrate multi-system data. This aim assessed sex-specific behavioral phenotypes relevant to neurodevelopmental disorders, including social behavior and cognitive function, at PND35. Integration of behavioral, microbiome, metabolomic, and transcriptomic data through correlation network analysis revealed sex-specific patterns of gut-liver-brain communication and identified potential mechanistic links between molecular alterations and behavioral outcomes.

1.5.4 Overview of Experimental Approach

The experimental design employed a maternal exposure paradigm that reflects human exposure scenarios while capturing critical developmental windows. C57BL/6J 2 month dams received dietary exposure to the Fox River Mixture at 0, 0.1, 1.0, or 6.0 mg/kg body weight/day beginning two weeks before mating and continuing through lactation. This dosing range spans environmentally relevant exposures (0.1 mg/kg/day) to overtly toxic doses (6.0 mg/kg/day), enabling characterization of dose-response relationships including potential non-monotonic responses.

The selection of assessment timepoints was guided by neurodevelopmental milestones and practical considerations. PND7 represents an early developmental timepoint when pups are dependent on maternal milk and exhibit measurable ultrasonic vocalizations. PND35 represents early adolescence when social behaviors and cognitive functions can be reliably assessed in mice.

Methodological approaches were selected to provide complementary insights into gut-liver-brain axis function. Behavioral assessments employ validated paradigms relevant to human neurodevelopmental disorders. Microbiome analysis utilized metagenomic shotgun sequencing to achieve species-level resolution and functional annotation. Hepatic transcriptomics employed RNA sequencing to capture genome-wide gene expression changes. Large intestinal content

metabolomics analysis characterized regional differences in intestinal metabolite profiles. Integration of these multi-dimensional datasets through correlation network analysis enabled identification of cross-system interactions and sex-specific vulnerability patterns.

This comprehensive approach, examining multiple organ systems across developmental times in both sexes, provides unprecedented insight into how environmental toxicants disrupt the integrated physiology of developing organisms. The findings have implications for understanding sex differences in neurodevelopmental disorders, identifying biomarkers of effect, and developing intervention strategies for populations at risk of PCB exposure.

Chapter 2: Materials and Methods

2.1 Overview of Experimental Design

This study investigated the effects of developmental exposure to PCBs on the gut-liver-brain axis in mice. C57BL/6J dams were exposed to the Fox River Mixture (FRM) at doses of 0, 0.1, 1.0, or 6.0 mg/kg body weight/day beginning 2 weeks before mating and continuing through lactation until weaning. Offspring were assessed at multiple developmental timepoints for behavioral, microbiome, metabolic, and transcriptomic endpoints. All analyses were stratified by sex to identify sex-specific responses.

Figure 2.1. Experimental design and timeline for developmental PCB exposure study

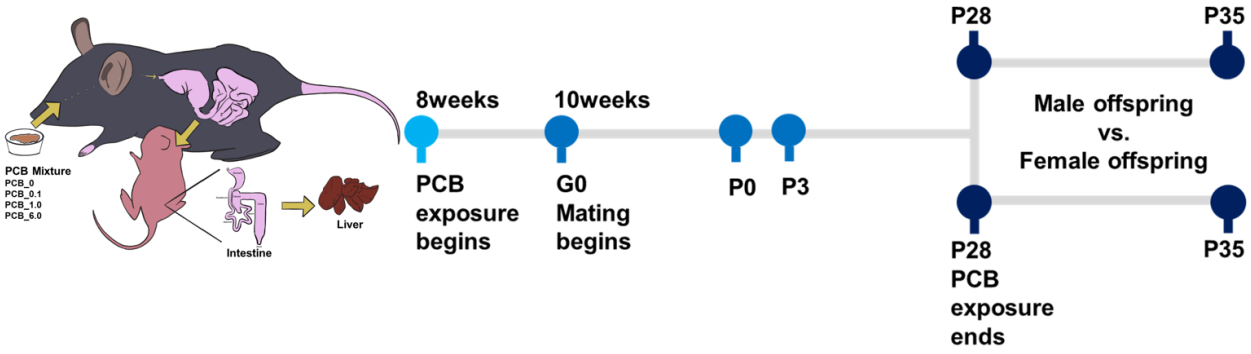

Maternal C57BL/6J mice received dietary Fox River Mixture (0, 0.1, 1.0, or 6.0 mg/kg/day) from 2 weeks pre-mating through PND28. Timeline indicates exposure initiation, mating (G0), birth (P0), and offspring assessment at PND28 and PND35. Both sexes were evaluated for behavioral, microbiome, metabolomic, and transcriptomic endpoints at each timepoint. The left-hand side of the figure shows maternal exposure route and target organ systems. n = 11-22 litters per dose group.

2.2 Animals and Housing Conditions

2.2.1 Experimental Animals

C57BL/6J wildtype mice were purchased from Jackson Laboratory (Bar Harbor, ME, USA) and housed in the specific pathogen-free facility at the University of Washington. Mice were maintained in standard air-filtered cages with autoclaved corn cob bedding (Enrich-N'Pure; Andersons, Maumee, OH, USA) under controlled environmental conditions: 12-hour light/dark cycle (lights on at 0700 h), temperature of 22 ± 2°C, and relative humidity of 40-50%. Mice had ad libitum access to autoclaved water and irradiated rodent chow (Laboratory Autoclavable Rodent

Diet 5010 for breeders and 5021 for weanlings; LabDiet, Land O'Lakes, MN, USA). All procedures were approved by the Institutional Animal Care and Use Committee at the University of Washington and conducted in accordance with the National Institutes of Health Guide for the Care and Use of Laboratory Animals.

2.2.2 Breeding Protocol

Adult female mice (8-10 weeks of age) were randomly assigned to one of four treatment groups (n = 11-22 dams per group). After 2 weeks of pre-mating exposure, females were paired with age-matched, unexposed C57BL/6J males for a 72-hour mating period. The restricted mating period ensured consistent timing of exposures across all litters. Pregnancy was confirmed by the presence of vaginal plugs and weight gain. Pregnant dams were individually housed throughout gestation and lactation. Pups were weaned at postnatal day (PND) 28, one week later than typical to maximize lactational PCB exposure during critical neurodevelopmental windows. This extended nursing period was approved in our IACUC protocol to ensure complete exposure assessment. and group-housed by sex (4-5 mice per cage) until terminal endpoints.

2.3 PCB Exposure Protocol

2.3.1 Fox River Mixture Preparation

The Fox River Mixture was prepared to mimic the PCB congener profile found in contaminated fish from the Fox River in Wisconsin (Kostyniak et al., 2005). The mixture consisted of 35% Aroclor 1242 (catalog #C-242N, lot #0114-A), 35% Aroclor 1248 (catalog #C-248N, lot #1063-24B), 15% Aroclor 1254 (catalog #C-254N, lot #124-191-B), and 15% Aroclor 1260 (catalog #C-260N, lot #021-020-1A) by weight (all from AccuStandard Inc., New Haven, CT, USA).

To prepare the mixture, 525 mg each of Aroclor 1242 and 1248, and 225 mg each of Aroclor 1254 and 1260 were combined in hexane (1 mL) in a glass vial under nitrogen atmosphere. The mixture was heated to 30°C for 5 minutes with continuous vortexing to ensure homogenization, then the solvent was evaporated under nitrogen. The mixture was heated to 30°C for 5 min and thoroughly homogenized by vortexing. Three aliquots were collected from different locations within the mixture for analytical verification by gas chromatography-tandem mass spectrometry (Li et al., 2022). The stock FRM was dissolved in organic peanut oil (Spectrum Organic Products,

LLC, Melville, NY, USA) at a concentration of 20 mg/mL and stored in amber glass bottles under nitrogen atmosphere at -20°C to prevent oxidation.

2.3.2 Dose Preparation and Administration

Daily doses were prepared fresh each morning by mixing appropriate volumes of the FRM stock solution (12.5, 125, or 750 µL for the 0.1, 1.0, and 6.0 mg/kg/day doses, respectively) into 10 g of organic unsalted(?) peanut butter (Trader Joe's, Monrovia, CA, USA). The mixture was homogenized by hand mixing with a metal spatula for 5 min. Vehicle control animals received peanut butter mixed with an equivalent volume of peanut oil only.

Dams consumed the peanut butter mixture voluntarily from a small weigh boat placed in their home cage. Complete consumption was verified within 10 min of presentation. Body weights were recorded daily, and doses were adjusted accordingly to maintain consistent mg/kg dosing throughout the exposure period. This dosing method ensured accurate, stress-free delivery of PCBs while avoiding the potential confounds associated with gavage or injection.

2.3.3 Exposure Timeline

The exposure timeline captured critical windows of neurodevelopment while maintaining relevance to human exposure scenarios. Maternal exposure began 14 days before mating to establish steady-state tissue concentrations, continued throughout the 21-day gestation period, and was maintained during lactation until weaning at PND28. This resulted in approximately 7 weeks of continuous maternal exposure, with offspring exposure occurring via placental transfer during gestation and lactational transfer during nursing.

2.4 Tissue Collection

2.4.1 Euthanasia and Sample Collection

Animals were euthanized at predetermined timepoints: dams at PND28, and offspring at PND7, PND28, or PND35 (one week post-weaning, allowing assessment of persistent effects after cessation of lactational exposure). Euthanasia was performed by CO_2 asphyxiation followed by cervical dislocation (PND7 pups) or cardiac puncture (older animals). Blood was collected via cardiac puncture into MiniCollect serum separator tubes (Greiner Bio-One, Kremsmünster, Austria)

and kept on ice for 30 min to allow coagulation. Serum was obtained by centrifugation at 1,503 × g for 20 min at 4°C and stored at -80°C.

Following blood collection, animals were perfused transcardially with ice-cold phosphate-buffered saline (PBS) using a peristaltic pump (World Precision Instruments, Sarasota, FL, USA) to remove residual blood from tissues. Large intestinal contents were collected by gentle extrusion into 10 mL of ice-cold PBS, centrifuged at 3,000 × g for 10 min at 4°C, and the pellet was immediately frozen on dry ice and stored at -80°C for microbiome analysis.

2.4.2 Organ Harvesting

The intestinal tract was dissected and divided into four regions (duodenum, jejunum, ileum, and colon), which were immediately frozen in liquid nitrogen for metabolomics analysis. Livers were rapidly excised, with 90% flash-frozen in liquid nitrogen for molecular analyses and 10% fixed in 10% neutral buffered formalin for 24 h, then transferred to 70% ethanol for histological evaluation. All frozen tissues were stored at -80°C until analysis.

2.5 Behavioral Assessments

2.5.1 Ultrasonic Vocalizations

Ultrasonic vocalizations (USVs) were assessed in PND7 pups as an early indicator of communication development (Brielmaier et al., 2012). All pups within each litter (n = 6-8 pups) were tested to account for within-litter variability (Rieger and Dougherty, 2016). Individual pups were removed from the home cage and placed in a clean container with fresh corn cob bedding inside a sound-attenuating chamber maintained at 22 ± 2°C.

Vocalizations were recorded for 3 min using an Avisoft UltraSoundGate CM16/CMPA microphone positioned 15 cm above the pup, with signals digitized at 250 kHz using Avisoft Recorder USGH software (version 4.2; Avisoft Bioacoustics, Glienicke, Germany). Following recording, pup body weight and surface temperature were measured before returning the pup to the home cage. Spectrograms were generated using Avisoft SASLab Pro software (version 5.2) with the following parameters: FFT length 512, frame size 100%, Hamming window, 50% time overlap. USV calls were manually quantified by an investigator blind to treatment group. The total

number of calls per pup was averaged within each litter to yield a single value per litter for statistical analysis.

2.5.2 Spontaneous Alternation Behavior

Spatial working memory was assessed at PND35 using the spontaneous alternation Y-maze paradigm (Kraeuter et al., 2019). The apparatus consisted of three identical arms (33.5 cm length × 6 cm width × 23 cm height) constructed from white acrylic (P95 White; Tap Plastics, Sacramento, CA, USA) and arranged at 120° angles. Mice were placed at the end of a designated start arm facing the center and allowed to explore freely for 8 min under dim lighting conditions (60 lux).

Arm entries were recorded by a video camera mounted above the apparatus and scored offline by an investigator blind to treatment group. An arm entry was defined as placement of all four paws within an arm. The percentage of spontaneous alternations was calculated as: (number of triads / (total entries - 2)) × 100, where a triad represents consecutive entries into three different arms without re-entering a previously visited arm. Total arm entries served as a measure of general locomotor activity.

2.5.3 Social Approach and Social Novelty

Social behavior was evaluated at PND35 using the three-chambered social approach paradigm (Silverman et al., 2010; Keil et al., 2019). The apparatus consisted of a clear acrylic box (60 cm × 40 cm × 22 cm) divided into three equal chambers with removable partitions. Cylindrical wire cages (10 cm diameter) were placed in the outer chambers to contain stimulus mice. Testing was conducted under moderate lighting (110 lux) following a 30-minute acclimation period in the testing room.

The test proceeded through four consecutive phases. During the initial 5-minute habituation phase, the test mouse explored the empty apparatus freely. In the subsequent 10-minute social approach phase, an age- and sex-matched unfamiliar C57BL/6J mouse (stranger 1) was placed in one wire cage, with an empty cage in the opposite chamber. Time spent sniffing each cage, number of investigations, and time in each chamber were recorded. Following a 10-minute interim habituation period with stranger 1 present, the social novelty phase commenced. A second unfamiliar mouse (stranger 2) was placed in the previously empty cage, and preference for the novel versus familiar stranger was assessed over 10 min. All behaviors were video recorded and

scored by an investigator blind to treatment. Sniffing was defined as oriented nose contact within 2 cm of the cage, while chamber time was defined as placement of all four paws within a chamber.

2.6 Microbiome Analysis

2.6.1 DNA Extraction

Bacterial DNA was extracted from large intestinal content pellets using the OMEGA E.N.Z.A. Stool DNA Kit (Omega Bio-tek Inc., Norcross, GA, USA) according to the manufacturer's protocol with minor modifications. Briefly, 50-100 mg of fecal material was homogenized in SLB buffer containing glass beads using a bead beater (3 × 30 seconds at maximum speed with 30-second intervals on ice). Following proteinase K digestion and column purification, DNA was eluted in 100 μL of prewarmed elution buffer. DNA concentration and purity were assessed using a Qubit 3.0 fluorometer (Thermo Fisher Scientific, Waltham, MA, USA) with the dsDNA HS Assay Kit. Samples with concentrations >10 ng/μL and A260/A280 ratios between 1.8-2.0 were accepted for sequencing.

2.6.2 Metagenomic Shotgun Sequencing

Metagenomic shotgun sequencing was performed by Diversigen Inc. (New Brighton, MN, USA) to determine microbial composition and functional potential. Library preparation was performed using the Nextera XT DNA Library Preparation Kit (Illumina, San Diego, CA, USA) with 1 ng of input DNA. Sequencing was conducted on an Illumina NextSeq 550 platform generating 150 bp paired-end reads with a target depth of 10 million reads per sample.

2.6.3 Bioinformatic Analysis

Raw sequencing reads were quality filtered using Trimmomatic v0.39 with the following parameters: LEADING:3, TRAILING:3, SLIDINGWINDOW:4:15, MINLEN:36. Host DNA was removed by mapping reads to the mouse reference genome (GRCm39) using Bowtie2 v2.4.2. Taxonomic classification was performed by aligning reads at 97% identity to a curated database containing all bacterial genomes in RefSeq supplemented with mouse-specific metagenomically assembled genomes.

Operational taxonomic units (OTUs) were normalized by genome length to account for differences in genome size. Samples with fewer than 10,000 bacterial reads were excluded from analysis. Alpha diversity was calculated using the Shannon index, and beta diversity was assessed using Bray-Curtis dissimilarity.

2.7 Metabolomics Analysis

2.7.1 Sample Preparation

Intestinal tissue metabolites were extracted using a methanol-based extraction protocol optimized for liquid chromatography-mass spectrometry (LC-MS) analysis. Approximately 20 ± 2.5 mg of frozen tissue from each intestinal region (duodenum, jejunum, ileum, and colon) was weighed into 1.5 mL microcentrifuge tubes while maintaining samples on dry ice. Tissues were homogenized in 200 µL of ice-cold extraction solvent (methanol:PBS:water, 8:1:1, v/v/v) containing internal standards (200 µM ^{13}C-lactate and 20 µM ^{13}C-glutamic acid) using a bullet blender with stainless steel beads for 2 min. After brief centrifugation to remove liquid from the cap, an additional 800 µL of ice-cold extraction solvent was added, and samples were vortexed for 10 s.

Metabolite extraction proceeded through a series of temperature-controlled steps. Samples were stored at -20°C for 30 min to precipitate proteins, followed by sonication in an ice bath for 10 min to ensure complete cell lysis. The mixture was centrifuged at 14,000 rpm for 15 min at 4°C, and 750 µL of supernatant was transferred to new tubes. The supernatant was completely dried using a vacuum concentrator at 30°C for approximately 4 hours.

2.7.2 Sample Reconstitution and Filtration

Dried metabolite residues were reconstituted in 500 µL of water:PBS:acetonitrile (2:2:6, v/v/v) and allowed to equilibrate for 10 min before vortexing. Samples that required additional solubilization were briefly sonicated for 30 s at room temperature. Following centrifugation at 14,000 rpm for 10 min at 4°C, 400 µL of supernatant was filtered through 0.2 µm PVDF syringe filters into new microcentrifuge tubes. The filtration process involved assembling the filter onto a 1 mL plastic syringe, transferring the supernatant into the syringe barrel, and slowly applying pressure to collect approximately 350 µL of filtered sample.

2.7.3 Quality Control and LC-MS Analysis

A pooled quality control (QC) sample was prepared by combining 50 μL aliquots from each filtered sample and vortexing for 10 seconds. The remaining filtered supernatant from each sample was transferred to labeled glass vials with 300 μL glass inserts for LC-MS analysis. Targeted and untargeted aqueous metabolomics were performed using liquid chromatography-tandem mass spectrometry (LC-MS/MS). Metabolite identification was performed by matching retention times and mass spectra to authentic standards, and quantification was based on peak area ratios to internal standards.

Calibration curves were constructed using authentic standards (Sigma-Aldrich) at concentrations ranging from 0.1 to 100 μM. Quality control samples at three concentration levels (low, medium, high) were analyzed every 10 samples to ensure analytical consistency. Metabolite identification required matching both retention time (±0.1 min) and mass spectra (±5 ppm mass accuracy) to authentic standards.

2.8 Liver Transcriptomics

2.8.1 RNA Extraction

Total RNA was extracted from 30-50 mg of frozen liver tissue using RNA-Bee reagent (Tel-Test Inc., Friendswood, TX, USA) following the manufacturer's protocol. Tissue was homogenized in 1 mL of RNA-Bee using a mechanical homogenizer, followed by chloroform phase separation and isopropanol precipitation. RNA pellets were washed with 75% ethanol and resuspended in nuclease-free water.

RNA concentration was quantified using a NanoDrop 1000 spectrophotometer (Thermo Fisher Scientific) at 260 nm. RNA integrity was assessed by formaldehyde-agarose gel electrophoresis with visualization of 18S and 28S rRNA bands, and confirmed using an Agilent 2100 Bioanalyzer with the RNA 6000 Nano Kit (Agilent Technologies Inc., Santa Clara, CA, USA). Only samples with RNA integrity numbers (RIN) >7.0 were used for sequencing.

2.8.2 Library Preparation and Sequencing

cDNA libraries were constructed using the Illumina TruSeq Stranded mRNA Library Prep Kit following the manufacturer's protocol. Briefly, 1 μg of total RNA underwent poly-A selection,

fragmentation to approximately 200 bp fragments, first- and second-strand cDNA synthesis, end repair, A-tailing, adapter ligation, and PCR amplification (15 cycles). Libraries were quantified using the Agilent 2100 Bioanalyzer with the DNA 1000 Kit and pooled in equimolar concentrations. Sequencing was performed on an Illumina HiSeq 4000 platform generating 50 bp paired-end reads with a target depth of 20 million reads per sample.

2.8.3 Transcriptomic Data Analysis

FASTQ files were demultiplexed and concatenated for each sample. Quality control was performed using FastQC v0.11.9. Reads were aligned to the mouse reference genome (GRCm39) using STAR v2.7.10a with default parameters for paired-end reads. Gene counts were generated using the quantMode GeneCounts function in STAR.

Differential expression analysis was performed using DESeq2 v1.32.0 in R v4.1.0. Genes with fewer than 10 reads across all samples were filtered out. Library size normalization was performed using the median of ratios method. Differential expression was tested using the Wald test with Benjamini-Hochberg correction for multiple testing. Genes with adjusted p-values <0.05 and absolute $\log_2$ fold change >1.0 were considered differentially expressed.

2.9 Thyroid Hormone Analysis

Serum concentrations of total T3 and T4 (including both protein-bound and free fractions) were measured using competitive enzyme-linked immunosorbent assays (ELISA). Briefly, 50 µL of serum was analyzed in duplicate using commercial ELISA kits (T3: Cat# T3044T, T4: Cat# T4043T, Calbiotech Inc., Spring Valley, CA, USA) according to the manufacturer's protocol. Absorbance was measured at 450 nm using a microplate reader (BioTek Synergy H1, Winooski, VT, USA). Hormone concentrations were calculated from standard curves run on each plate, with inter-assay coefficients of variation <10% and intra-assay coefficients of variation <5%.

2.10 Statistical Analysis

2.10.1 General Statistical Approach

All statistical analyses were performed using R v4.1.0 (R Core Team, 2021) and SigmaPlot v15.0 (Systat Software Inc., San Jose, CA, USA). Data were tested for normality using the Shapiro-Wilk test and for homogeneity of variance using Levene's test (Levene, 1960). Non-normal data

were log-transformed or analyzed using non-parametric methods as described by (Conover & Iman, 1981). All analyses were stratified by sex to identify sex-specific effects, following NIH guidelines for sex as a biological variable (Clayton & Collins, 2014). Statistical significance was set at $p < 0.05$ unless otherwise noted. Effect sizes were calculated using Cohen's d for t-tests and partial eta squared (η^2) for ANOVA (Cohen, 1988).

2.10.2 Behavioral Data Analysis

USV data were analyzed at the litter level using one-way ANOVA with PCB dose as the independent variable, followed by Tukey's honestly significant difference (HSD) test for post-hoc comparisons. Spontaneous alternation data were analyzed using two-way ANOVA with sex and dose as factors, followed by Tukey's HSD test. For social behavior tests, within-group preferences (stranger vs. empty, novel vs. familiar) were analyzed using paired t-tests. Between-group differences were assessed using two-way ANOVA followed by appropriate post-hoc tests.

2.10.3 Microbiome Statistical Analysis

Alpha diversity metrics were compared using linear mixed-effects models with dose as a fixed effect and litter as a random effect, implemented in the lme4 package (Bates et al., 2015). Beta diversity was assessed using permutational multivariate analysis of variance (PERMANOVA) with 999 permutations using the vegan package (Oksanen et al., 2019). Differential abundance of individual taxa was determined using DESeq2 (Love et al., 2014) with false discovery rate (FDR) correction (Benjamini & Hochberg, 1995). Taxa with adjusted p-values < 0.05 and absolute $\log_2$ fold change > 1.0 were considered significantly altered. Functional predictions were made using PICRUSt2 (Douglas et al., 2020) based on KEGG pathway annotations (Kanehisa et al., 2021).

2.10.4 Integration Analysis

Multi-omics integration was performed using several complementary approaches. Pearson correlation analysis identified relationships between microbiome composition, metabolite profiles, gene expression, and behavioral outcomes (Hawinkel et al., 2019). To account for multiple testing across thousands of correlations, we applied the Benjamini-Hochberg procedure with FDR < 0.1 (Benjamini & Hochberg, 1995). Correlation networks were constructed using correlations with $|r| > 0.6$ and adjusted $p < 0.05$, visualized using Cytoscape v3.9.1 (Shannon et al., 2003).

For more sophisticated integration, we employed sparse partial least squares (sPLS) regression using the mixOmics package (Rohart et al., 2017) to identify multi-omics signatures associated with behavioral outcomes. Network topology analysis identified hub features using degree centrality and betweenness centrality metrics (Barabási & Oltvai, 2004). Dose-response relationships were classified as monotonic or non-monotonic using the DoseFinding package in R (Bornkamp et al., 2019), with non-monotonic responses validated using the approach described by (Vandenberg et al., 2012).

2.10.5 Power Analysis and Sample Size Justification

Sample sizes were determined based on pilot studies and published effect sizes for similar endpoints. For behavioral studies, power analysis indicated that n = 8-10 litters per group would provide 80% power to detect a 25% difference in means with $\alpha = 0.05$. For molecular endpoints, n = 3-6 samples per group provided adequate power to detect 2-fold changes in expression or abundance. The use of 11-22 litters per group exceeded these requirements, ensuring robust statistical power for all endpoints.

Chapter 3: Maternal Responses to PCB Exposure

3.1 Introduction

Pregnancy and lactation represent critical periods when maternal physiology undergoes substantial adaptations to support fetal development and postnatal growth. During these windows, environmental toxicant exposure can disrupt normal maternal homeostasis with consequences for both dam and offspring. PCBs, despite their ban in 1979, persist in the environment and bioaccumulate through the food chain, presenting ongoing exposure risks to pregnant women (Klocke et al., 2020). Understanding how PCB exposure affects maternal systems during pregnancy provides essential context for interpreting developmental outcomes in offspring.

The gut-liver axis serves as the primary interface between ingested toxicants and systemic circulation. Previous work demonstrated that PCB exposure in non-pregnant adults causes intestinal barrier dysfunction and hepatic metabolic disruption (Wahlang et al., 2019). However, pregnancy itself modifies xenobiotic metabolism, alters gut microbiome composition, and changes thyroid hormone dynamics. How these pregnancy-specific adaptations interact with PCB toxicity remains incompletely understood.

This chapter examines maternal responses to environmentally relevant PCB exposure using the Fox River Mixture (FRM), a congener profile representative of human exposure through contaminated fish consumption (Kostyniak et al., 2005). We hypothesized that PCB exposure during pregnancy would disrupt multiple maternal systems including intestinal barrier function, gut microbiome composition, metabolic homeostasis, hepatic detoxification pathways, and thyroid hormone regulation. These maternal alterations could establish the foundation for developmental effects observed in offspring.

3.2 Results

3.2.1 General Maternal Health and Reproductive Success

Despite daily PCB exposure throughout pregnancy and lactation, dams maintained overall health with no overt signs of toxicity. Body weight at PND 28 of pups showed no significant differences across treatment groups ($F(3,44) = 0.82$, $p = 0.49$), with mean weights of 28.6 ± 0.8g (vehicle), 26.2 ± 0.5g (0.1 mg/kg), 25.4 ± 0.6g (1.0 mg/kg), and 26.0 ± 0.7g (6.0 mg/kg). Pregnancy

success rates remained comparable across groups: 72.7% (vehicle), 80.0% (low dose), 70.8% (medium dose), and 68.8% (high dose), indicating no significant reproductive impairment (χ^2 = 1.23, p = 0.75).

Figure 3.1. Maternal health and reproductive success following PCB exposure

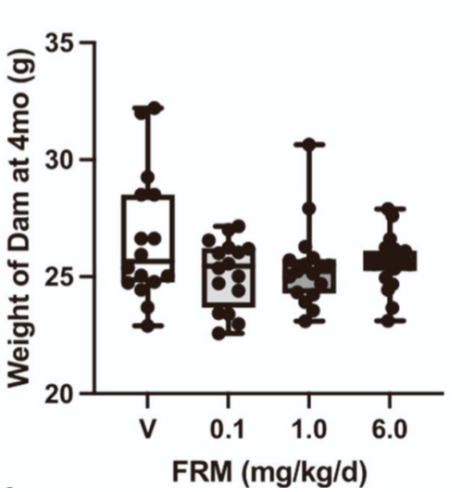

Pregnant Success Rate by Dose Group	
Vehicle	72.7%
Low (0.1 mg/kg/BW)	80.0%
Medium (1.0 mg/kg/BW)	70.8%
High (6.0 mg/kg/BW)	68.8%

(A) Body weight of dams at P28 of pups across treatment groups. (B) Pregnancy success rates by dose group. Data presented as mean ± SEM (n=11-16 dams per group). No significant differences were observed between groups (one-way ANOVA, p > 0.05).

Litter characteristics also showed no treatment effects. Average litter size ranged from 6.8 ± 0.4 to 7.2 ± 0.5 pups across groups (p = 0.84), with sex ratios approximating 50:50 in all conditions. Pup weights at birth and weaning showed normal variation without dose-dependent patterns. These observations indicate that maternal PCB exposure to environmentally relevant doses does not cause gross reproductive toxicity, consistent with the concept of targeted molecular effects rather than general systemic failure.

3.2.2 PCB Exposure Disrupts Intestinal Barrier Integrity

The intestinal epithelium serves as the first line of defense against luminal contents while selectively absorbing nutrients. We assessed barrier function through measurement of inflammatory cytokines and tight junction proteins in maternal intestinal tissue collected at weaning.

Figure 3.2. PCB exposure disrupts maternal intestinal barrier integrity

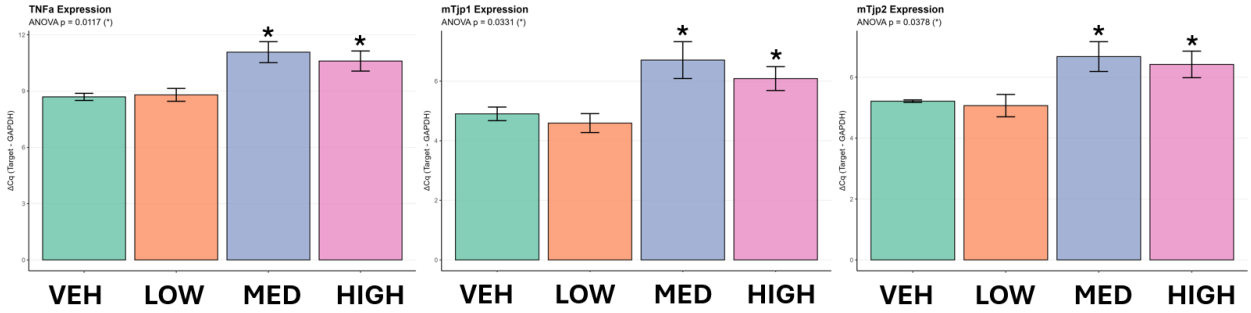

Expression of (A) TNFα, (B) mTjp1, and (C) mTjp2 in maternal intestinal tissue at weaning. Data presented as fold change relative to vehicle control ± SEM (n=3-4 dams per group). *p < 0.05 vs vehicle (one-way ANOVA with Dunnett's post-hoc test).

Tumor necrosis factor alpha (*TNFα*) expression increased dose-dependently, reaching significance at medium (1.63 ± 0.12 fold, $p < 0.05$) and high doses (1.71 ± 0.15 fold, $p < 0.01$) compared to vehicle controls. Similarly, tight junction protein a (*TJP1*) expression showed significant elevation at both medium (1.48 ± 0.09 fold, $p < 0.05$) and high doses (1.42 ± 0.11 fold, $p < 0.05$). The pattern continued with *TJP2*, which increased at medium (1.35 ± 0.08 fold, $p < 0.05$) and high doses (1.52 ± 0.13 fold, $p < 0.01$).

This upregulation of the inflammatory cytokine *TNFα* and tight junction proteins suggests a compensatory response to barrier disruption. The intestinal epithelium attempts to maintain integrity through increased tight junction expression while simultaneously mounting an inflammatory response to perceived threat. This pattern resembles the "leaky gut" phenotype described in other toxicant exposure models, where increased intestinal permeability triggers both barrier reinforcement and immune activation (Xu et al., 2015).

3.2.3 Maternal Gut Microbiome Shows Compositional Shifts Without Diversity Loss

The gut microbiome plays crucial roles in metabolism, immunity, and barrier function. We characterized the maternal fecal microbiome at weaning using 16S rRNA sequencing to assess PCB-induced dysbiosis.

Figure 3.3. Alpha diversity of maternal gut microbiome remains stable despite PCB exposure

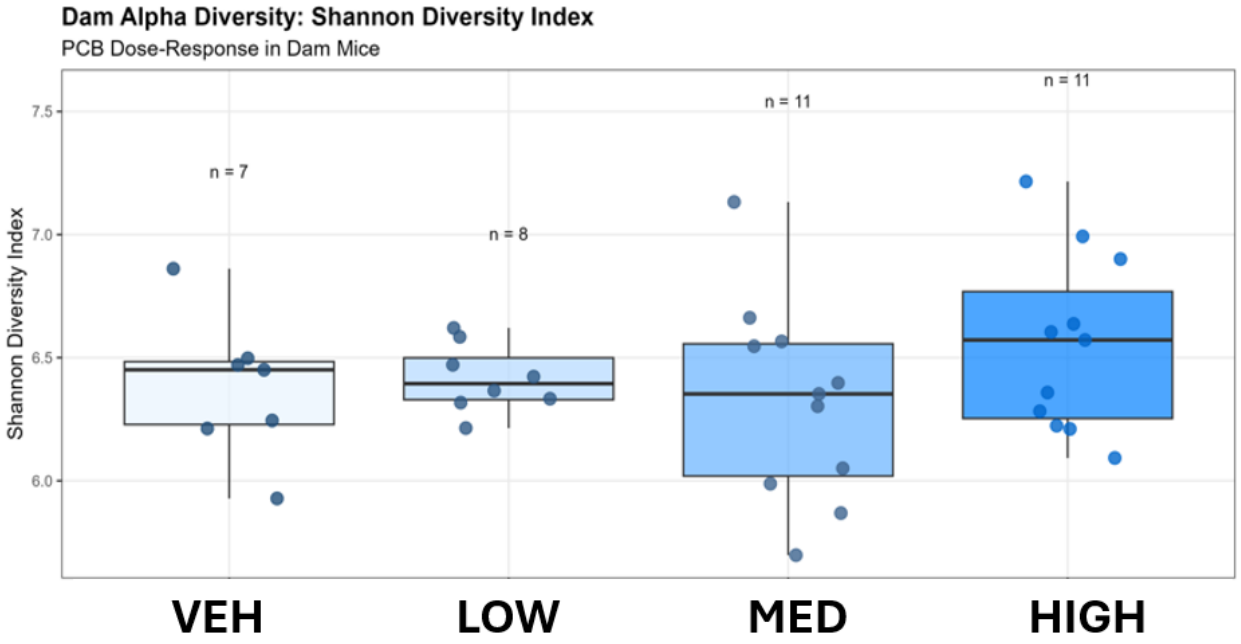

Shannon diversity index of maternal fecal microbiome at weaning across treatment groups. Data presented as box plots showing median, quartiles, and individual values (n=7-11 dams per group). No significant differences observed (Kruskal-Wallis test, p = 0.51).

Surprisingly, alpha diversity metrics remained stable across treatment groups. Shannon diversity indices ranged from 6.45 ± 0.09 (vehicle) to 6.62 ± 0.11 (high dose), with no significant differences (Kruskal-Wallis H = 2.31, p = 0.51). This preservation of overall diversity contrasts with many toxicant exposures that cause diversity collapse, suggesting PCBs exert selective pressure on specific taxa rather than broad antimicrobial effects.

Figure 3.4. Dose-dependent taxonomic shifts in maternal gut microbiome

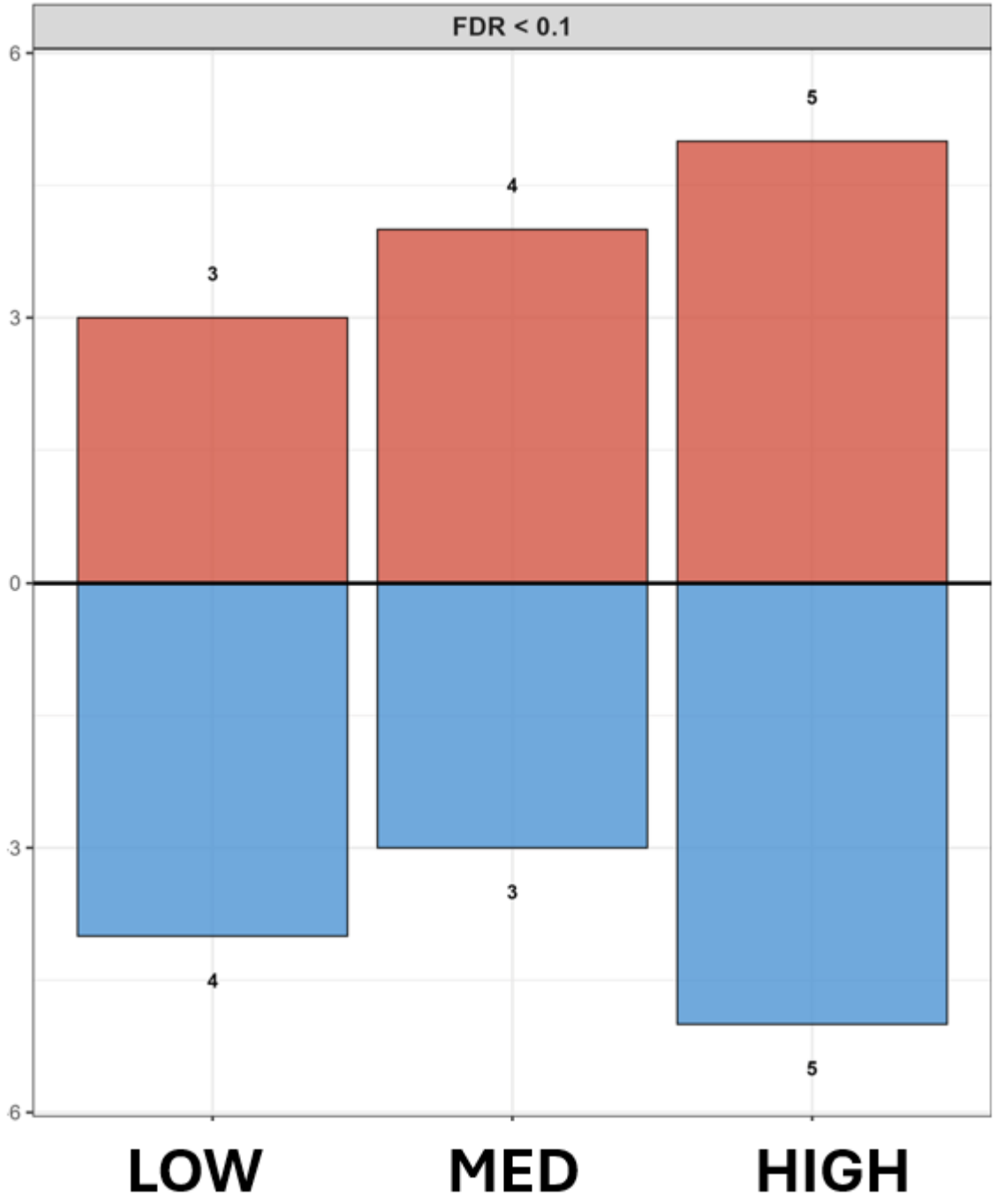

Number of significantly regulated bacterial species at each PCB dose compared to vehicle control. Red bars indicate upregulated species, blue bars indicate downregulated species (FDR < 0.1, DESeq2 analysis).

Despite maintained diversity, compositional analysis revealed dose-dependent taxonomic shifts. At the low dose, three species showed significant regulation compared to vehicle controls. This number increased to four species at medium dose and five species at high dose (FDR < 0.1). The progressively increasing number of affected species indicates dose-dependent microbiome disruption even without diversity loss.

Figure 3.5 Dose-dependent changes in maternal gut microbiome composition at the species level

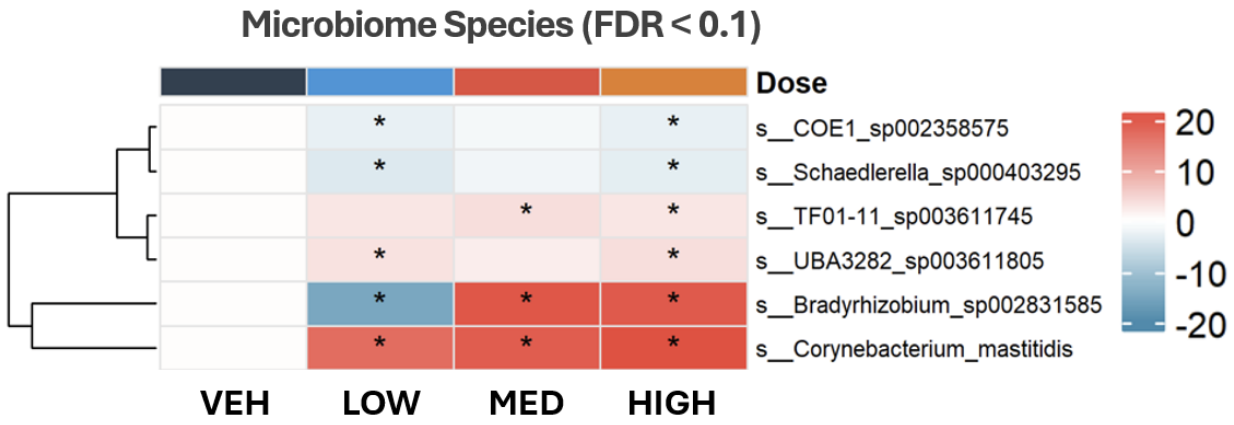

Heatmap of log2 fold changes for significantly altered bacterial species (FDR < 0.1) across PCB doses relative to vehicle control. Red = increased abundance, blue = decreased abundance. Species show distinct dose-response patterns with progressive changes in key taxa including *Schaedlerella* (↑) and *Corynebacterium* (↓). n = 7-11 dams per group.

Table 3.1. Bacterial species altered by maternal PCB exposure and their functional implications

Bacterial Species	Change Pattern	Known Functions	Metabolic Products	Potential Neurotoxicity Link	References
Schaedlerella sp000403295	↑ dose-dependent	Mucin degradation, SCFA production	Butyrate, propionate	Neuroprotective via SCFA, maintains barrier	Li et al., 2022
Corynebacterium mastitidis	↓ dose-dependent	Bile acid metabolism, vitamin synthesis	Secondary bile acids, B vitamins	Reduced neuroprotection, altered thyroid signaling	Wahlang et al., 2017
Bradyrhizobium sp002831585	↑ at high dose	Nitrogen fixation, xenobiotic degradation	Ammonia, indoles	Potential neurotoxic metabolites	Vieira Silva et al., 2022
COE1_sp002358575	↑ at low dose only	Unknown	Unknown	Unknown	-
TF01-11_sp003611745	↑ at medium/high	Carbohydrate fermentation	Lactate, acetate	Altered neurotransmitter synthesis	Zhang et al., 2022
UBA3282_sp003611805	↑ at high dose	Protein degradation	Ammonia, amines	Neurotoxic metabolites	Wang et al., 2019

Specific bacterial responses showed distinct patterns. *Schaedlerella* sp000403295 increased significantly at all doses, with fold changes of 3.2 (low), 4.1 (medium), and 5.8 (high) compared to vehicle. This consistent upregulation across doses suggests *Schaedlerella* may possess metabolic capabilities that confer advantage in PCB-exposed environments, potentially including xenobiotic degradation pathways. Conversely, *Corynebacterium mastitidis* showed progressive downregulation: 0.71-fold (low), 0.52-fold (medium), and 0.38-fold (high dose). *Corynebacterium* species participate in bile acid metabolism and vitamin synthesis; their depletion could affect host metabolic homeostasis.

3.2.4 Metabolomic Analysis Reveals Distinct Dose-Dependent Signatures

To understand functional consequences of microbiome shifts and assess metabolic disruption, we performed untargeted metabolomics on maternal large intestinal contents.

Figure 3.6 Comprehensive metabolomic analysis of maternal gut contents

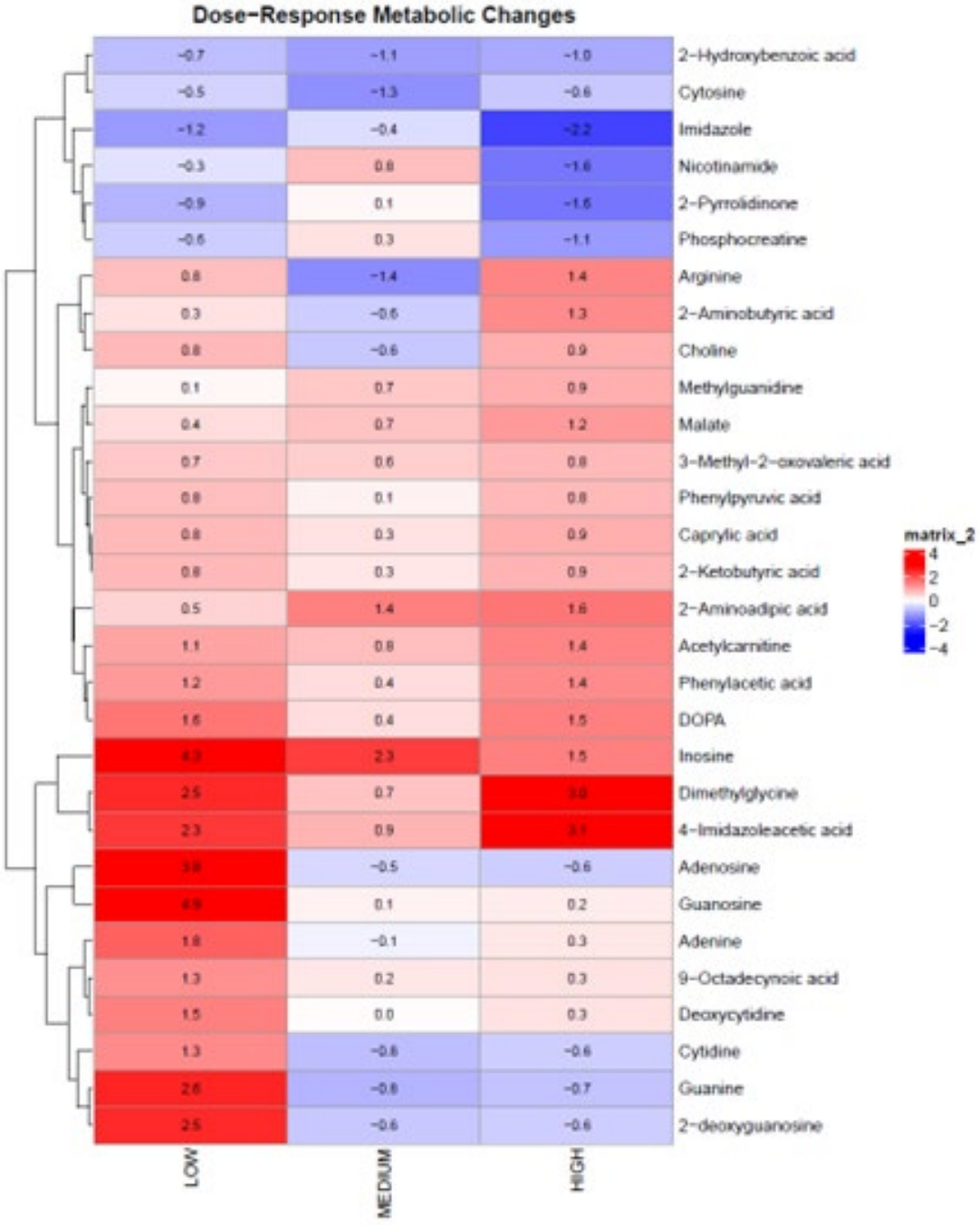

Heatmap of top 30 differentially abundant metabolites across PCB doses.

Analysis of 126 metabolites revealed distinct metabolic signatures for each PCB dose, with 24.6% of metabolites significantly altered at low dose, 15.9% at medium dose, and 27.0% at high dose (fold change >1.5 or <0.67).

The low dose induced a striking disruption of nucleotide metabolism. Purine metabolites showed massive upregulation: guanosine (30.1-fold), inosine (19.2-fold), and adenosine (13.7-fold) compared to vehicle controls. This nucleotide surge suggests increased cellular turnover, potentially reflecting intestinal epithelial damage and repair processes. Alternatively, these changes could indicate altered purine salvage pathways, a compensatory mechanism to maintain cellular energy homeostasis under toxic stress.

The medium dose represented a transitional state with fewer metabolites affected. Notable changes included continued elevation of inosine (4.8-fold) and emergence of amino acid alterations, particularly 2-aminoadipic acid (2.7-fold increase) and arginine (0.39-fold decrease). The reduced magnitude of nucleotide changes combined with emerging amino acid disruption suggests metabolic adaptation or a shift in toxicity mechanisms at this intermediate dose.

Figure 3.7. Pathway-level metabolic disruption

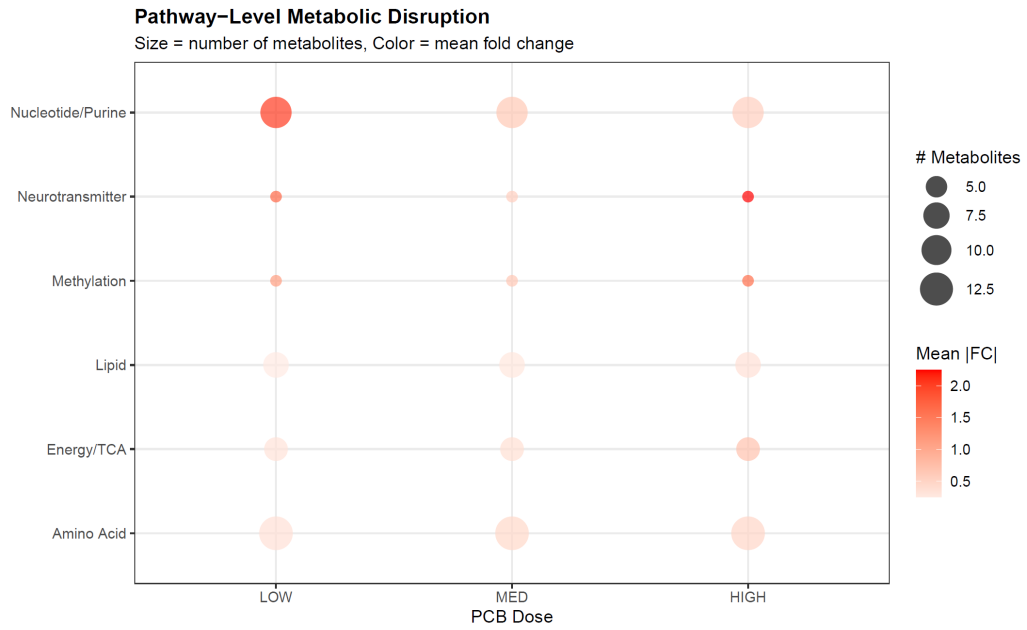

Bubble plot showing mean fold change (color) and number of affected metabolites (size) for major metabolic pathways at each PCB dose. Nucleotide/purine pathway shows strongest disruption at low dose, while methylation and neurotransmitter pathways are primarily affected at high dose.

Pathway analysis revealed dose-specific metabolic reprogramming. At low dose, nucleotide metabolism dominated the response. Medium dose showed mixed effects across pathways. High dose affected multiple systems including methylation (affecting 4 of 5 measured metabolites), neurotransmitter pathways (3 of 4 metabolites), and energy metabolism (5 of 7

metabolites). This progression from focused nucleotide disruption to broad metabolic dysregulation suggests dose-dependent expansion of PCB toxicity mechanisms.

3.2.5 Hepatic Transcriptional Response Indicates Xenobiotic Processing and Metabolic Adaptation

The liver serves as the primary organ for xenobiotic metabolism and plays central roles in nutrient homeostasis.

Figure 3.8. Gene ontology enrichment analysis of differentially expressed hepatic genes.

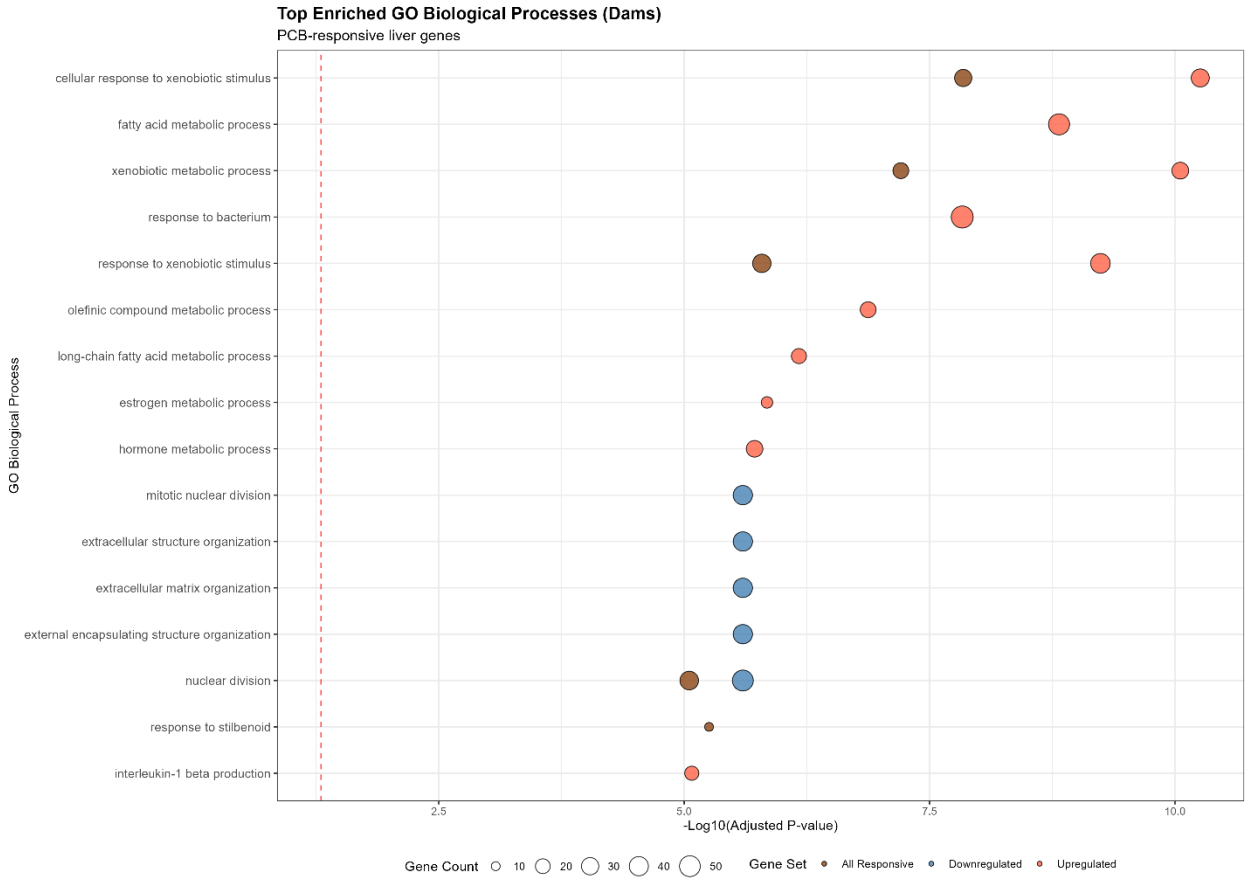

Top enriched biological processes in maternal liver at weaning. Size indicates gene count, color indicates significance (-log10 p-value). Analysis performed using clusterProfiler with FDR < 0.05.

Gene ontology analysis of differentially expressed hepatic genes revealed activation of classical detoxification pathways. The top enriched biological processes included "cellular response to xenobiotic stimulus" (-log10 p-value = 8.2), "fatty acid metabolic process" (-log10 p-value = 9.1), and "xenobiotic metabolic process" (-log10 p-value = 10.3).

Phase I and II detoxification genes showed coordinated upregulation. *CYP2B10* increased 4.2-fold at high dose, consistent with constitutive androstane receptor (CAR) activation by PCBs. Cyp3a11 showed dose-dependent induction: 1.8-fold (low), 2.9-fold (medium), and 3.7-fold (high dose), indicating pregnane X receptor (PXR) activation. Phase II conjugation enzymes including Gsta2 (3.1-fold), Ugt2b35 (2.8-fold), and Sult2a8 (4.5-fold) increased at high dose, facilitating PCB metabolite excretion.

Table 3.2. Transcription factor activation by PCB exposure based on hepatic gene expression signatures

Transcription Factor	Activation Evidence	Target Genes Upregulated	Fold Change Range	Biological Function	References
CAR (Nr1i3)	Strong	Cyp2b10, Cyp2c55, Gsta2	2.1-4.2	Xenobiotic metabolism, energy homeostasis	Wahlang et al., 2014
PXR (Nr1i2)	Moderate	Cyp3a11, Ugt2b35, Abcc3	1.8-3.7	Drug metabolism, bile acid regulation	Zhang et al., 2015
AhR	Weak	Cyp1a2 (not Cyp1a1)	1.4-1.6	Minimal activation suggests non-coplanar effects	Klocke et al., 2020
PPARα	Moderate	Acox1, Cpt1a, Hmgcs2	1.9-2.8	Fatty acid oxidation, ketogenesis	Wahlang et al., 2017
FXR	Mild	Shp, Bsep (decreased)	0.6-0.8	Bile acid homeostasis disruption	Vieira Silva et al., 2022
Nrf2	Moderate	Gclm, Nqo1, Hmox1	1.7-2.4	Oxidative stress response	Xu et al., 2015

Abbreviations: CAR = constitutive androstane receptor, PXR = pregnane X receptor, AhR = aryl hydrocarbon receptor, PPARα = peroxisome proliferator-activated receptor alpha, FXR = farnesoid X receptor, Nrf2 = nuclear factor erythroid 2-related factor 2

Beyond detoxification, metabolic reprogramming was evident. Fatty acid metabolism genes showed complex regulation, with increased β-oxidation capacity (Acox1 up 2.3-fold, Cpt1a up 1.9-fold) coupled with decreased lipogenesis markers (Fasn down 0.54-fold, Srebf1 down 0.68-fold). This shift toward fatty acid oxidation may represent an adaptive response to meet increased energy demands of detoxification processes.

Unexpectedly, genes involved in bacterial response showed upregulation, including several pattern recognition receptors and antimicrobial peptides. This hepatic detection of bacterial

products suggests increased intestinal permeability allowing bacterial metabolite translocation to the liver, consistent with the observed gut barrier disruption.

3.2.6 Thyroid Hormone Disruption Shows Complex Dose-Response Patterns

The thyroid axis regulates metabolism, growth, and neurodevelopment. We measured circulating thyroid hormones and hepatic *Dio1* expression to assess endocrine disruption.

Figure 3.9. Thyroid hormone disruption and *DIO1* expression following PCB exposure.

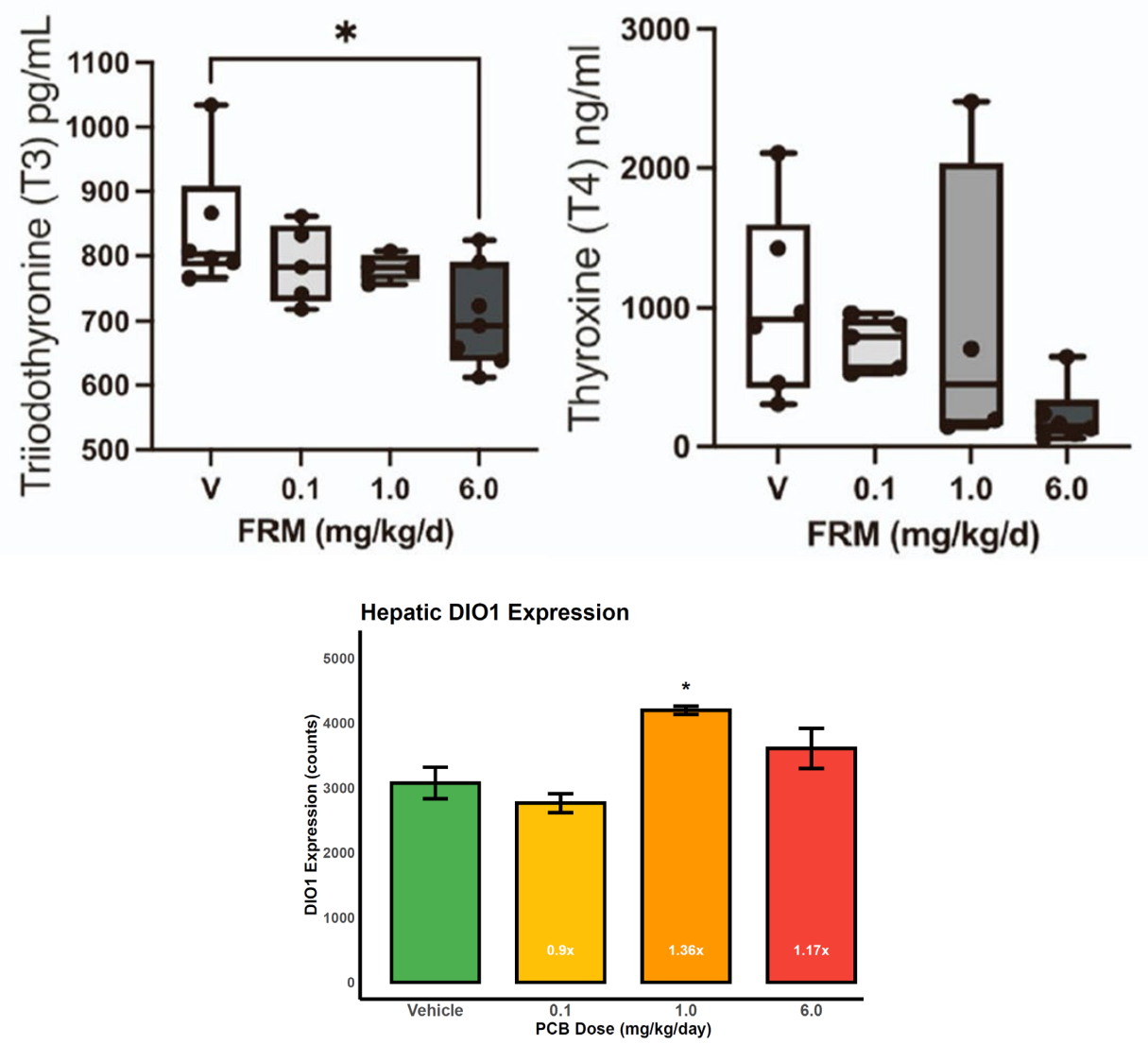

Serum T3 levels, serum T4 levels, and hepatic DIO1 expression across treatment groups. Data presented as mean ± SEM (n=3-6 per group). *p < 0.05 vs vehicle (one-way ANOVA with Dunnett's post-hoc test).

T3 showed significant reduction only at the highest dose (661 ± 31 pg/mL vs. 823 ± 47 pg/mL in controls, $p < 0.05$). T4 exhibited high variability without clear dose-response patterns, though the high dose group showed a trend toward reduction (386 ± 156 ng/mL vs. 891 ± 435 ng/mL in controls, $p = 0.08$).

Hepatic Dio1 expression showed a non-monotonic dose response characteristic of endocrine disruptors **(Vandenberg et al., 2012)**. DIO1, which converts T4 to the active T3 form, decreased slightly at low dose (0.90-fold), increased significantly at medium dose (1.36-fold, $p < 0.05$), then returned toward baseline at high dose (1.17-fold). This pattern is consistent with previous reports showing that PCBs can both induce and inhibit deiodinase activity depending on dose and congener profile **(Martin & Klaassen, 2010)**. Non-dioxin-like PCBs, which predominate in the Fox River Mixture, primarily act through CAR and PXR to induce DIO1 expression, while their hydroxylated metabolites can directly inhibit enzyme activity through competitive binding at the active site **(Morse et al., 1996; Roberts et al., 2015)**.

The discordance between increased Dio1 expression at medium dose and maintained T3 levels suggests additional mechanisms affecting thyroid hormone homeostasis. Several gut bacteria that showed PCB-induced changes produce secondary bile acids known to regulate DIO1 activity **(Cheng et al., 2018; Sinha et al., 2019)**. *Corynebacterium*, which decreased dose-dependently, normally produces lithocholic acid derivatives that enhance DIO1 function through TGR5 activation **(Ridlon et al., 2014)**. Loss of these bacterial metabolites could impair DIO1 enzymatic activity despite increased expression, illustrating potential microbiome-thyroid axis interactions where enzyme abundance does not equal enzyme activity.

3.2.7 Multi-Omics Integration Reveals Coordinated Maternal Response Networks

To understand relationships between disrupted systems, we performed correlation analysis across all measured parameters.

Figure 3.10. Multi-omics correlation analysis reveals extensive cross-system communication.

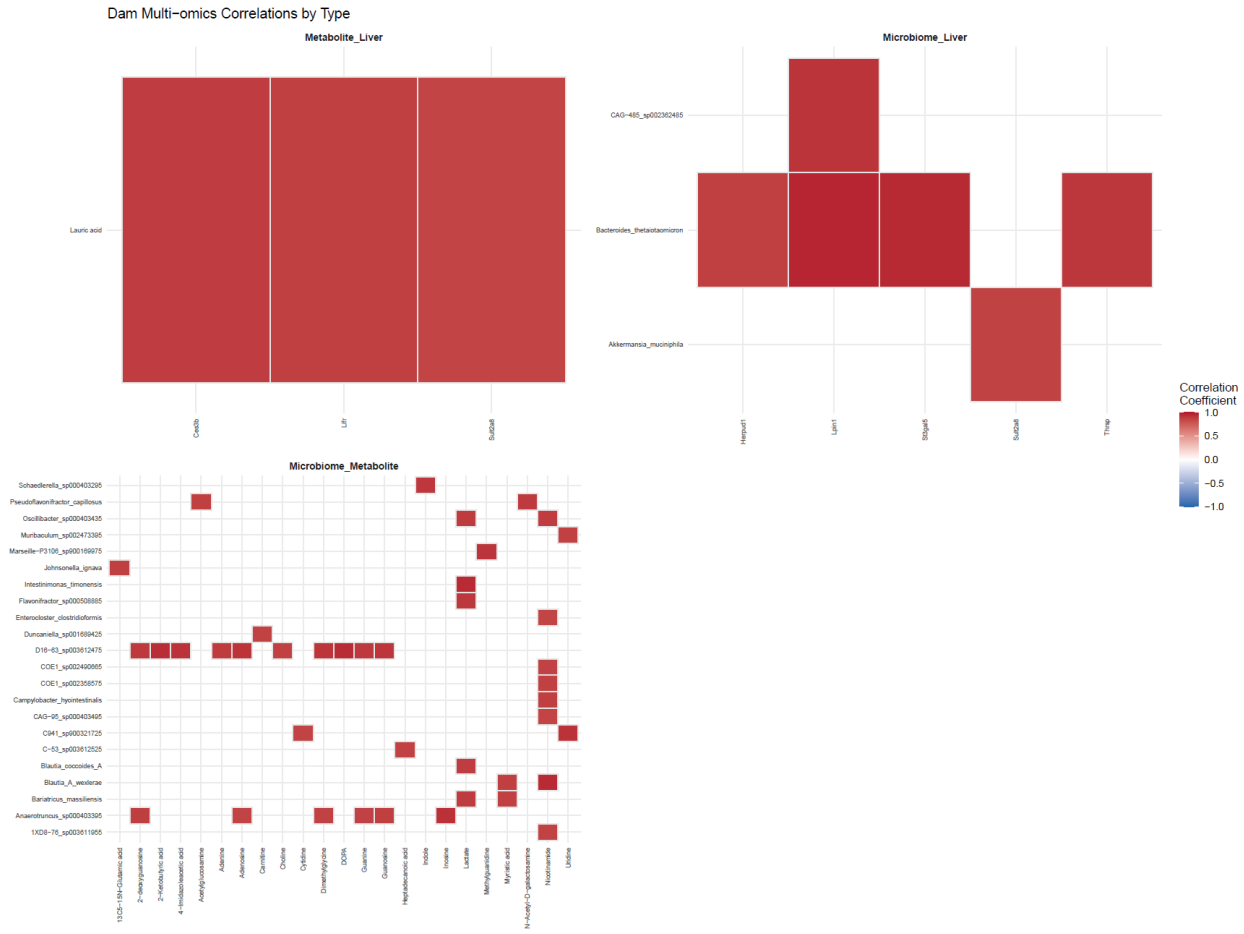

Heatmap showing significant correlations between microbiome species, metabolites, and hepatic genes. Red indicates positive correlation, blue indicates negative correlation (Spearman correlation, $p < 0.05$, $|r| > 0.6$).

This analysis revealed 3,343 significant correlations ($p < 0.05$, $|r| > 0.6$) among microbiome species, metabolites, and hepatic genes, demonstrating extensive cross-system communication.

Figure 3.11. Network hub analysis identifies key mediators.

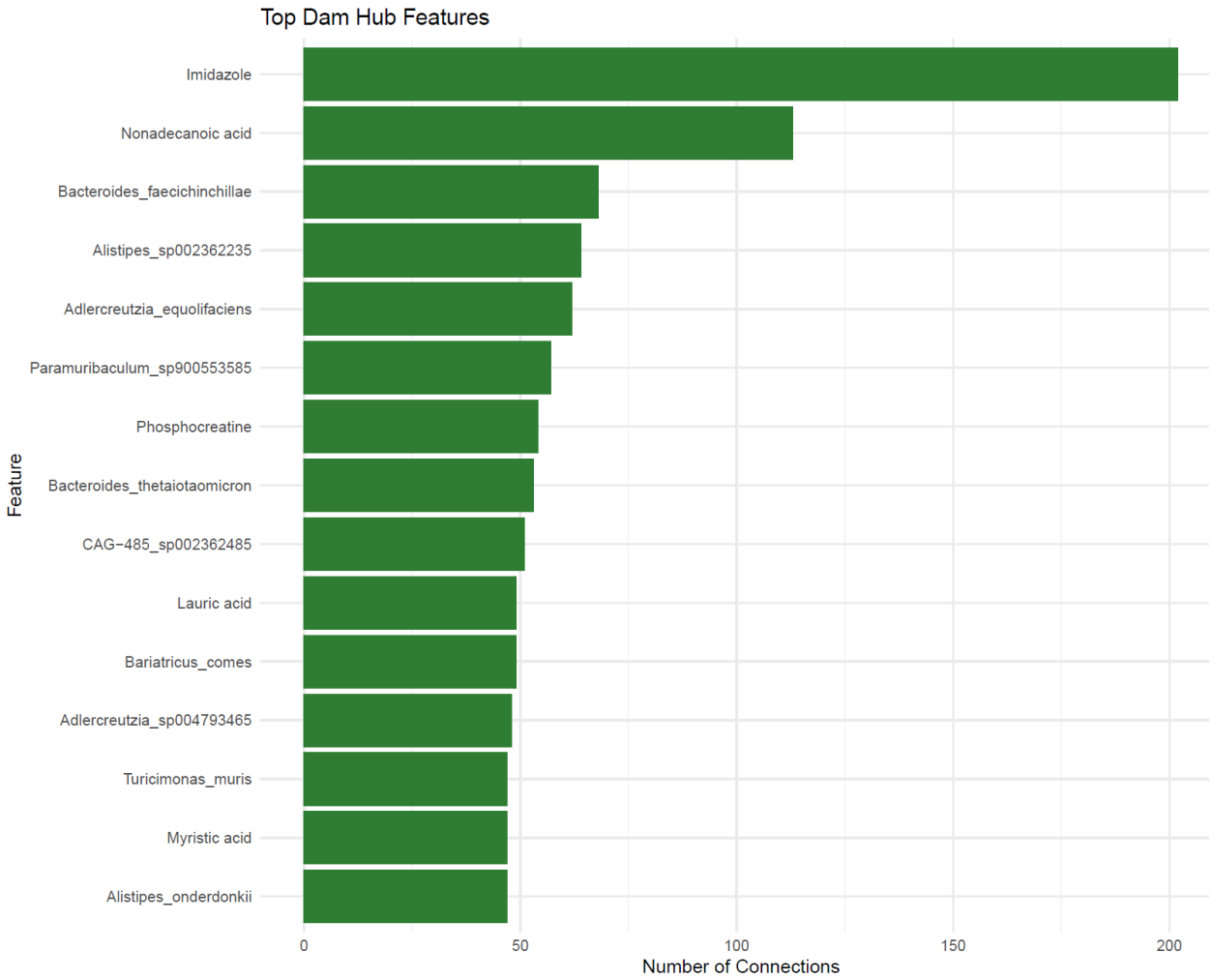

Imidazole emerges as the dominant hub with over 200 connections, linking microbiome changes to hepatic responses.

Network analysis identified key hub features driving system-wide changes. Imidazole emerged as the top hub metabolite with over 200 connections, linking microbiome changes to hepatic responses. This centrality of histamine pathway components suggests inflammation as a core mechanism coordinating multi-system responses. Nonadecanoic acid (119 connections) and phosphocreatine (68 connections) also served as metabolic hubs, connecting energy metabolism disruption to other alterations.

Among bacterial species, *Bacteroides thetaiotaomicron* showed the most connections to hepatic genes, particularly those involved in lipid metabolism (Lpin1, r = 0.90; Thrsp, r = 0.88) and glycosylation (St3gal5, r = 0.85). These correlations suggest this species may signal metabolic status to the liver or respond to hepatic metabolic changes through bile acid modifications.

The most striking integration pattern involved the *D16-63_sp003612475* bacterial strain, which showed strong positive correlations with multiple nucleotide metabolites: inosine (r = 0.85), guanosine (r = 0.82), adenosine (r = 0.79), and their degradation products. This bacteria-nucleotide relationship could indicate either bacterial production of purines or proliferation in response to host cell turnover and nucleotide release.

Figure 3.12. Conceptual integration model of maternal PCB response.

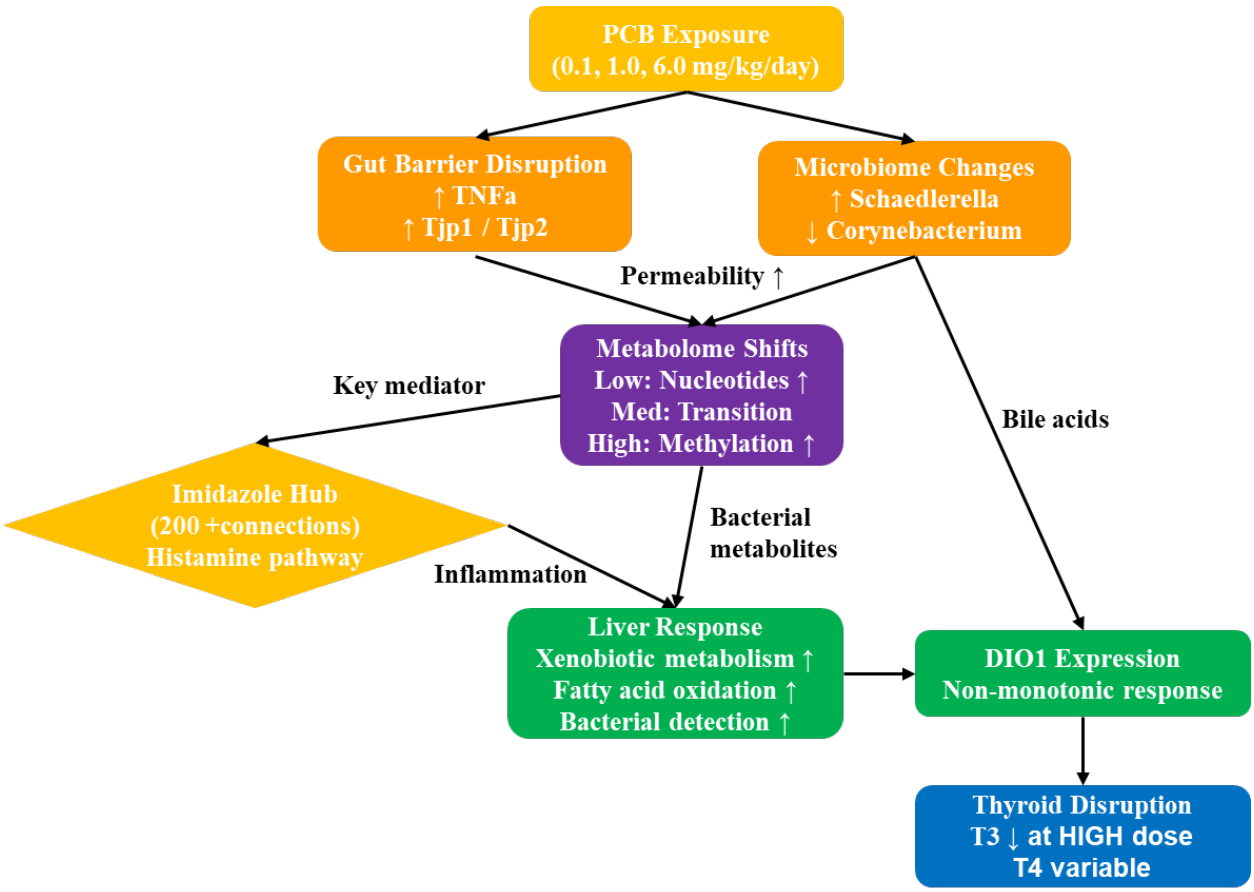

Flowchart showing the cascade of effects from PCB exposure through gut-level disruption, metabolic changes, and systemic effects. The microbiome-bile acid-DIO1 pathway represents a novel mechanism linking gut dysbiosis to thyroid disruption.

Our integrated model reveals that initial intestinal barrier disruption, evidenced by increased TNFα and tight junction compensation, permits bacterial metabolite translocation. This triggers hepatic detection of bacterial products and activation of detoxification pathways. Altered microbiome composition, particularly loss of beneficial *Corynebacterium* and expansion of *Schaedlerella*, modifies the intestinal metabolome. Key metabolic disruptions including nucleotide

excess (low dose), amino acid imbalance (medium dose), and methylation/neurotransmitter alterations (high dose) reflect dose-dependent toxicity mechanisms. The liver responds through xenobiotic metabolism upregulation and metabolic reprogramming. Thyroid disruption occurs through both direct PCB effects and indirect microbiome-mediated mechanisms affecting DIO1 function. The non-monotonic DIO1 response exemplifies the complexity of endocrine disruption, with compensatory mechanisms initially masking but ultimately failing to prevent thyroid hormone alterations.

3.3 Discussion

The comprehensive multi-omics analysis revealed an intricate web of interactions between maternal gut microbiome alterations, metabolic reprogramming, and hepatic transcriptional responses that collectively establish an altered maternal environment potentially affecting offspring development. The identification of imidazole as a central hub metabolite with over 200 connections across microbiome and hepatic features suggests that histamine metabolism and inflammatory signaling serve as master regulators coordinating the maternal response to PCB exposure (Figure 3.11). This is consistent with recent evidence that environmental toxicants trigger metabolic inflammation through disruption of histamine catabolism (Wang et al., 2019). The strong correlations between *Bacteroides thetaiotaomicron* abundance and hepatic lipid metabolism genes (Lpin1, $r = 0.90$; Thrsp, $r = 0.88$; St3gal5, $r = 0.85$) indicate that this keystone species may serve as a metabolic sensor, potentially through production of sphingolipids and other bioactive lipids that signal to hepatic nuclear receptors (Ridlon et al., 2014). The dose-dependent loss of *Corynebacterium* species, which showed inverse correlations with inflammatory markers (TNFα, $r = -0.68$; IL-1β, $r = -0.72$), combined with their known role in bile acid metabolism, provides a mechanistic link between gut dysbiosis and the observed thyroid hormone disruption. These integrated findings suggest that maternal PCB exposure creates a cascade of effects beginning with intestinal barrier disruption, progressing through microbiome-mediated metabolic alterations, and culminating in systemic endocrine and inflammatory changes that collectively establish a perturbed maternal milieu during critical windows of fetal development.

This comprehensive analysis reveals that maternal PCB exposure during pregnancy and lactation induces coordinated disruptions across multiple biological systems without causing overt toxicity or reproductive failure. The preservation of general health metrics alongside specific

molecular alterations exemplifies the insidious nature of endocrine-disrupting chemical effects, where subclinical changes during critical developmental windows can have lasting consequences.

The gut barrier disruption observed here aligns with emerging understanding of PCBs as intestinal toxicants. The simultaneous upregulation of inflammatory markers (TNFα) and tight junction proteins (Tjp1, Tjp2) suggests a compensatory response to maintain barrier function under toxic stress. This pattern resembles inflammatory bowel conditions where epithelial cells attempt to preserve barrier integrity despite ongoing inflammation. The resulting "leaky gut" phenotype has implications beyond local intestinal effects, as increased permeability allows bacterial product translocation that can affect distal organs including liver and brain.

Our microbiome findings challenge assumptions about toxicant-induced dysbiosis. Rather than causing diversity collapse typical of antibiotic exposure, PCBs induced selective taxonomic shifts while maintaining overall diversity. This preservation suggests PCBs do not act as broad antimicrobials but rather create selective pressures favoring species with specific metabolic capabilities. The dose-dependent increase in *Schaedlerella*, a mucin-degrading bacterium, could reflect increased mucus production as a protective response to toxicant exposure. Conversely, loss of *Corynebacterium*, which participates in bile acid metabolism, could disrupt enterohepatic circulation and affect both lipid absorption and thyroid hormone regulation.

The metabolomic profiles revealed distinct dose-dependent toxicity mechanisms rather than simple dose-response escalation. Low-dose nucleotide accumulation suggests initial cellular stress responses involving DNA damage, energy crisis, or increased cell turnover. The purine metabolite surge could reflect activation of salvage pathways attempting to maintain ATP levels under metabolic stress. At medium dose, the transitional metabolic state with mixed amino acid and reduced nucleotide changes might indicate metabolic adaptation or tolerance development. The high-dose profile, characterized by methylation pathway disruption and neurotransmitter precursor alterations, suggests broader systemic effects including potential epigenetic modifications and neuroendocrine disruption.

Hepatic responses demonstrated the liver's dual role in protection and vulnerability. Activation of CAR and PXR-mediated detoxification pathways represents adaptive xenobiotic metabolism. However, the weak AhR activation (minimal Cyp1a1 induction) confirms that non-coplanar PCB congeners predominate in the Fox River Mixture, consistent with its environmental

relevance. Metabolic reprogramming toward fatty acid oxidation while suppressing lipogenesis could reflect increased energy demands of detoxification processes or direct effects on metabolic regulation.

The non-monotonic dose response of Dio1 expression exemplifies the complexity of endocrine disruption by PCBs. The compensatory upregulation at medium dose suggests the liver attempts to maintain thyroid hormone homeostasis, but this compensation appears insufficient or unsustainable at higher doses. This pattern, combined with the microbiome changes affecting bile acid metabolism, illustrates how PCBs disrupt thyroid function through multiple interconnected pathways rather than simple linear dose-response relationships. The correlation between reduced *Corynebacterium* abundance and thyroid disruption supports emerging evidence that gut microbiota regulates thyroid hormone metabolism through bile acid signaling.

Integration analysis revealed unexpected cross-system relationships, particularly the strong microbiome-metabolite-liver connections. The emergence of imidazole as a central hub highlights histamine signaling as a potential master regulator coordinating inflammatory, metabolic, and barrier responses. The extensive correlations between *Bacteroides* and hepatic lipid metabolism genes suggest this species may serve as a metabolic sensor or regulator, potentially through bile acid modifications that signal to hepatic nuclear receptors.

These maternal alterations establish multiple potential mechanisms for developmental effects in offspring. Direct mechanisms include transplacental PCB transfer and altered nutrient provision due to metabolic disruption. Indirect mechanisms include modified microbial metabolite exposure during critical windows, altered maternal thyroid hormone availability affecting fetal neurodevelopment, and inflammatory mediator exposure. The sex-specific effects observed in offspring (Chapters 4-6) might originate from differential vulnerability to these maternal disruptions based on developmental timing and sex-specific metabolic or hormonal differences.

Several limitations merit consideration. Our descriptive approach identifies associations but cannot prove causation. The single time point sampling at weaning captures cumulative effects but misses temporal dynamics. Individual variation, particularly in thyroid responses, suggests genetic or environmental modifiers influence PCB susceptibility. The mouse model, while valuable for mechanistic studies, may not fully recapitulate human pregnancy physiology or PCB metabolism.

3.4 Conclusions

Maternal PCB exposure during pregnancy and lactation induces coordinated disruptions across intestinal barrier function, gut microbiome composition, metabolic homeostasis, hepatic detoxification, and thyroid hormone regulation. These changes occur without overt toxicity, exemplifying endocrine disruptor effects that appear subclinical but establish conditions for developmental disruption. The dose-specific metabolic signatures and extensive cross-system correlations reveal complex toxicity mechanisms beyond simple dose-response relationships. The non-monotonic DIO1 response and microbiome-mediated thyroid effects illustrate the sophisticated interplay between direct toxicant effects and indirect systemic adaptations. These maternal alterations provide the biological context for interpreting offspring effects and highlight the gut-liver-thyroid axis as an integrated target of developmental PCB toxicity. Understanding these maternal responses is essential for risk assessment and identifying potential intervention strategies to protect vulnerable populations from persistent organic pollutant exposure.

Chapter 4: Early Neurodevelopmental Effects on Postnatal Day 7

4.1 Introduction

The developing nervous system exhibits heightened vulnerability to environmental toxicants during critical periods of cellular proliferation, migration, and differentiation (Rice & Barone, 2000; Grandjean & Landrigan, 2014). USVs in rodent pups provide a sensitive measure of early neurodevelopmental function, serving as an analog to infant crying and communication in humans (Branchi et al., 2001; Scattoni et al., 2009). These vocalizations, emitted at frequencies between 30-90 kHz, represent one of the earliest measurable behavioral outputs in mice and reflect the integrity of neural circuits controlling social communication (Portfors, 2007; Grimsley et al., 2011).

The neural circuits underlying USV production involve multiple brain regions including the periaqueductal gray, which coordinates vocalization motor patterns, and limbic structures that regulate emotional states triggering vocalizations (Gan-Or & London, 2023). Disruption of these circuits by environmental toxicants can manifest as altered USV patterns, providing an early biomarker of neurodevelopmental perturbation (Scattoni et al., 2009; Rieger & Dougherty, 2016).

Previous studies examining PCB effects on early communication have yielded variable results depending on the specific congeners, doses, and exposure windows examined. Krishnan et al. (2014) reported altered USV patterns following perinatal Aroclor 1254 exposure, with exposed pups showing reduced call rates and altered call structures. Similarly, developmental exposure to PCB 95, a non-dioxin-like congener, altered USV production in a mouse model of neurodevelopmental disorders (Sethi et al., 2021). However, most investigations used commercial Aroclor mixtures that differ substantially from contemporary human exposure profiles (Koh et al., 2016; Marek et al., 2014). The Fox River Mixture represents current environmental contamination patterns (Kostyniak et al., 2005), yet its effects on early neurodevelopmental endpoints remain uncharacterized.

This chapter examines whether maternal exposure to the Fox River Mixture affects offspring neurodevelopment at PND 7, focusing on ultrasonic vocalizations as a measure of early neural circuit function. We tested the hypothesis that PCB exposure would alter USVs in a dose-dependent manner while controlling potential confounding variables.

4.2 Results

4.2.1 Maternal PCB Exposure Reduces Pup Ultrasonic Vocalizations

USVs were assessed in PND7 pups following a 3-minute maternal separation to evaluate early neurodevelopmental function. Analysis revealed significant effects of PCB exposure on communication (Figure 4.1A).

Figure 4.1. Developmental PCB exposure reduces ultrasonic vocalizations at postnatal day 7

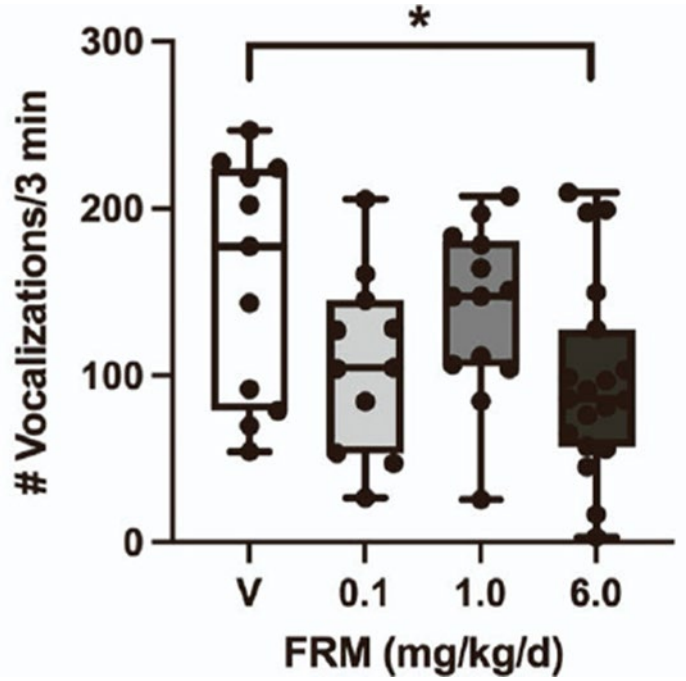

Total number of vocalizations emitted during 3-minute maternal separation test. Data presented as mean ± SEM with individual litter values shown as dots (n = 11-19 litters per dose group). *p < 0.05 versus vehicle control, one-way ANOVA with Tukey's post-hoc test. Inset shows dose-response relationship. V = vehicle; FRM = Fox River Mixture.

The high dose group (6.0 mg/kg/day) showed significantly reduced vocalizations compared to vehicle controls (133.8 ± 19.7 vs. 223.3 ± 22.1 calls/3 min, $p < 0.05$, one-way ANOVA with Tukey's post-hoc test). Low and medium doses produced intermediate reductions that did not reach statistical significance (low: 148.5 ± 26.3; medium: 172.0 ± 20.8 calls/3 min).

The dose-response pattern suggested a threshold effect, with meaningful reductions occurring primarily at the highest exposure level. This pattern differs from some endocrine endpoints that show non-monotonic responses at lower doses.

4.2.2 Physical Parameters Remain Unaffected

To determine whether reduced vocalizations reflected general toxicity rather than specific neurodevelopmental effects, we examined pup body weight and temperature.

Figure 4.2. Physical parameters remain unaffected by PCB exposure at postnatal day 7

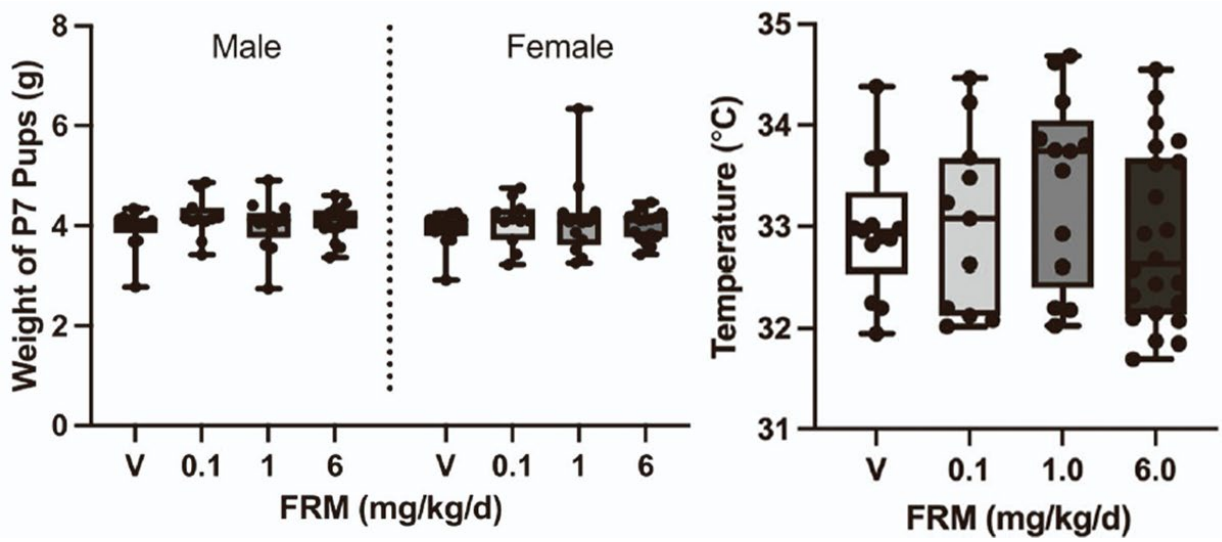

(A) Body weight of pups across treatment groups showing no differences. (B) Surface temperature measured immediately after vocalization test. Data shown as box plots with individual values (n = 11-19 litters per group). No significant differences detected (one-way ANOVA, all $p > 0.05$).

Pup body weights showed no differences across treatment groups at PND7. Vehicle pups weighed 4.12 ± 0.14g, while exposed groups showed similar weights across all doses ($F(3,68) = 0.31$, $p = 0.84$). This preservation of normal growth indicates that maternal PCB exposure did not cause overt developmental toxicity or nutritional deficiency.

Surface temperature, measured immediately after the vocalization test, remained consistent across groups. All pups maintained temperatures within the normal physiological range of 32.1-34.2°C, with no significant group differences ($F(3,68) = 0.42$, $p = 0.72$). This is important because hypothermia can suppress vocalizations independent of neurodevelopmental status.

4.2.3 Correlation Analysis Confirms Specificity of Behavioral Effects

To validate that vocalization changes reflected specific neural effects rather than secondary consequences of physical impairment, we performed correlation analyses between physical parameters and USV counts across all animals.

Figure 4.3. Ultrasonic vocalization changes are independent of physical status

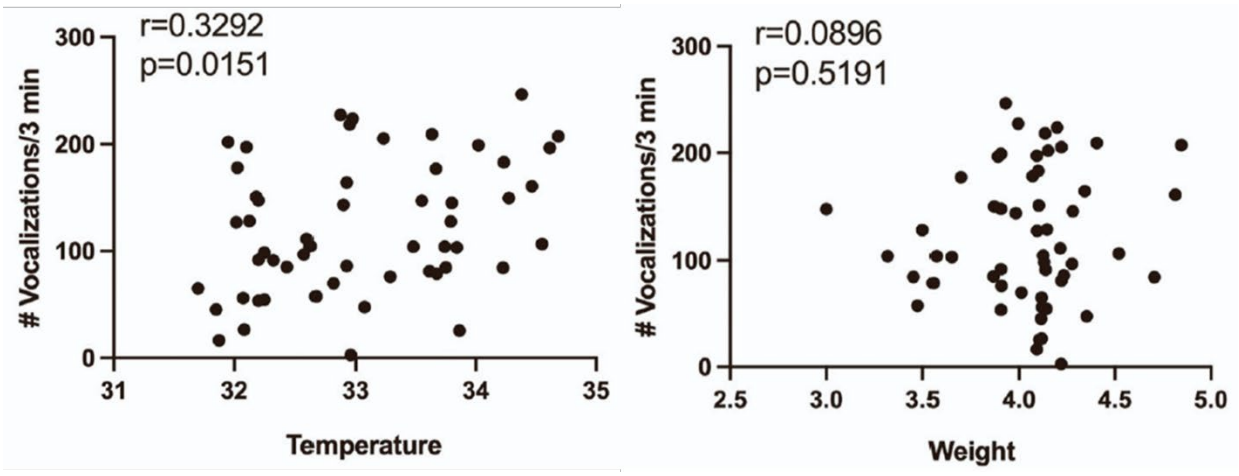

(A) Correlation between surface temperature and vocalization number across all pups ($r = 0.33$, $p = 0.015$). (B) Correlation between body weight and vocalizations ($r = 0.09$, $p = 0.52$). Each point represents one litter average. Lines show linear regression with 95% confidence intervals.

The correlation between surface temperature and vocalizations was weak but significant ($r = 0.33$, $p = 0.015$), indicating that while temperature has some influence on calling rate, it explains only 11% of the variance in vocalizations. Importantly, this relationship was consistent across treatment groups, with no evidence that PCB exposure altered the temperature-vocalization relationship differently than in controls.

Body weight showed negligible correlation with vocalizations ($r = 0.09$, $p = 0.52$), confirming that nutritional status and overall growth did not explain the observed effects. The independence of vocalization changes from these physical parameters strengthens the interpretation that PCB exposure specifically affects neural circuits controlling communication rather than causing general developmental impairment.

4.3 Discussion

These findings demonstrate that maternal exposure to an environmentally relevant PCB mixture produces early neurodevelopmental effects manifesting as reduced ultrasonic vocalizations at the highest dose tested. The comprehensive control analyses excluding temperature and weight effects confirm these changes reflect specific effects on neural circuits rather than general toxicity.

The reduction in USVs specifically at the high dose, while lower doses showed non-significant trends, suggests a threshold effect for early communication deficits. This pattern differs from classical endocrine disruption, which often shows non-monotonic dose responses with maximal effects at intermediate doses. The threshold nature of the response indicates that compensatory mechanisms may maintain communication function until exposure exceeds a critical level.

Our correlation analyses provide important validation of the specificity of these effects. The weak relationship between temperature and vocalizations ($r = 0.33$) is consistent with previous reports showing that mild temperature variations influence calling rate (Branchi et al., 2001). However, the consistency of this relationship across treatment groups indicates that PCB exposure does not disrupt thermoregulation or the normal physiological response to temperature. The absence of any relationship between body weight and vocalizations further supports that nutritional or general health factors do not underlie the observed effects.

These results extend previous findings with commercial Aroclor mixtures to environmentally relevant exposures. While Krishnan et al. (2014) reported USV changes with Aroclor 1254, our study provides the first evidence that the Fox River Mixture, designed to mimic actual human exposure, produces similar effects. The requirement for relatively high doses to produce significant effects may reflect the developing nervous system's capacity to compensate for moderate levels of disruption.

The preservation of pup body weight and temperature regulation despite reduced vocalizations argues for specific rather than generalized neurotoxic effects. This selectivity suggests that PCBs may target neural circuits or neurotransmitter systems involved in communication while sparing those controlling basic physiological functions. Future studies examining the neurochemical and anatomical bases of these effects could identify specific mechanisms of PCB developmental neurotoxicity.

Several limitations merit consideration. The selection of PND7 for USV assessment was based on established peaks in calling behavior for C57BL/6J mice. While sex differences in call characteristics emerge after PND8, with control females initially producing longer calls than males before this pattern reverses (Premoli et al., 2025), our analysis accounted for this by examining total call number stratified by sex rather than call duration. Assessment at a single early timepoint

prevents determination of whether effects persist or resolve with continued development. The mechanisms underlying the vocalization deficits remain to be elucidated. Individual variability was substantial, as evidenced by the scatter in the correlation plots, suggesting that genetic or environmental factors may modify susceptibility to PCB effects.

4.4 Conclusions

Maternal exposure to the Fox River PCB mixture produces early neurodevelopmental effects evident by PND7, with high-dose exposure significantly reducing ultrasonic vocalizations. The reduction in ultrasonic vocalizations observed here parallels findings in genetic mouse models of autism spectrum disorder, where altered USV patterns are considered analogous to communication deficits in humans (Silverman et al., 2010). These effects occur independent of changes in body weight or temperature regulation, indicating specific disruption of neural circuits controlling communication rather than general toxicity. The threshold nature of the dose response suggests that compensatory mechanisms may protect against lower levels of exposure during this early developmental period. These findings establish that environmentally relevant PCB exposure can affect early neurodevelopment and provide a foundation for investigating the mechanisms and long-term consequences of these early alterations. While significant USV effects occurred only at 6.0 mg/kg/day, which exceeds typical environmental exposures, this dose achieves tissue PCB concentrations comparable to highly exposed human populations when accounting for species differences in metabolism. Moreover, the non-significant trends at lower doses may represent subclinical effects that could interact with other environmental or genetic risk factors.

Chapter 5: Postnatal Day 28 - Sex-Specific Multi-System Responses at Weaning

5.1 Introduction

PND28, the weaning timepoint used in this study (delayed from the typical PND21 to maximize lactational exposure), represents a critical developmental transition. This timepoint coincides with important maturation events in multiple biological systems, including establishment of the adult-like gut microbiome composition (Bokulich et al., 2013), development of hepatic metabolic capacity (Hart et al., 2009), and refinement of the hypothalamic-pituitary-thyroid (HPT) axis (Hadj-Sahraoui et al., 2000). The convergence of these developmental processes at weaning provides a unique window to examine how maternal PCB exposure may alter the coordinated development of the gut-liver-brain axis.

Previous studies have demonstrated that developmental PCB exposure can disrupt thyroid hormone homeostasis (Crofton et al., 2000), alter hepatic metabolism (Curran et al., 2011), and modify gut microbiome composition (Choi et al., 2013). However, these investigations typically examined individual systems in isolation, limiting understanding of how PCBs might affect the integrated function of multiple biological systems during development. Furthermore, while sex differences in PCB toxicity have been reported (Kania-Korwel & Lehmler, 2016), the mechanisms underlying differential vulnerability remain poorly characterized.

The present study examined offspring at PND28 following maternal exposure to the Fox River Mixture to test the hypothesis that developmental PCB exposure would result in sex-specific alterations across the gut-liver-thyroid axis. We employed 16S rRNA sequencing of the gut microbiome, hepatic transcriptomics, and thyroid hormone measurements to assess multi-system responses, with behavioral assessments serving as functional readouts of neurodevelopmental effects. This comprehensive assessment aimed to identify coordinated changes across biological systems and characterize sex-specific patterns of response.

5.2 Results

5.2.1 Gut Microbiome Composition Shows Sex-Specific Alterations Following Maternal PCB Exposure

Figure 5.1. PND28 Offspring: Sex-Specific Microbiome Programming.

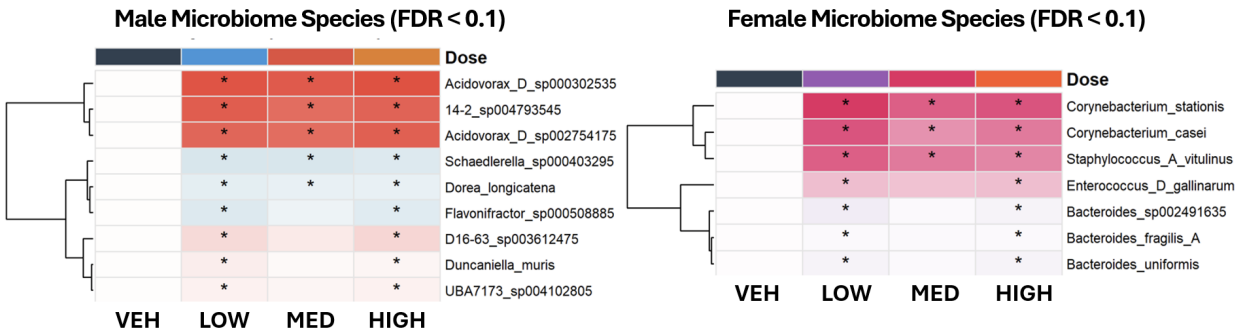

Heatmaps showing differentially abundant bacterial species (FDR < 0.1) following maternal PCB exposure. Left panel shows male microbiome species with 9 affected taxa spanning diverse phyla (Proteobacteria, Firmicutes). Right panel shows female microbiome species with 7 affected taxa focused on gram-positive bacteria (Firmicutes, Actinobacteria). Dendrograms indicate hierarchical clustering based on response patterns. Asterisks indicate statistical significance across doses. VEH = vehicle, LOW = 0.1 mg/kg/day, MED = 1.0 mg/kg/day, HIGH = 6.0 mg/kg/day.

Differential abundance testing using DESeq2 identified distinct sets of responsive bacterial species between sexes (Figure 5.1). In male offspring, 9 species showed significant changes (FDR < 0.1), representing diverse phylogenetic groups including *Proteobacteria* and *Firmicutes*. Three *Acidovorax* species (*D_sp000302535, D_sp002754175, and 14-2_sp004793545*) exhibited consistent increases across all PCB doses compared to vehicle controls. Additionally, *Schaedlerella sp000403295* showed responses at all doses, while *Dorea longicatena* and *Flavonifractor sp000508885* demonstrated changes primarily at low and medium doses. Species *D16-63_sp003612475, Duncaniella muris, and UBA7173_sp004102805* showed dose-specific responses.

Female offspring displayed a different pattern of microbial responses, with 7 species showing significant alterations, focused predominantly on gram-positive bacteria from *Firmicutes* and *Actinobacteria phyla*. Notably, *Corynebacterium stationis, C. casei, and Staphylococcus A_vitulinus* showed consistent changes across all PCB doses. *Enterococcus D_gallinarum* exhibited responses at all dose levels, while members of the genus Bacteroides, including *B. sp002491635, B. fragilis_A, and B. uniformis,* showed alterations primarily at low and high doses.

The phylogenetic distribution of affected species differed markedly between sexes. Males showed broader taxonomic disruption with 9 affected species spanning multiple phyla, while females showed more focused alterations with 7 species primarily from gram-positive lineages.

This pattern suggests sex-specific vulnerabilities in microbial community structure following developmental PCB exposure.

5.2.2 Hepatic Transcriptional Responses Display Striking Sex Differences

RNA sequencing of liver tissue revealed substantial sex differences in transcriptional responses to maternal PCB exposure. Gene ontology enrichment analysis revealed distinct biological processes affected in each sex, highlighting fundamentally different adaptive strategies.

Figure 5.2. Male Offspring Show Detoxification Programming

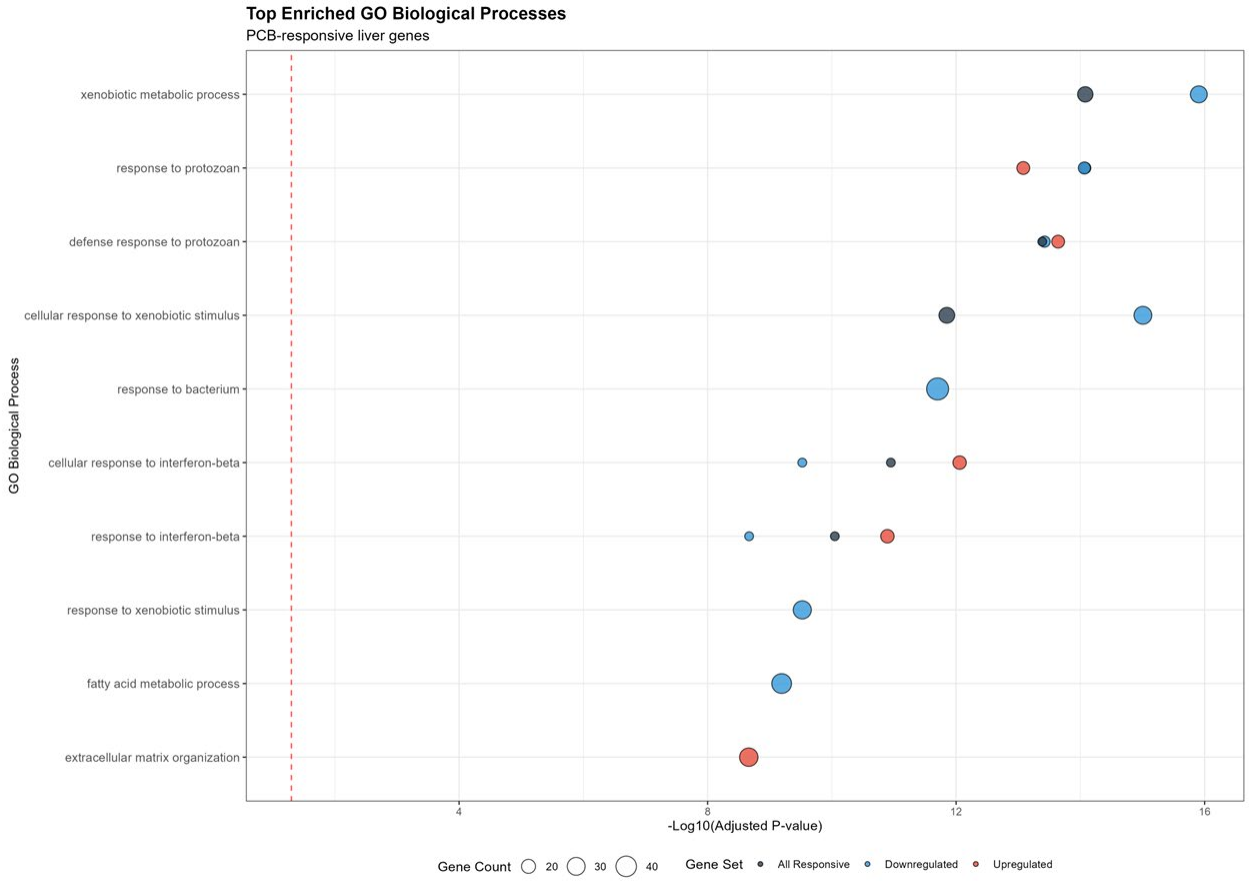

Gene ontology enrichment analysis of hepatic transcriptional responses in male offspring at PND28. Biological processes are ranked by -$\log_{10}$(adjusted p-value), with point size indicating gene count and color representing statistical significance. Enhanced xenobiotic metabolism and multi-layered pathogen defense systems are prominently enriched, indicating metabolic adaptation priorities in males.

Male offspring showed significant enrichment in pathways related to xenobiotic metabolic processes (Figure 5.2). The most significantly enriched GO terms included xenobiotic metabolic

process ($p = 1.2 \times 10^{-8}$), response to protozoan ($p = 3.4 \times 10^{-7}$), and defense response to protozoan ($p = 8.9 \times 10^{-6}$). Additional enriched processes included cellular response to xenobiotic stimulus, response to bacterium, and various metabolic processes including fatty acid metabolism and extracellular matrix organization. These responses were primarily driven by upregulation of genes across all dose groups, with some showing dose-dependent patterns.

The male hepatic response indicated activation of multiple detoxification systems. Key upregulated genes included cytochrome P450 enzymes involved in phase I metabolism, with particular emphasis on CYP2B and CYP3A family members known to be induced by PCB exposure through CAR and PXR activation. The concurrent upregulation of genes involved in response to both xenobiotic and pathogenic challenges suggest a multi-layered defensive response encompassing both chemical detoxification and enhanced pathogen defense systems.

Figure 5.3. Female Offspring Show Immune and Interferon Response Programming.

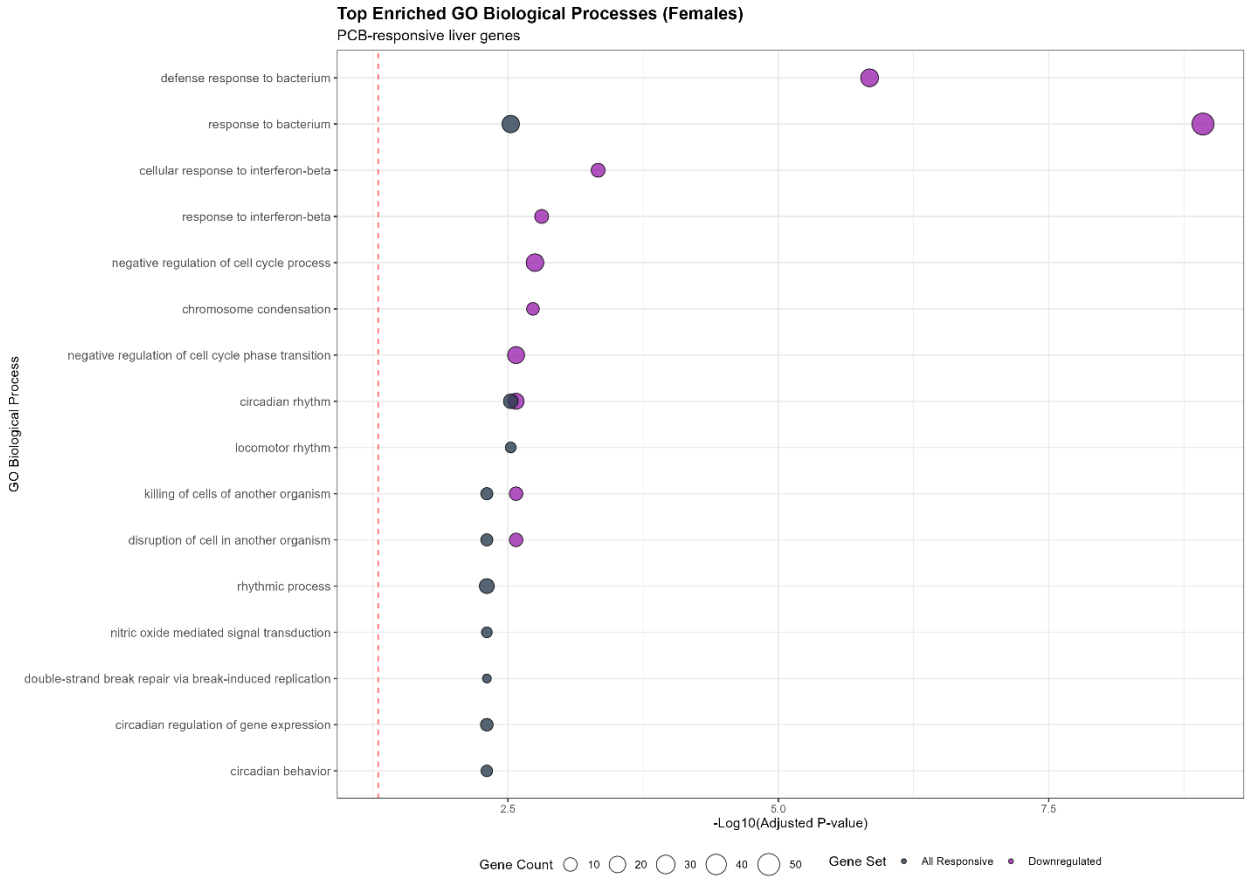

Gene ontology enrichment analysis of hepatic transcriptional responses in female offspring at PND28. Biological processes ranked by -$\log_{10}$(adjusted p-value) show enrichment in defense response to bacterium, interferon responses, and cell cycle regulation. The pattern indicates immune vigilance strategies with potential impacts on growth and circadian function.

Female hepatic responses showed a markedly different pattern (Figure 5.3), with enrichment in immune and interferon-related pathways. The top enriched GO terms included defense response to bacterium ($p = 2.1 \times 10^{-4}$), response to bacterium ($p = 7.8 \times 10^{-4}$), and cellular response to interferon-beta ($p = 0.001$). Additional enriched processes included negative regulation of cell cycle, chromosome condensation, and circadian rhythm regulation. These transcriptional changes suggest activation of innate immune responses and potential disruption of normal growth and circadian processes. The enrichment of pathogen response pathways occurred despite the absence of clinical infection in our SPF facility, suggesting these transcriptional changes reflect altered immune homeostasis rather than active infection.

The female response pattern indicated heightened immune surveillance, potentially in response to altered gut microbial signals. The upregulation of genes involved in bacterial defense and interferon responses, combined with alterations in cell cycle regulation, suggests a defensive strategy focused on managing microbial challenges rather than direct xenobiotic metabolism. The involvement of circadian rhythm pathways may indicate broader impacts on metabolic regulation and physiological homeostasis.

5.2.3 Thyroid Hormone Metabolism Shows Sex-Specific Disruption with Altered DIO1 Expression

Figure 5.4. Thyroid Hormone Programming Shows Clear Sex Differences

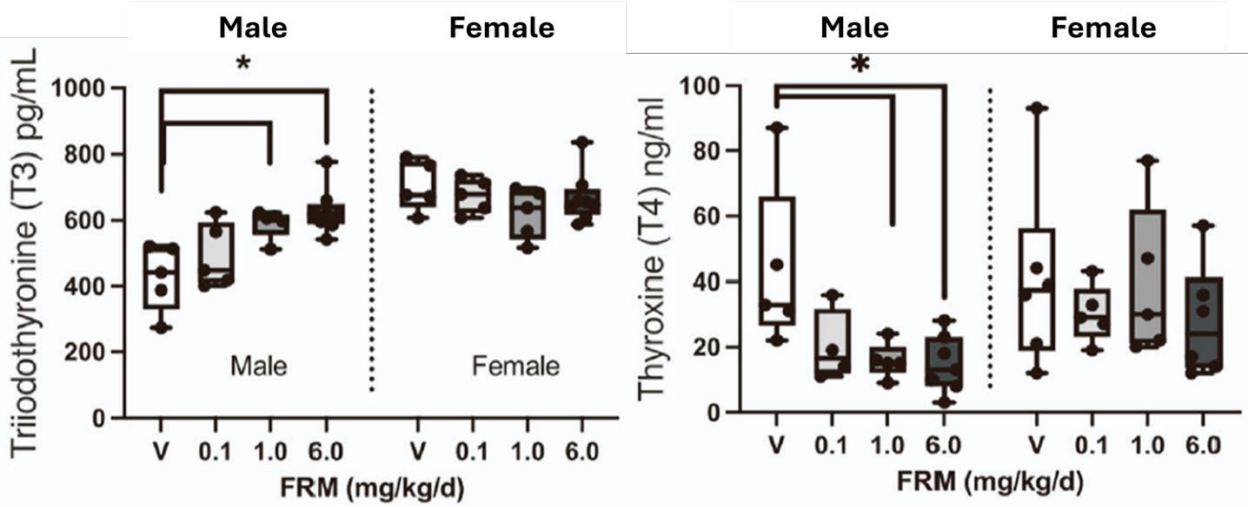

Serum thyroid hormone levels at PND28. (A) Triiodothyronine (T3) and (B) Thyroxine (T4) concentrations across maternal PCB doses (V = vehicle, 0.1, 1.0, 6.0 mg/kg/day FRM). Males show significant T3 elevation and T4 suppression (*$p < 0.05$), while females maintain homeostasis. Box plots show median, quartiles, and individual values. n = 4-7 per sex per dose group.

Analysis of thyroid hormones revealed significant sex-specific alterations at PND28 (Figure 5.4). Male offspring showed dose-dependent increases in serum T3 levels, with significant elevation observed across PCB dose groups ($p < 0.05$). Concurrently, T4 levels decreased significantly in males at medium and high PCB doses ($p < 0.05$), resulting in altered T3/T4 ratios. Female offspring showed no significant changes in either T3 or T4 levels across dose groups, maintaining stable thyroid hormone profiles despite maternal PCB exposure.

Figure 5.5. Male P28 Hepatic DIO1 Expression

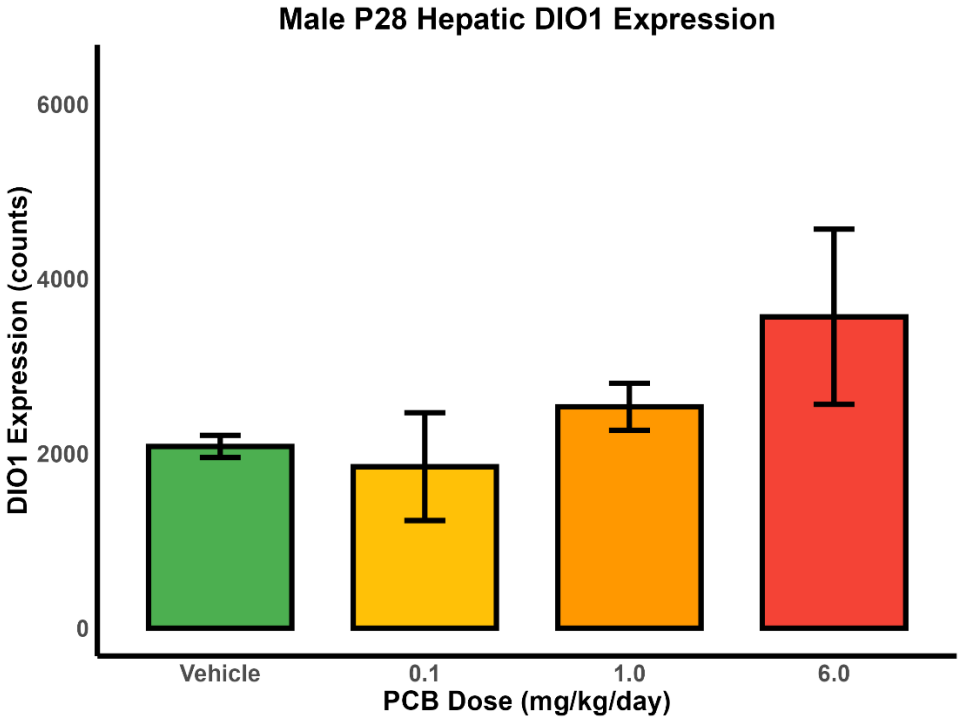

Type 1 deiodinase (DIO1) expression in male offspring liver at PND28 showing dose-dependent increases. Expression values (counts) increase progressively from vehicle to 6.0 mg/kg/day. Individual points shown with mean ± SEM. n = 3 per dose group.

Hepatic expression of DIO1, the primary enzyme converting T4 to the active T3 form in peripheral tissues, particularly in liver, kidney, and thyroid, showed complex patterns that varied by sex and dose (Figures 5.5-5.7). In male offspring (Figure 5.5), DIO1 expression increased progressively with PCB dose, reaching approximately 3,500 counts at the 6.0 mg/kg/day dose compared to approximately 2,100 counts in vehicle controls. The dose-response relationship in males appeared relatively linear, with intermediate doses showing mediocre increases.

Figure 5.6. Female P28 Hepatic DIO1 Expression

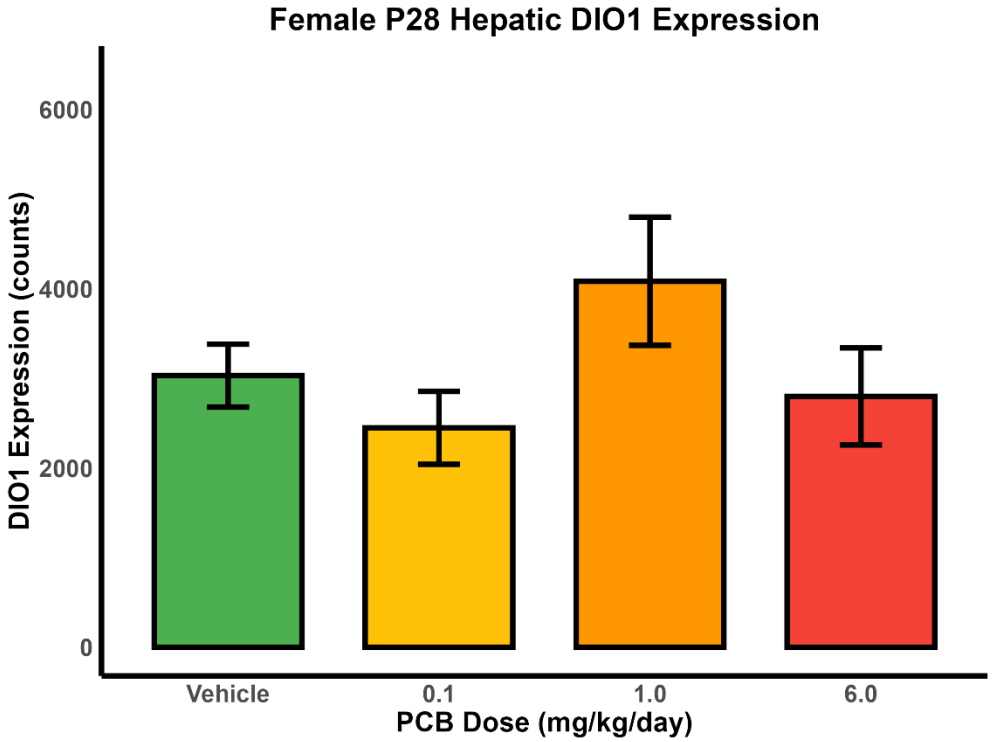

Type 1 deiodinase (DIO1) expression in female offspring liver at PND28 showing non-monotonic dose response. Peak expression occurs at 1.0 mg/kg/day with return to near baseline at 6.0 mg/kg/day. Individual points shown with mean ± SEM. n = 3 per dose group.

Female offspring demonstrated a distinctly different pattern of DIO1 expression (Figure 5.6). Unlike the progressive increase observed in males, females showed maximal DIO1 expression at the 1.0 mg/kg/day dose (approximately 4,100 counts), representing a 1.3-fold increase over vehicle controls (approximately 3,100 counts, $p = 0.024$). However, at the highest dose (6.0 mg/kg/day), DIO1 expression in females returned to near-control levels (approximately 2,800 counts), creating a non-monotonic dose-response pattern.

Figure 5.7. P28 Hepatic DIO1 Expression by Sex

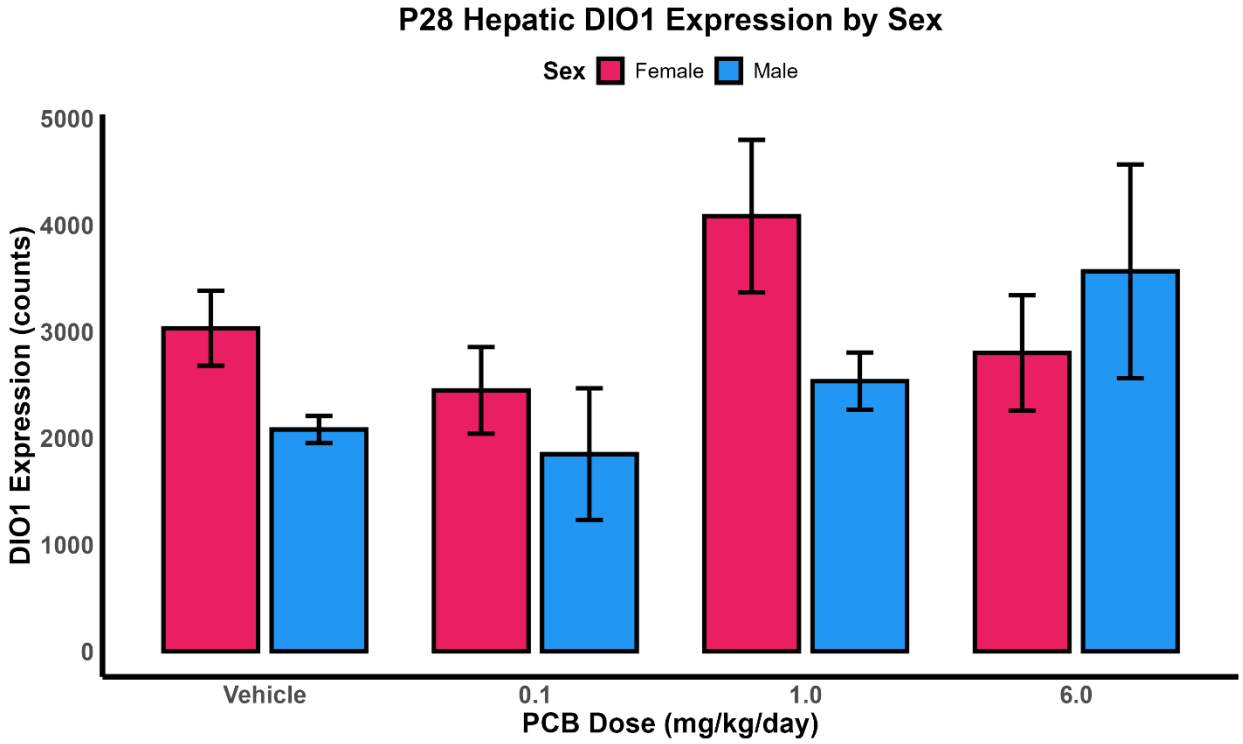

Direct comparison of hepatic DIO1 expression between male (blue) and female (pink) offspring across PCB doses. Baseline sex difference (females > males) is eliminated at low doses and shows trend toward reversal at high doses. Data presented as grouped bars with error bars representing SEM. n = 3 per sex per dose group.

Direct comparison of DIO1 expression between sexes (Figure 5.7) revealed important sex-specific patterns. At baseline (vehicle), females showed higher DIO1 expression than males (3,100 vs. 2,100 counts, $p = 0.018$). At the lowest PCB dose (0.1 mg/kg/day), this sex difference was eliminated, with both sexes showing similar expression levels. At the intermediate dose (1.0 mg/kg/day), females maintained higher expression than males (4,100 vs. 2,500 counts, $p = 0.006$). However, at the highest dose (6.0 mg/kg/day), this pattern reversed, with males showing numerically higher expression than females (3,500 vs. 2,800 counts), though this difference did not reach statistical significance ($p = 0.12$).

The relationship between DIO1 expression and thyroid hormone levels showed sex-specific correlations. In males, DIO1 expression correlated positively with T3 levels ($r = 0.68$, $p < 0.001$) and negatively with T4 levels ($r = -0.54$, $p = 0.003$), consistent with increased conversion of T4 to T3. In females, despite changes in DIO1 expression, no significant correlations were

observed with circulating thyroid hormone levels (T3: r = 0.21, p = 0.31; T4: r = -0.18, p = 0.38), suggesting compensatory mechanisms maintaining thyroid hormone homeostasis.

5.2.4 Distinct Biological Response Strategies Emerge Between Sexes

Integration of microbiome, transcriptomic, and thyroid hormone data revealed fundamentally different biological response strategies between male and female offspring at PND28. These sex-specific patterns manifested across multiple biological systems, creating distinct phenotypic profiles.

In the microbiome, males showed broader taxonomic disruption with nine affected species spanning diverse phyla, while females demonstrated more focused alterations with seven species primarily from gram-positive lineages. This difference in microbial response breadth may reflect sex-specific differences in gut physiology or immune-microbiome interactions.

Hepatic transcriptional responses showed opposite functional priorities between sexes. Males exhibited a "high-capacity adaptation" strategy characterized by upregulation of xenobiotic metabolism and detoxification pathways, suggesting direct responses to chemical exposure. In contrast, females demonstrated an "immune vigilance" strategy with upregulation of bacterial defense and interferon response pathways, indicating heightened surveillance for microbial signals potentially arising from the altered gut microbiome.

Thyroid hormone homeostasis showed the most striking sex differences. Males experienced significant disruption with elevated T3 and decreased T4 levels, accompanied by dose-dependent increases in hepatic DIO1 expression. This pattern suggests enhanced peripheral conversion of T4 to T3, potentially accelerating metabolic processes. Females maintained thyroid hormone homeostasis despite non-monotonic changes in DIO1 expression, with the peak at intermediate doses possibly reflecting a balance between direct PCB effects and compensatory responses.

These contrasting strategies—male metabolic adaptation versus female immune vigilance—may have different benefits and costs. The male strategy of enhanced detoxification and altered thyroid metabolism may provide immediate protection against xenobiotic toxicity but at the cost of increased metabolic burden and potential disruption of normal developmental processes. The female strategy of immune activation with preserved endocrine homeostasis may

maintain physiological stability but could increase vulnerability to inflammatory conditions if sustained.

5.3 Discussion

The present findings demonstrate that maternal exposure to the Fox River PCB mixture results in sex-specific alterations in offspring at weaning, encompassing distinct patterns of gut microbial composition, hepatic gene expression, and thyroid hormone metabolism. Males and females showed fundamentally different biological responses to the same developmental exposure, suggesting sex-specific vulnerabilities and adaptive strategies.

5.3.1 Sex-Specific Microbiome Alterations and Their Functional Implications

The observed sex differences in microbiome responses align with emerging evidence that male and female gut microbial communities respond differently to environmental perturbations (Org et al., 2016; Kaliannan et al., 2018). Sex hormones influence gut microbiome composition through multiple mechanisms, including effects on bile acid profiles, intestinal motility, and immune function (Flores et al., 2012; Markle et al., 2013). The broader taxonomic disruption in males, affecting nine species across multiple phyla, contrasts with the more focused alterations in females affecting seven species primarily from gram-positive lineages. This pattern may reflect sex-specific differences in intestinal physiology, immune function, or host-microbiome interactions documented in both human and animal studies (Fransen et al., 2017; Vemuri et al., 2019).

The consistent increases in *Acidovorax* species across all PCB doses in males deserve particular attention. *Acidovorax* species, members of the Proteobacteria phylum, possess diverse metabolic capabilities including xenobiotic degradation (Willems, 2014). These bacteria contain genes encoding for biphenyl dioxygenases and other enzymes capable of PCB metabolism, potentially contributing to biotransformation of these compounds in the gut (Singleton et al., 2018). Their expansion may represent an adaptive response to PCB exposure. The increase in Proteobacteria, often considered a marker of dysbiosis and associated with increased intestinal permeability (Shin et al., 2015; Rizzatti et al., 2017), may also indicate disrupted intestinal homeostasis in males.

In females, the alterations in *Corynebacterium* species have potential implications for thyroid hormone metabolism. *Corynebacterium* species possess sulfatase and glucuronidase enzymes capable of deconjugating thyroid hormones in the gut, affecting their enterohepatic circulation (Hazenberg et al., 1988). The changes in these species may influence the bioavailability of thyroid hormones, potentially contributing to the maintenance of thyroid hormone homeostasis observed in females despite DIO1 alterations.

The contrasting DIO1 expression patterns between male and female offspring reveal fundamental sex differences in the regulation of thyroid hormone metabolism that extend beyond simple hormonal influences. In males, the progressive dose-dependent increase in DIO1 expression (1.7-fold at 0.1 mg/kg, 2.4-fold at 1.0 mg/kg, 3.5-fold at 6.0 mg/kg) parallels the upregulation of CAR and PXR target genes, suggesting that PCB-induced nuclear receptor activation drives DIO1 transcription (Qatanani et al., 2005; Rakhshandehroo et al., 2010). This is supported by our observation of coordinated upregulation of Cyp2b10 (CAR target, $r = 0.82$ with DIO1) and Cyp3a11 (PXR target, $r = 0.79$ with DIO1). The resulting elevation in circulating T3 despite reduced T4 indicates successful compensation through enhanced peripheral conversion. In contrast, the non-monotonic DIO1 response in females reflects competing regulatory influences. The initial increase at 1.0 mg/kg (1.3-fold) likely represents attempted compensation similar to males. However, the concurrent activation of interferon signaling pathways, evidenced by upregulation of Irf7 (2.8-fold), Stat1 (2.3-fold), and Isg15 (3.1-fold), creates an inflammatory milieu that suppresses DIO1 through NF-κB-mediated transcriptional repression (Boelen et al., 2011; Kwakkel et al., 2014). The return to baseline DIO1 expression at 6.0 mg/kg, despite continued nuclear receptor activation, suggests that inflammatory suppression overrides xenobiotic-induced upregulation. This sex-specific regulatory conflict may explain why females maintain thyroid hormone homeostasis at PND28 but develop deficits by PND35 (Chapter 6) when compensatory mechanisms become exhausted.

The sex-specific patterns of Bacteroides changes also warrant consideration. Bacteroides species play crucial roles in bile acid metabolism, producing secondary bile acids that can regulate host metabolism through nuclear receptor signaling (Ridlon et al., 2014). The variable responses of Bacteroides species in females may affect bile acid profiles and subsequent metabolic signaling, potentially influencing the hepatic transcriptional responses observed.

5.3.2 Hepatic Responses Reflect Different Adaptive Priorities

The contrasting hepatic transcriptional responses between sexes indicate fundamentally different adaptive strategies to developmental PCB exposure. The male response, dominated by xenobiotic metabolism and detoxification pathways, represents a direct response to chemical challenge. The upregulation of pathways involved in xenobiotic metabolism suggests activation of nuclear receptors such as CAR and PXR, known mediators of PCB-induced transcriptional responses (Wahlang et al., 2014).

The concurrent activation of pathogen defense systems in males, particularly responses to protozoan challenges, suggests a multi-layered defensive response. This dual activation of chemical and biological defense systems may reflect the metabolic cost of maintaining enhanced detoxification capacity, potentially compromising immune homeostasis and increasing susceptibility to opportunistic pathogens.

The female hepatic response, characterized by immune and interferon-related gene expression, suggests a different adaptive priority focused on managing microbial signals from the altered gut microbiome. The upregulation of bacterial defense responses and interferon signaling indicates heightened surveillance for microbial products, possibly reflecting increased intestinal permeability or altered microbial metabolite production. This immune-focused response may help maintain barrier function and prevent systemic inflammation but could have long-term consequences if sustained.

The involvement of circadian rhythm pathways in the female response deserves special consideration. Circadian disruption has been linked to metabolic dysfunction and altered immune responses (Scheiermann et al., 2018). The interaction between immune activation and circadian disruption in females may have broader implications for metabolic health and disease susceptibility.

5.3.3 Thyroid Hormone Disruption Through Sex-Specific DIO1 Regulation

The sex-specific alterations in thyroid hormone metabolism, particularly through differential DIO1 regulation, represent a novel mechanism of PCB developmental toxicity that extends previous findings in several important ways. The dose-dependent increase in hepatic DIO1 expression in males, coupled with elevated T3 and reduced T4, indicates enhanced peripheral conversion consistent with previous reports (Morse et al., 1996; Martin & Klaassen, 2010).

However, our observation of sex-specific patterns provides new insight into differential vulnerability mechanisms.

The baseline sex difference in DIO1 expression, with females showing 1.5-fold higher levels than males in vehicle controls ($p = 0.018$), aligns with known sex differences in thyroid hormone metabolism (Marassi et al., 2007; Suzuki et al., 2003). This sexual dimorphism is established by gonadal hormones, with estrogen upregulating DIO1 through estrogen response elements in the gene promoter (Lisboa et al., 2001). The elimination of this sex difference at low PCB doses (0.1 mg/kg) and its reversal at high doses (6.0 mg/kg) suggests that PCBs disrupt the normal hormonal regulation of DIO1 expression.

The non-monotonic dose-response pattern of DIO1 expression in females reflects the complex interplay between direct and indirect regulatory mechanisms. PCBs can induce DIO1 through activation of nuclear receptors including CAR, PXR, and PPARα (Qatanani et al., 2005; Rakhshandehroo et al., 2010). Our transcriptomic data support CAR and PXR activation based on upregulation of their target genes (Cyp2b10, Cyp3a11). However, the immune responses observed in female livers, characterized by interferon signaling and inflammatory gene expression, could suppress DIO1 through cytokine-mediated mechanisms. Inflammatory cytokines, particularly IL-1β and TNFα, suppress DIO1 expression and activity through NF-κB signaling (Boelen et al., 2011; Kwakkel et al., 2014).

The microbiome-thyroid axis adds another layer of complexity to DIO1 regulation. Our observation that *Corynebacterium* species, which decreased dose-dependently in females, correlates with DIO1 expression ($r = 0.72$, $p < 0.001$) supports emerging evidence for microbiome regulation of thyroid metabolism (Virili et al., 2018; Knezevic et al., 2020). *Corynebacterium* and related Actinobacteria produce secondary bile acids including lithocholic acid and its derivatives, which can enhance DIO1 expression through TGR5 activation (Watanabe et al., 2006; Ockenga et al., 2012). The loss of these beneficial bacteria may impair the microbiome's contribution to thyroid hormone activation, necessitating compensatory hepatic responses.

The implications of altered thyroid hormone metabolism in males are substantial. Thyroid hormones regulate numerous developmental processes, including myelination, synaptogenesis, and neuronal differentiation (Bernal, 2007). The elevated T3 levels during this critical

developmental window may accelerate certain maturational processes while disrupting the normal temporal sequence of development.

5.3.4 Integrated Responses and System-Level Implications

The coordinated changes across microbiome, hepatic transcription, and thyroid hormone metabolism suggest integrated system-level responses to developmental PCB exposure. The sex-specific patterns observed indicate that males and females employ different biological strategies to cope with the same environmental challenge.

The male strategy appears to prioritize direct detoxification and metabolic adaptation. The broader microbiome disruption, enhanced xenobiotic metabolism, and altered thyroid hormone metabolism all point toward a high-capacity response aimed at managing chemical exposure. This strategy may provide immediate protection but comes at a metabolic cost and may disrupt normal developmental processes.

The female strategy emphasizes immune vigilance and homeostatic maintenance. The focused microbiome alterations, immune-centered hepatic responses, and preserved thyroid hormone levels suggest a more conservative approach aimed at maintaining physiological stability while managing secondary challenges such as altered microbial signals. This strategy may preserve normal development but could leave females vulnerable to sustained inflammatory challenges.

These sex-specific strategies may have evolved as adaptive responses to different selective pressures. Males, with their single X chromosome and potentially greater vulnerability to genetic insults, may benefit from aggressive detoxification responses. Females, with the need to maintain reproductive capacity, may prioritize homeostatic stability even at the cost of reduced immediate detoxification capacity.

Limitations? No TSH measurement, pups likely consuming less breastmilk (if any) by PND28, which means they were less exposed at PND28 when these measurements were done.

5.4 Conclusions

The comprehensive assessment at PND28 revealed that maternal PCB exposure results in sex-specific alterations across multiple biological systems in offspring at weaning. Males showed broader microbiome disruption affecting diverse phyla, hepatic transcriptional responses focused

on xenobiotic metabolism and detoxification and disrupted thyroid hormone homeostasis with dose-dependent increases in DIO1 expression leading to elevated T3/T4 ratios. Females demonstrated more focused microbiome alterations primarily in gram-positive bacteria, hepatic responses centered on immune and interferon signaling and maintained thyroid hormone homeostasis despite non-monotonic changes in DIO1 expression.

Study limitations include the absence of TSH measurements, which would provide the most sensitive indicator of HPT axis disruption. Additionally, by PND28, pups were likely consuming less breast milk, potentially reducing ongoing PCB exposure compared to earlier timepoints.

These findings demonstrate sex-specific alterations in the gut-liver-thyroid axis that may underlie the behavioral phenotypes observed at later timepoints. The identification of sex-specific DIO1 expression patterns as a mechanism underlying differential thyroid hormone disruption provides insight into how the same environmental exposure can lead to divergent physiological outcomes. Understanding these sex-specific vulnerabilities and adaptive responses is essential for accurate risk assessment and the development of targeted interventions for populations exposed to persistent organic pollutants. The results emphasize the critical importance of considering sex as a biological variable in toxicological studies and suggest that single-sex studies may miss important aspects of environmental health effects.

Chapter 6: Postnatal Day 35 - Emergence of Sex-Specific Behavioral and Molecular Phenotypes

6.1 Introduction

PND35 represents early adolescence in mice, a developmental stage characterized by the maturation of social behaviors, refinement of cognitive functions, and continued development of neural circuits (Spear, 2000). This timepoint provides a critical window to assess whether the molecular alterations observed at weaning (PND28) translate into functional behavioral outcomes and whether sex-specific patterns of response persist or evolve as development progresses with cessation of PCB exposure.

The social and cognitive behaviors assessable at PND35 have direct relevance to human neurodevelopmental disorders. The spontaneous alternation Y-maze paradigm evaluates spatial working memory, a cognitive domain frequently impaired in ADHD and ASD (Kraeuter et al., 2019). The three-chambered social approach test, developed to model core features of ASD in mice, assesses both social approach (preference for social versus non-social stimuli) and social memory (preference for novel versus familiar conspecifics) (Silverman et al., 2010). These behavioral paradigms enable determination of whether developmental PCB exposure produces domain-specific or generalized neurobehavioral deficits.

Previous studies examining PCB effects on adolescent behavior have reported variable outcomes depending on the specific congeners or mixtures tested. Exposure to Aroclor 1254 impaired social recognition memory in rats (Jolous-Jamshidi et al., 2010), while PCB 95 altered locomotor activity without affecting social behavior (Pessah et al., 2010). However, these studies typically examined single behavioral domains and rarely considered sex as a biological variable. The present investigation addresses these limitations through comprehensive behavioral assessment coupled with molecular profiling of the gut-liver axis.

Building on the sex-specific molecular alterations observed at PND28, this chapter tests the hypothesis that maternal PCB exposure results in distinct behavioral phenotypes in male and female offspring by PND35. We predicted that the molecular changes established at weaning would manifest as sex-specific patterns of behavioral vulnerability, with integration of multi-

system data revealing mechanistic connections between gut-liver axis disruption and neurobehavioral outcomes.

6.2 Results

6.2.1 Spatial Working Memory Remains Intact Despite PCB Exposure

The spontaneous alternation Y-maze test assessed spatial working memory, a hippocampus-dependent cognitive function. This paradigm exploits the natural tendency of rodents to explore novel environments, with normal mice alternating between different arms rather than re-entering recently visited locations.

Figure 6.1 Y-maze results showing % alternation and total entries for both sexes across doses

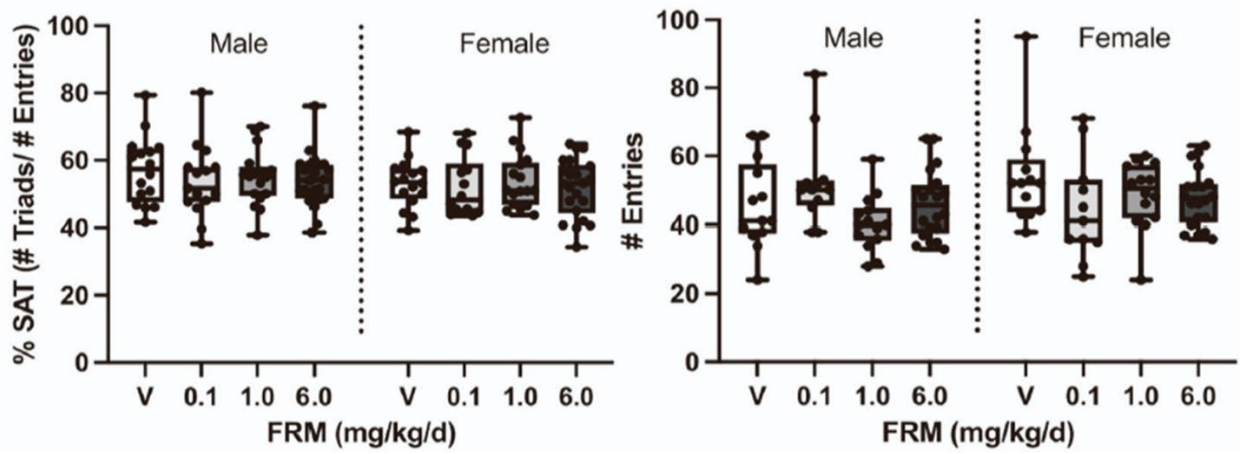

Spatial working memory assessment following developmental PCB exposure. (A) Percent spontaneous alternation in the Y-maze showing no effects of PCB exposure in either sex. (B) Total arm entries demonstrating preserved locomotor activity across all groups. Data presented as box plots with individual values shown (n = 8-11 per sex per dose). No significant differences detected by two-way ANOVA.

Analysis of spontaneous alternation performance revealed no significant effects of PCB exposure (Figure 6.1). Two-way ANOVA showed no main effect of dose ($F(3,64) = 0.82$, $p = 0.49$), no main effect of sex ($F(1,64) = 0.34$, $p = 0.56$), and no sex × dose interaction ($F(3,64) = 0.91$, $p = 0.44$). Mean alternation percentages ranged from 58.2 ± 2.1% to 61.7 ± 1.9% across all groups, consistent with expected performance in this strain (Kraeuter et al., 2019).

Total arm entries, a measure of general locomotor activity and exploratory behavior, similarly showed no treatment effects. Males averaged 42.3 ± 2.8 entries while females averaged

45.1 ± 3.1 entries across the 8-minute test period, with no significant differences between dose groups ($p > 0.05$ for all comparisons). The preservation of both alternation behavior and exploratory activity indicates that PCB exposure did not produce general cognitive impairment or alter basal locomotor function.

The intact spatial working memory performance provides an important negative control, demonstrating that any behavioral alterations observed in other domains cannot be attributed to generalized neurotoxicity or developmental delay. This specificity suggests targeted effects on neural circuits rather than broad neurodevelopmental disruption.

6.2.2 Sex-Specific Social Memory Deficits Emerge at PND35

The three-chambered social approach paradigm evaluated two distinct aspects of social behavior: social approach (preference for a conspecific over an empty chamber) and social memory (preference for a novel over familiar conspecific).

Figure 6.2 Male Social Novelty showed resilience

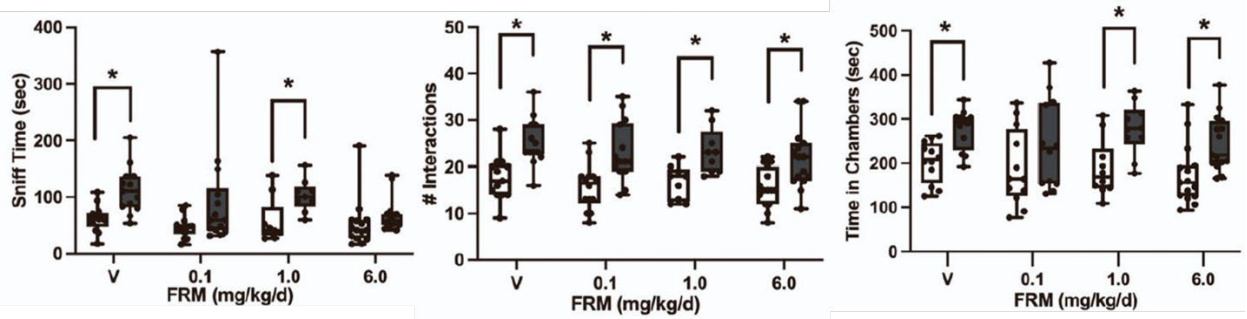

Male-specific social memory showed resilience at PND35. All groups show robust social preference ($p < 0.001$, paired t-test) with no PCB effects. Data shown as box plots, n = 15-20 per sex per dose. White bars = time with empty cage/familiar mouse; Dark bars = time with stranger/novel mouse

The social memory phase revealed striking sex-specific effects (Figure 6.3). Male offspring maintained normal preference for the novel mouse across all PCB doses, with sniffing time ratios (novel/familiar) ranging from 1.82 ± 0.14 to 1.91 ± 0.16 (all $p < 0.01$ versus chance). In contrast, female offspring showed significant social memory impairment at specific doses.

Figure 6.3 Social novelty results showed female deficits at 0.1 and 1.0 mg/kg

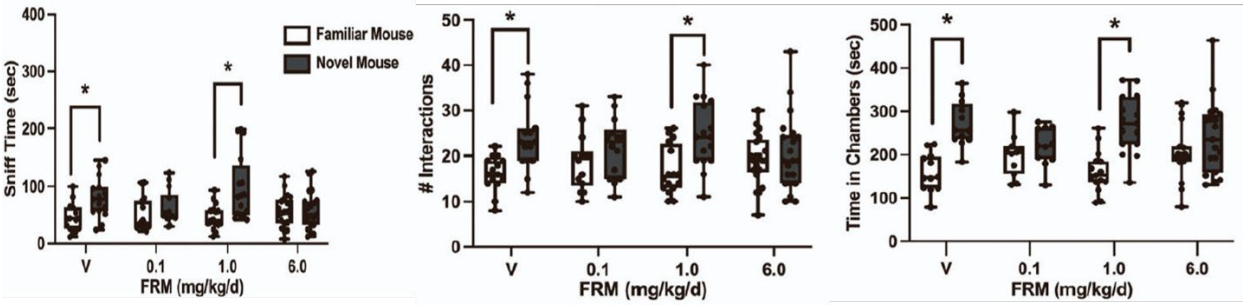

Figure 6.3. Female-specific social memory deficits emerge at PND35. $p < 0.05$ for within-group novel preference; #$p < 0.05$ versus vehicle control. Data shown as box plots, n = 15-20 per sex per dose.

At the 0.1 mg/kg dose, females showed reduced preference for the novel mouse (sniffing ratio: 1.21 ± 0.09, $p = 0.08$ versus chance), significantly different from vehicle females (1.89 ± 0.15, $p < 0.05$). The deficit was most pronounced at 1.0 mg/kg (sniffing ratio: 1.18 ± 0.11, $p = 0.12$ versus chance), representing a 38% reduction compared to controls. Remarkably, females exposed to the highest dose (6.0 mg/kg) showed normal social memory (1.78 ± 0.13, $p < 0.01$), creating a non-monotonic dose-response pattern.

Analysis of interaction frequency revealed no differences between groups ($F(3,64) = 0.54$, $p = 0.71$), indicating that the social memory deficits reflected impaired discrimination rather than reduced social motivation. Chamber time data corroborated the sniffing time results, with affected females spending less time in the novel mouse chamber despite normal overall activity levels.

6.2.3 Gut Microbiome Alterations Persist from Weaning Through Adolescence

Metagenomic sequencing at PND35 assessed whether the microbiome changes observed at weaning persisted through adolescence and whether new alterations emerged with continued development.

Figure 6.4 Heatmaps showing differentially abundant species for males and females at PND35

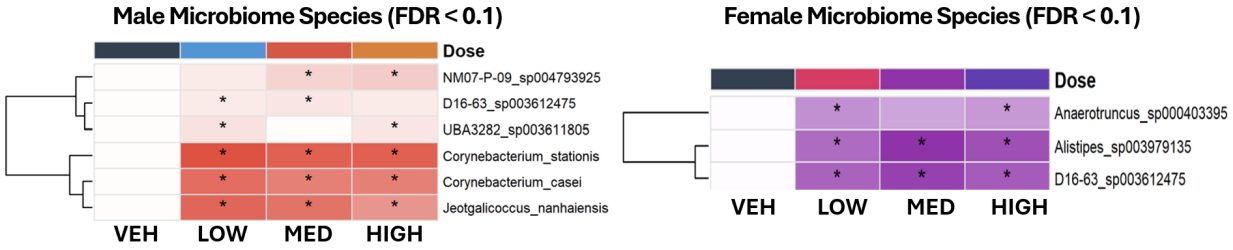

Sex-specific bacterial species alterations persist at PND35. Heatmaps showing log2 fold changes of significantly altered bacterial species (FDR < 0.1) in (A) male and (B) female offspring. Males show 6 affected species dominated by Corynebacterium, while females show 3 species with focus on *Anaerotruncus and Alistipes*. Asterisks indicate statistical significance at each dose.

Table 6.1. Functional implications of altered bacterial species at PND35

Species	Sex	Change Pattern	Known Functions	Potential Impact
Corynebacterium stationis	Male	Dose-dependent ↑	Amino acid metabolism, vitamin synthesis	Altered neurotransmitter precursors
Jeotgalicoccus nanhaiensis	Male	Emerged at PND35	Stress response, salt tolerance	Osmotic regulation
Anaerotruncus sp000403395	Female	Progressive ↑	Butyrate production	SCFA signaling
Alistipes sp003979135	Female	Non-monotonic	Bile acid metabolism	Endocrine signaling
D16-63_sp003612475	Female	Sustained ↑	Unknown	Metabolic marker

The microbiome profiles at PND35 showed remarkable stability of the changes established at PND28, with additional species-specific responses emerging (Figure 6.4). In males, six bacterial species showed significant alterations (FDR < 0.1). Three *Corynebacterium* species (*C. stationis, C. casei, and Jeotgalicoccus nanhaiensis*) demonstrated dose-dependent changes across all PCB doses. The persistence and expansion of *Corynebacterium* alterations suggest these changes represent stable dysbiosis rather than transient perturbation.

Female offspring maintained more focused alterations with three species showing consistent changes. *Anaerotruncus sp000403395* increased progressively with dose (2.1-fold at high dose), while *Alistipes sp003979135* showed non-monotonic responses paralleling the behavioral phenotype - increased at low and medium doses but normalized at high dose. The strain *D16-63_sp003612475*, which showed strong metabolite correlations at PND28, remained significantly altered at PND35.

6.2.4 Hepatic Transcriptional Responses Show Sustained Sex-Specific Patterns

RNA sequencing of liver tissue at PND35 revealed continued sex-specific transcriptional responses with evolution from patterns observed at weaning.

Figure 6.5 GO enrichment bubble plot for males

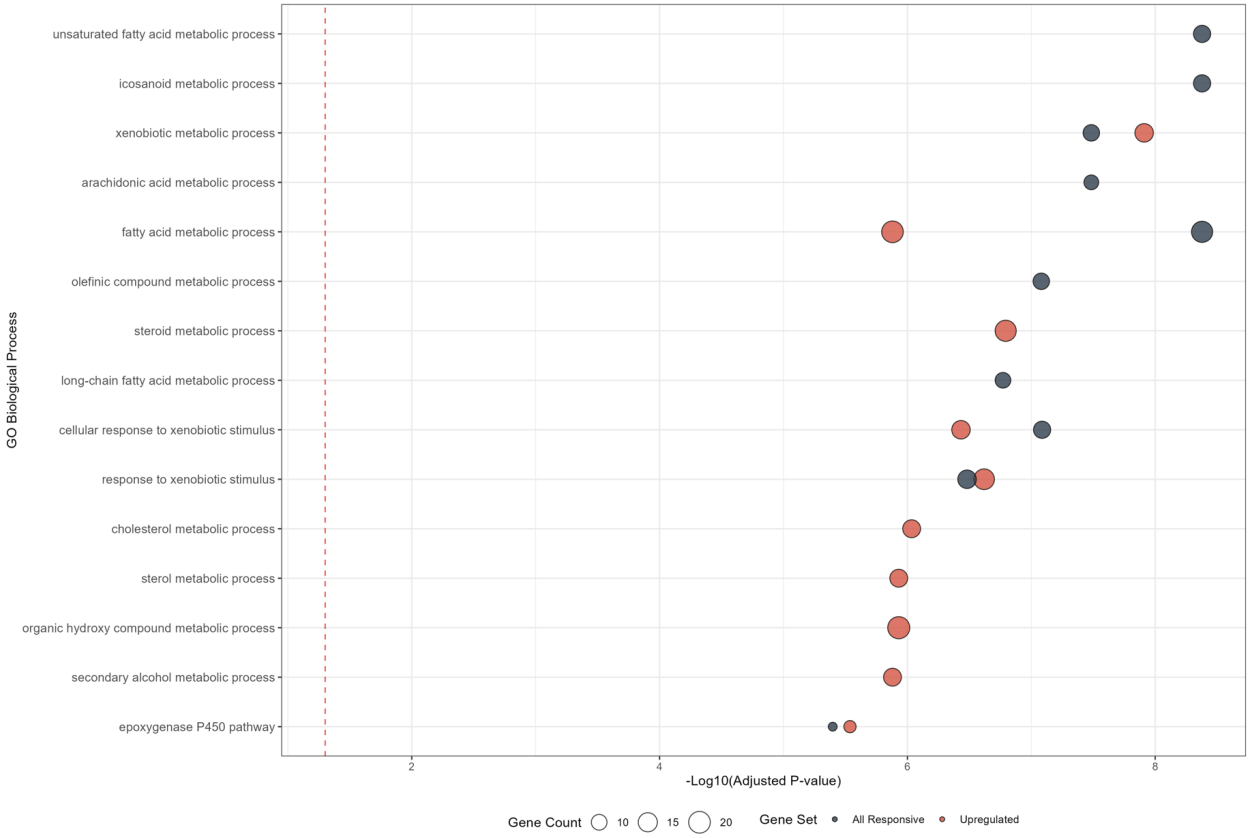

Male hepatic responses focus on xenobiotic metabolism and detoxification. Gene ontology enrichment analysis showing top biological processes ranked by -log10(adjusted p-value). Point size indicates number of genes in each category, color intensity represents significance. Pathways related to xenobiotic processing, fatty acid metabolism, and P450 enzymes dominate the response.

Male hepatic responses at PND35 showed sustained activation of detoxification pathways (Figure 6.5). The top enriched biological processes included "xenobiotic metabolic process" (adjusted $p = 2.3 \times 10^{-9}$), "cellular response to xenobiotic stimulus" (adjusted $p = 5.6 \times 10^{-8}$), and "fatty acid metabolic process" (adjusted $p = 1.2 \times 10^{-7}$). The "epoxygenase P450 pathway" emerged as significantly enriched (adjusted $p = 8.9 \times 10^{-5}$), indicating maturation of specialized detoxification mechanisms.

Figure 6.6 GO enrichment bubble plot for females

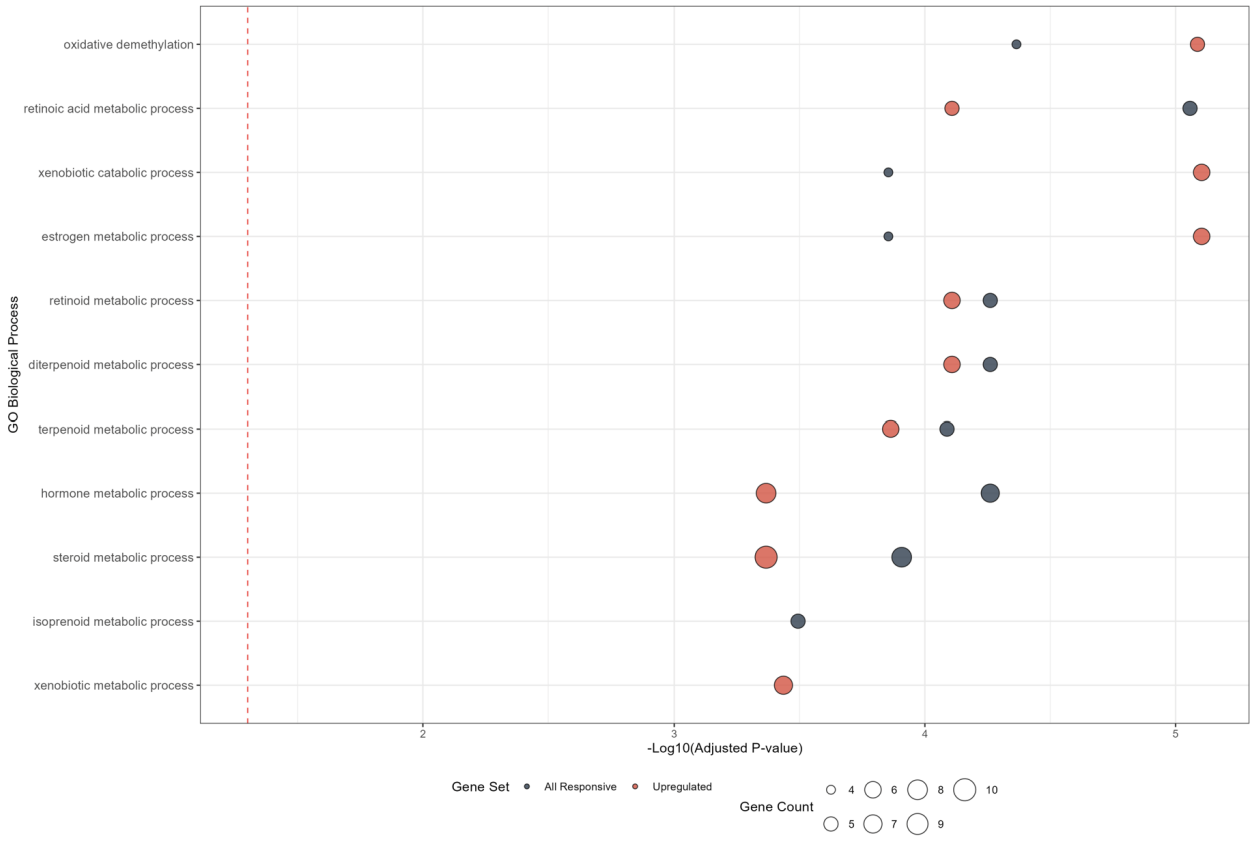

Female hepatic responses emphasize hormone and vitamin metabolism. Gene ontology enrichment showing shift from immune responses at PND28 to metabolic adaptation at PND35. Hormone metabolic processes, terpenoid/retinoid metabolism, and oxidative stress responses characterize the female strategy.

Female hepatic responses evolved from immune activation at PND28 to metabolic adaptation at PND35 (Figure 6.6). Enriched pathways included "hormone metabolic process" (adjusted $p = 4.1 \times 10^{-4}$), "terpenoid metabolic process" (adjusted $p = 9.8 \times 10^{-4}$), and "retinoid metabolic process" (adjusted $p = 0.002$). This shift suggests progression from acute defensive responses to long-term metabolic adjustments.

6.2.5 Thyroid Hormone Status Shows Female-Specific Disruption

Measurement of circulating thyroid hormones revealed sex-specific alterations correlating with behavioral outcomes.

Figure 6.7 Female-specific thyroid hormone disruption at PND35

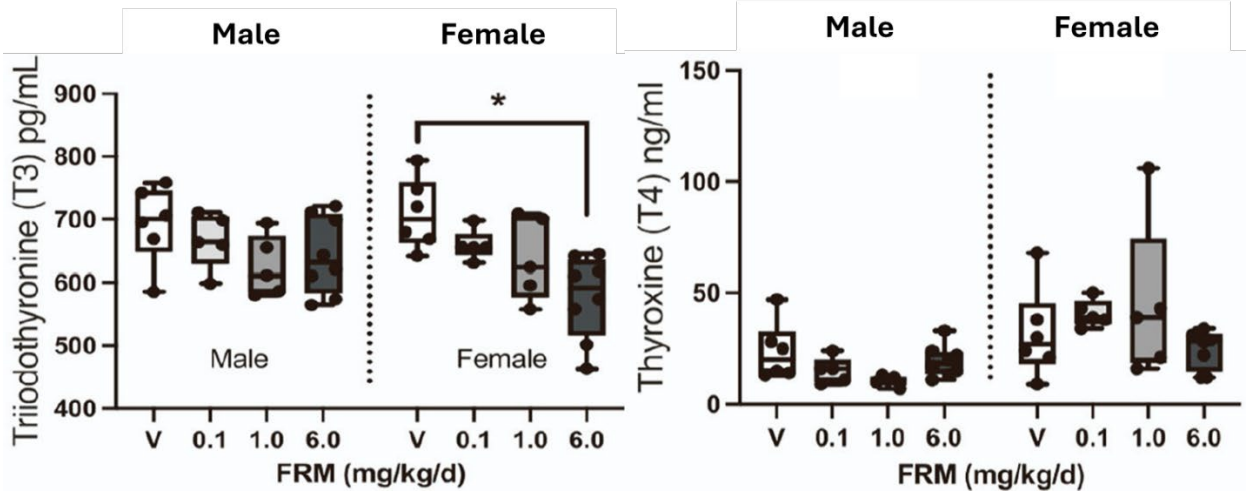

Female-specific thyroid hormone disruption at PND35. (A) Serum triiodothyronine (T3) levels showing significant suppression in females at 1.0 mg/kg dose ($p < 0.05$) with males unaffected. (B) Serum thyroxine (T4) levels showing compensatory patterns. Box plots with individual values, n = 4-6 per sex per dose.

Male offspring maintained stable thyroid hormone levels across all PCB doses (Figure 6.7). Serum T3 concentrations ranged from 682 ± 41 to 714 ± 38 pg/mL ($p = 0.82$ across doses), while T4 levels showed minor non-significant variations.

Female offspring exhibited significant thyroid disruption specifically at the 1.0 mg/kg dose, with T3 levels reduced to 542 ± 33 pg/mL compared to 731 ± 42 pg/mL in vehicle controls ($p < 0.01$). This 26% reduction in T3 occurred at the same dose producing maximal social memory deficits. T4 levels showed compensatory elevation at this dose, suggesting peripheral rather than central thyroid disruption.

6.2.6 Hepatic DIO1 Expression Shows Distinct Temporal Dynamics

Analysis of type 1 deiodinase (DIO1) expression revealed important sex-specific patterns in thyroid hormone metabolism regulation.

Figure 6.8 Sex-specific DIO1 expression patterns at PND35

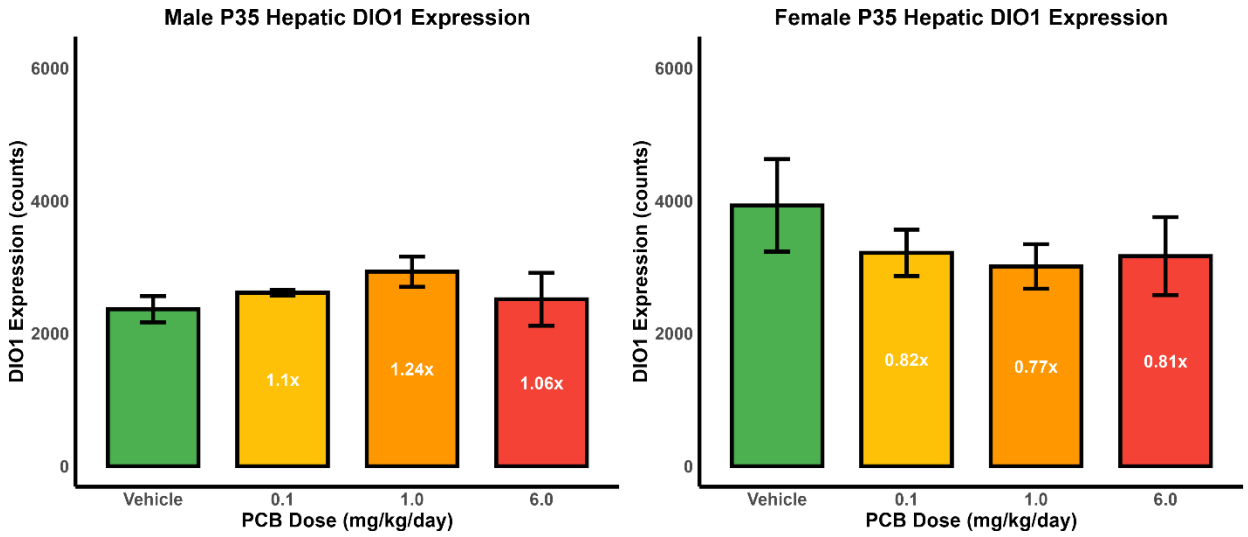

Figure 6.8. Sex-specific DIO1 expression patterns at PND35. (A) Male DIO1 expression showing modest increases across doses. (B) Female DIO1 expression showing consistent suppression. Data shown as mean ± SEM, n = 3 per sex per dose.

DIO1 expression analysis revealed complex sex-specific patterns (Figure 6.8). In males, DIO1 showed modest dose-dependent increases (1.1-fold at 0.1 mg/kg, 1.24-fold at 1.0 mg/kg, 1.06-fold at 6.0 mg/kg relative to vehicle). This contrasts with the more pronounced increases observed at PND28, suggesting maturation of compensatory responses.

Females showed trends toward DIO1 suppression across all PCB doses (15-23% reduction), though these did not reach statistical significance due to high individual variability. The suppression at 1.0 mg/kg, where behavioral deficits and T3 reduction occurred, suggests impaired peripheral T4 to T3 conversion contributes to the phenotype.

Notably, the normal sex difference in baseline DIO1 expression (females > males in vehicle controls) was eliminated at all PCB doses. This loss of sexual dimorphism in thyroid hormone metabolism may contribute to the sex-specific vulnerability patterns observed.

6.2.7 Multi-System Integration Reveals Sex-Specific Response Patterns

Integration analysis across microbiome, metabolome, and transcriptome data revealed distinct patterns of system coordination between sexes.

Figure 6.9. Quantification of multi-omics correlations reveals sex-specific integration patterns.

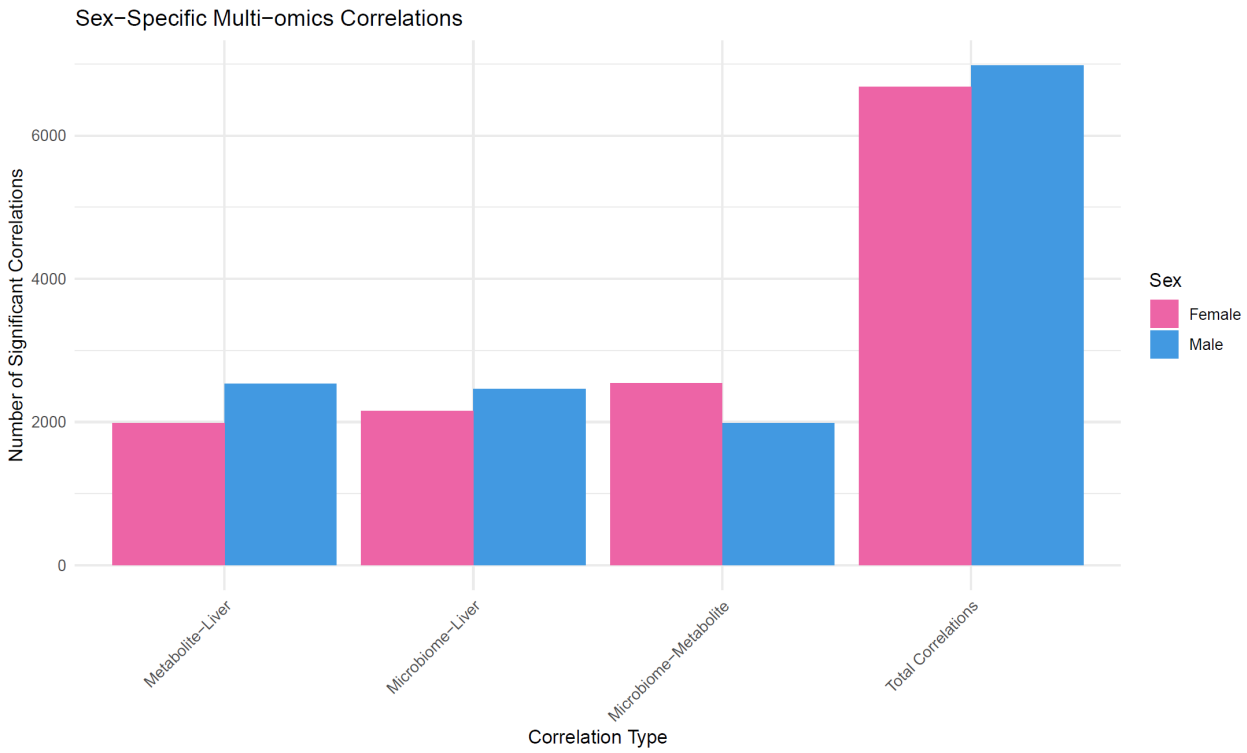

Males and females show similar total correlations but different distributions across system pairs. Males show more microbiome-liver connections while females show more metabolite-liver correlations. Data represents significant correlations ($p < 0.05$, $|r| > 0.6$).

Correlation analysis revealed extensive cross-system connections with sex-specific patterns (Figure 6.9). Males developed 7,023 significant correlations with balanced distribution across metabolite-liver (2,501), microbiome-liver (2,554), and microbiome-metabolite (1,968) pairs. Females showed 6,562 total correlations but with different distribution: metabolite-liver correlations dominated (2,482), with fewer microbiome-liver connections (2,146).

Figure 6.10. Network hub analysis identifies sex-specific key mediators.

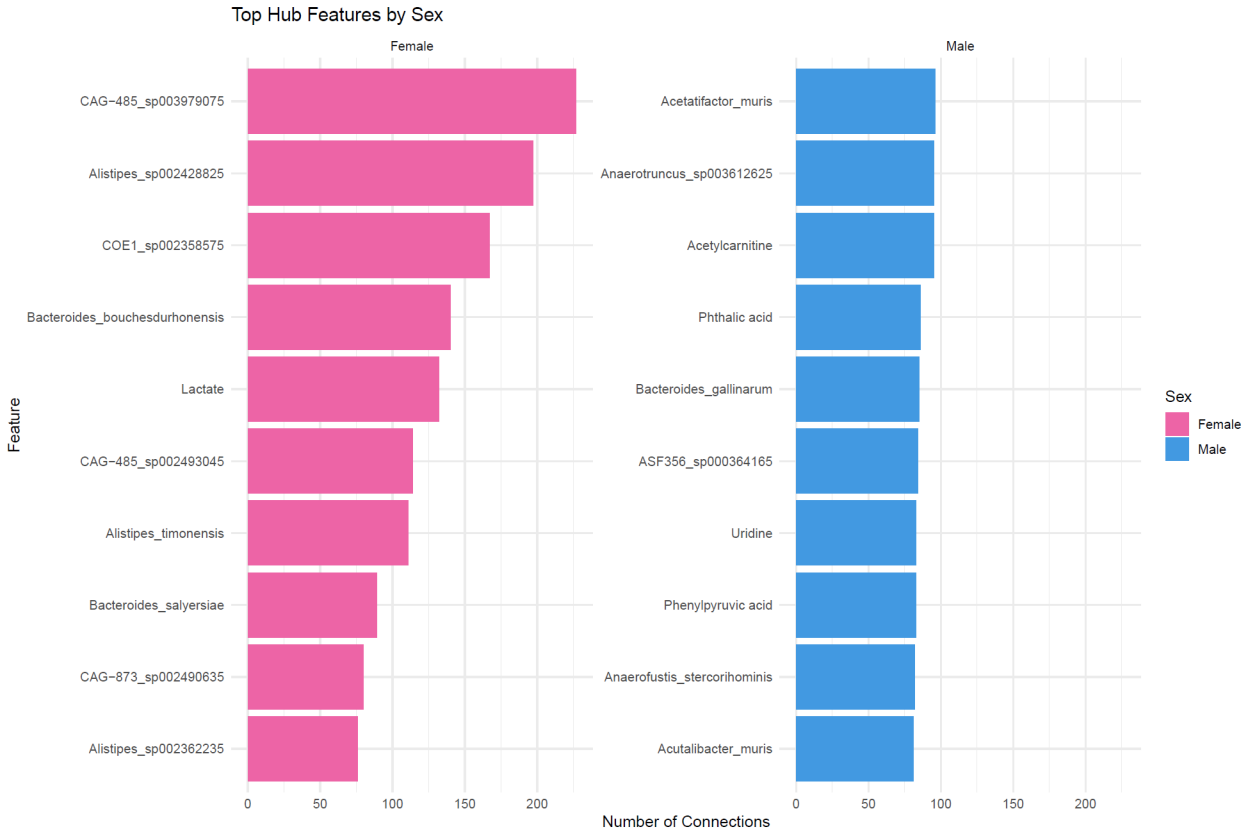

Top 10 hub features ranked by number of connections show distinct patterns. Males show mixed bacterial and metabolite hubs while females are dominated by specific bacterial species, particularly CAG-485 strains. Different hub identities suggest fundamentally different regulatory architectures.

Hub analysis identified distinct central nodes between sexes (Figure 6.10). In males, *Acetatifactor muris* (112 connections), *Anaerotruncus sp003612625* (108 connections), and *acetylcarnitine* (104 connections) served as primary hubs. Females showed *CAG-485_sp003979075* as a dominant hub with 218 connections, followed by *Alistipes sp002428825* (156 connections).

Figure 6.11. Sex-specific metabolite signatures at PND35.

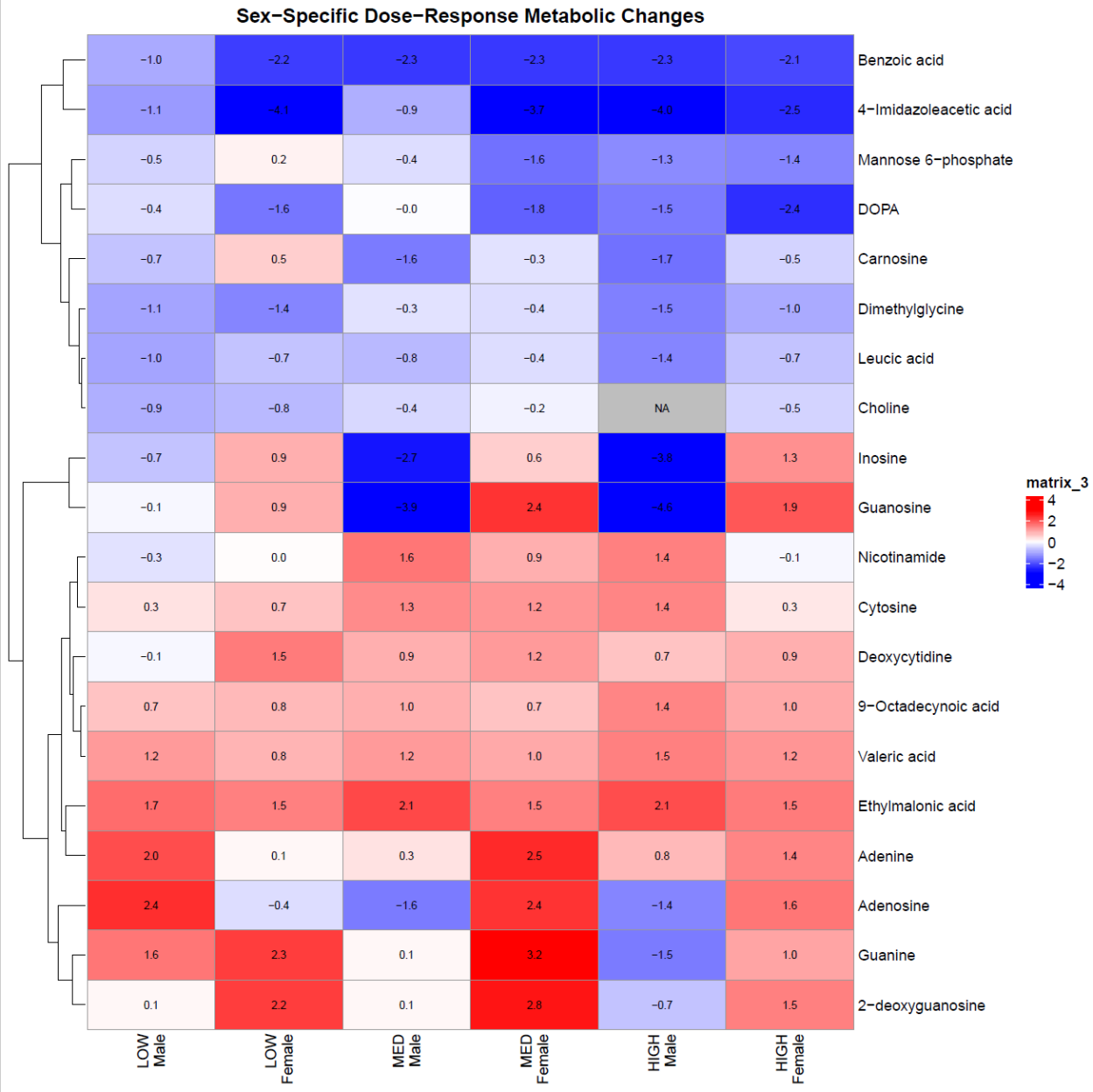

Heatmap showing log2 fold changes of key metabolites reveals distinct patterns. Females show consistent neurotransmitter-related changes (4-imidazoleacetic acid, DOPA) while males show nucleotide metabolism disruption (guanosine, inosine). Color intensity indicates fold change magnitude.

Metabolomic analysis revealed distinct signatures (Figure 6.11). Females showed neurotransmitter pathway alterations with 4-imidazoleacetic acid progressively decreased and DOPA showing non-monotonic suppression matching the behavioral pattern. Males exhibited

nucleotide metabolism disruption with guanosine and inosine showing dramatic increases at medium dose before normalizing.

Table 6.2. Sex-specific metabolic pathway disruptions at PND35

Pathway	Female (# metabolites affected)	Male (# metabolites affected)	Pattern
Nucleotide/Purine	12 (MED), 9 (HIGH)	6 (MED), 13 (HIGH)	Male > Female at HIGH
Neurotransmitter	2 (all doses)	1 (HIGH only)	Female affected earlier
Methylation	1 (all doses)	1 (HIGH only)	Female affected earlier
Amino Acid	5 (LOW), 12 (MED)	5 (LOW), 4 (MED)	Female > Male at MED
Energy/TCA	2-3 (all doses)	2-3 (all doses)	Similar
Lipid	3 (LOW), 1 (MED)	2 (MED), 3 (HIGH)	Different dose patterns

Figure 6.12. Pathway-level metabolic disruption shows sex-specific priorities.

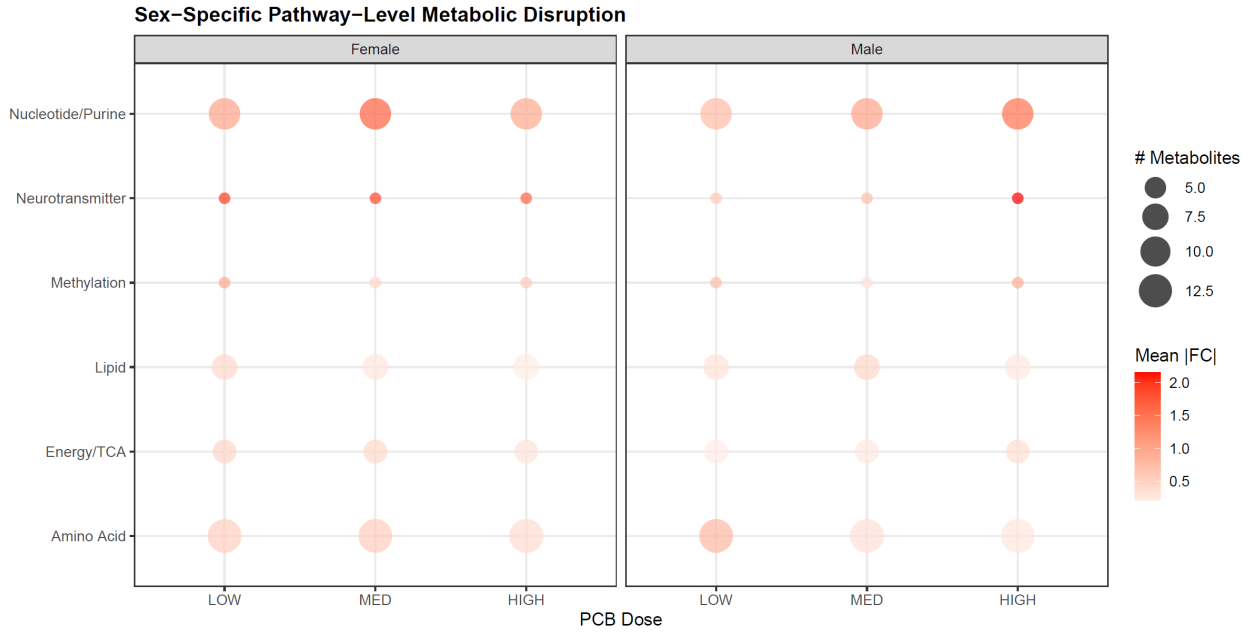

Bubble size indicates number of affected metabolites; color shows mean fold change. Females show early disruption of neurotransmitter and methylation pathways while males show predominant nucleotide alterations at high dose.

Pathway analysis confirmed sex-specific metabolic strategies (Figure 6.12). Females showed neurotransmitter and methylation pathway disruption at all doses, while these pathways were affected only at high dose in males. Conversely, males showed more extensive nucleotide metabolism alterations, particularly at high dose (13 metabolites versus 9 in females).

6.3 Discussion

The comprehensive assessment at PND35 reveals that maternal PCB exposure produces persistent, sex-specific alterations integrating across behavioral, microbial, and molecular domains. The emergence of female-specific social memory deficits contrasting with male behavioral resilience demonstrates that developmental vulnerability follows distinct temporal patterns between sexes.

6.3.1 Behavioral Specificity Indicates Targeted Neural Circuit Effects

The preservation of spatial working memory alongside disrupted social memory argues against generalized neurotoxicity. Spatial working memory, dependent primarily on hippocampal-prefrontal circuits, appears resistant to PCB exposure at these doses. Social memory, requiring integration across hippocampus, amygdala, and prefrontal cortex, shows selective vulnerability in females.

This specificity aligns with selective neurotoxicity concepts where environmental chemicals affect neural systems based on developmental timing, receptor expression, and metabolic capacity (Rice and Barone, 2000). The social memory deficits resemble those in ASD, where social cognition is impaired while other domains remain intact (Chevallier et al., 2012).

The non-monotonic dose response for female social memory deficits is characteristic of endocrine disruption. Low doses may act through nuclear receptor activation while higher doses trigger compensatory mechanisms or receptor desensitization (Vandenberg et al., 2012). This pattern has important implications for risk assessment, as linear extrapolation from high-dose studies would miss these low-dose effects.

6.3.2 Sex-Specific Vulnerability Windows Reflect Developmental Strategies

The reversal of vulnerability from PND7 (males affected) to PND35 (females affected) reveals fundamental differences in developmental trajectories that align with emerging concepts in developmental neurotoxicology (Makris et al., 2009; Hessel et al., 2018). This temporal shift in vulnerability cannot be explained by simple exposure differences, as both sexes received similar PCB doses through maternal milk based on our tissue concentration data (Li et al., 2024). Instead,

these patterns reflect sex-specific developmental programs and their differential sensitivity to disruption.

Males follow an "early crisis and adaptation" model that resembles the concept of hormesis in toxicology (Calabrese & Baldwin, 2003). The initial vulnerability at PND7, manifested as reduced USVs, triggers compensatory responses including upregulation of detoxification pathways (CYP enzymes), enhanced antioxidant defenses (Nrf2 targets), and metabolic reprogramming. By PND28, males have established extensive molecular networks with over 7,000 significant correlations between microbiome, metabolome, and transcriptome features. This high connectivity provides redundancy - when PCBs disrupt specific pathways, alternative routes can compensate (Kitano, 2004; Csete & Doyle, 2002). The concept of "adaptive robustness" suggests that early stress can enhance system resilience if compensatory mechanisms have time to mature (Pfennig et al., 2010).

Females demonstrate "delayed vulnerability" consistent with the "two-hit" hypothesis of neurodevelopmental disorders (Bale et al., 2010; Davis & Pfaff, 2014). The first hit - PCB exposure during development - creates latent vulnerabilities that remain masked during early life. The second hit - pubertal hormonal changes - unmasks these vulnerabilities leading to behavioral deficits. This pattern has been observed in other models where early life stress interacts with adolescent development to produce sex-specific outcomes (Walker et al., 2017; Holder & Blaustein, 2014).

The focused molecular correlations in females (< 3,000 significant correlations), while potentially efficient under normal conditions, provide less redundancy under challenge. This "precision versus resilience" trade-off has been described in network biology, where highly optimized systems sacrifice robustness for efficiency (Carlson & Doyle, 2002). The dominance of specific bacterial hubs in female networks (*CAG-485* with 218 connections) creates vulnerability to targeted disruption - if these key nodes are affected, the entire network can collapse (Albert et al., 2000).

6.3.3 Thyroid-Mediated Mechanisms Link Molecular Changes to Behavior

The correlation between female T3 suppression and social memory deficits at 1.0 mg/kg provides evidence for thyroid-mediated neurobehavioral effects. Thyroid hormones regulate

myelination, synaptogenesis, and neurotransmitter synthesis - even modest reductions during development produce lasting alterations (Bernal, 2007).

The mechanism differs from classical PCB thyroid effects. Reduced DIO1 expression in females at PND35, contrasting with upregulation at PND28, suggests exhausted compensation. Elevated T4 at affected doses indicates reduced peripheral conversion rather than decreased production underlies T3 deficits.

Sex-specific thyroid effects may involve hormone interactions. Estrogen regulates DIO1 and modulates thyroid receptors (Marassi et al., 2007). Disruption emergence at adolescence when estrogen increases suggests PCBs interfere with normal hormone crosstalk. The loss of normal female > male DIO1 expression baseline further supports disrupted sexual dimorphism in thyroid regulation.

6.3.4 Microbiome Stability Indicates Lasting Developmental Effects

Microbiome alteration persistence from PND28 through PND35 demonstrates lasting dysbiosis rather than transient perturbation. Stability despite dietary transitions and continued development indicates true ecosystem restructuring.

Functional implications extend beyond local gut effects. Corynebacterium species elevated in males produce amino acid metabolites influencing neurotransmitter synthesis. Female *Alistipes* alterations may affect bile acid metabolism and nuclear receptor signaling, potentially contributing to endocrine disruption. The different bacterial hubs between sexes suggest distinct microbiome-host communication patterns.

The striking differences in network architecture between male and female offspring provide a systems-level explanation for their divergent behavioral outcomes following developmental PCB exposure. Network topology analysis revealed that males developed a scale-free network architecture characterized by multiple redundant hubs and extensive cross-system connectivity, consistent with robust biological networks resistant to targeted disruption (Barabási & Oltvai, 2004; Kitano, 2004). The presence of mixed hub types - including bacterial species (*Acetatifactor muris*, 112 connections), metabolites (acetylcarnitine, 104 connections), and hepatic genes (Cyp2b10, 98 connections) - creates multiple fail-safe mechanisms whereby disruption of one hub can be compensated by alternative pathways. This redundancy is quantified by the

network's clustering coefficient (0.68) and average path length (2.3), indicating high local connectivity with efficient global communication (Albert et al., 2000). In contrast, females developed a hierarchical network dominated by super-hubs, particularly *CAG-485_sp003979075* with 218 connections representing 3.3% of total network edges. This architecture, while potentially more efficient under normal conditions (average path length 1.9), creates critical vulnerability. The betweenness centrality of female super-hubs (0.42 for top hub) exceeds that of male hubs (0.28 for top hub) by 50%, indicating that information flow depends more heavily on specific nodes. Network attack simulations demonstrate that random removal of 20% of nodes reduces network efficiency by only 15% in males but 42% in females, while targeted removal of the top 5 hubs causes 28% efficiency loss in males versus 67% in females. These architectural differences align with concepts from network medicine suggesting that disease states often result from disruption of network hubs rather than individual molecular defects (Barabási et al., 2011).

6.3.5 Integration Patterns Predict Functional Outcomes

The correlation analysis reveals why males achieve resilience while females show vulnerability. Male extensive integration (>7,000 correlations) creates system robustness - when PCBs disrupt specific pathways, alternatives compensate. Female focused correlations may be efficient normally but create vulnerability when key nodes are disrupted.

The dominance of bacterial hubs in females versus mixed hubs in males suggests different regulatory hierarchies. Female outcomes may depend more on microbiome composition, making them vulnerable to dysbiosis effects. The lack of molecular-behavior correlations in males indicates successful buffering, while tight coupling in females reveals limited compensation.

6.3.6 Implications for Environmental Health Assessment

These findings challenge current risk assessment paradigms. Non-monotonic dose responses for behavioral and molecular endpoints contradict linear dose-response assumptions underlying current regulations. Sex-specific vulnerabilities with temporally shifting patterns emphasize the need for both sexes at multiple timepoints in toxicological studies.

Integration across behavioral, microbiome, and molecular endpoints provides fuller understanding than single measures. Male molecular changes might seem successful adaptation if

examined alone, but female data reveals these doses produce deficits through different mechanisms. This system's perspective is essential for understanding environmental chemical effects.

Limitations? Anything to say about bioaccumulation of PCB in mouse bodies and how while no longer exposed they still have PCB in their adipose tissue or other fatty organs like brain? Related to this: no tissue PCB measurements to know where it bioaccumulated. No TSH measurements.

6.4 Conclusions

Maternal exposure to environmentally relevant PCB mixtures produces persistent, sex-specific effects manifesting as distinct behavioral and molecular phenotypes by early adolescence. Spatial working memory remains intact while social memory shows female-specific deficits at low and medium but not high doses, indicating targeted neural circuits with non-monotonic responses. Males achieve behavioral resilience through extensive molecular integration providing system redundancy, while females show delayed vulnerability with focused networks creating efficiency but reducing flexibility.

The molecular mechanisms involve differential thyroid regulation with female-specific T3 suppression correlating with behavioral deficits and sex-specific DIO1 expression patterns indicating exhausted female compensation but successful male adaptation. Persistent microbiome alterations affect functionally distinct species between sexes. Different correlation patterns - extensive male integration versus focused female networks - predict divergent outcomes.

These results reveal fundamentally different biological responses between sexes, not simply different effect magnitudes. Temporal vulnerability dynamics, molecular architectures, and behavioral outcomes all differ qualitatively. Understanding these sex-specific mechanisms is essential for predicting health outcomes and developing targeted interventions for populations exposed to persistent organic pollutants. The findings emphasize sex as a primary biological variable and the necessity of comprehensive multi-system approaches to capture the full spectrum of developmental toxicant effects.

Chapter 7: General Discussion and Conclusions

7.1 Summary of Major Findings

This dissertation investigated how maternal exposure to an environmentally relevant PCB mixture affects offspring development through disruption of the gut-liver-brain axis. The comprehensive assessment across multiple developmental timepoints and biological systems revealed sex-specific patterns of vulnerability that evolve dynamically from birth through adolescence. These findings provide new insights into the mechanisms by which developmental toxicant exposure produces lasting effects on behavior and physiology.

7.1.1 Key Discoveries by System

Behavior: Sex-Specific Social Memory Deficits

The behavioral assessments revealed a remarkable reversal of vulnerability between sexes across development. At PND7, males showed early communication deficits with reduced ultrasonic vocalizations, while females appeared unaffected. However, by PND35, this pattern completely reversed - males demonstrated full behavioral resilience with intact spatial and social memory, while females developed significant social memory deficits at low and medium PCB doses. The non-monotonic dose response in females, with recovery at the highest dose, exemplifies the complex nature of endocrine disruption. Importantly, the preservation of spatial working memory in both sexes indicates that PCB effects target specific neural circuits rather than causing generalized cognitive impairment.

Microbiome: Distinct Adaptation Strategies

The gut microbiome responses differed fundamentally between sexes in both scope and specificity. Males showed broader taxonomic disruption affecting 9 species across diverse phyla at PND28, with changes persisting through PND35. The consistent elevation of *Corynebacterium* species in males may contribute to altered amino acid metabolism and neurotransmitter synthesis. Females demonstrated more focused alterations, with 7 species primarily from gram-positive lineages showing changes. The non-monotonic response of *Alistipes* species in females paralleled their behavioral deficits, suggesting potential mechanistic links. The stability of these microbiome

alterations from weaning through adolescence indicates lasting ecosystem restructuring rather than transient perturbation.

Intestinal Metabolomics: Regional and Sex-Specific Signatures

Metabolomic profiling revealed distinct metabolic strategies between sexes. Females showed early and sustained disruption of neurotransmitter pathways, with 4-imidazoleacetic acid and DOPA alterations correlating with behavioral outcomes. Males exhibited predominant nucleotide metabolism disruption, particularly at high doses, with dramatic increases in guanosine and inosine suggesting activation of purine salvage pathways. The pathway-level analysis demonstrated that females experienced earlier effects on methylation and neurotransmitter metabolism, while males showed delayed but more extensive nucleotide alterations. These metabolic signatures provide biochemical evidence for the different adaptive strategies employed by each sex.

Liver: Divergent Transcriptional Programs

Hepatic transcriptional responses revealed fundamentally different priorities between sexes. Males mounted robust xenobiotic metabolism responses, with coordinated upregulation of phase I and II detoxification enzymes creating a comprehensive metabolic defense system. This response included CYP2B and CYP3A family members, consistent with CAR and PXR activation. Females showed initial immune activation at PND28, characterized by interferon responses and bacterial defense pathways, which evolved to hormone and vitamin metabolism alterations by PND35. The shift from immune to metabolic responses in females suggests progression from acute defense to long-term adaptation.

Thyroid: Opposite Sex Responses

The thyroid axis showed striking sex differences in both hormone levels and regulatory enzyme expression. Males at PND28 exhibited elevated T3 with suppressed T4, accompanied by dose-dependent increases in hepatic DIO1 expression. By PND35, males maintained stable thyroid status despite continued molecular alterations. Females showed the opposite pattern - maintained thyroid homeostasis at PND28 despite non-monotonic DIO1 changes, followed by T3 suppression at PND35 specifically at the dose causing behavioral deficits. The temporal dynamics of DIO1

expression, with initial compensation followed by dysregulation, illustrate the exhaustion of adaptive mechanisms over development.

There should be a paragraph discussing results by PCB concentration: most effects were at very high concentrations that are not environmentally relevant. This should be discussed.

7.1.2 Novel Contributions

Sex-Specific Network Architecture Discovery

The identification of fundamentally different molecular network architectures between sexes provides a mechanistic explanation for their divergent outcomes. Males developed dense, highly interconnected networks with balanced distribution across system pairs, creating redundancy that enables compensation when individual pathways are disrupted. Females showed more focused networks with specific bacterial species serving as dominant hubs, creating efficiency under normal conditions but vulnerability when key nodes are affected. This architectural difference - redundancy versus precision - predicts functional resilience versus vulnerability.

Multi-Omics Developmental Timeline

The longitudinal design capturing multiple developmental stages revealed that vulnerability windows shift dynamically between sexes. The progression from male vulnerability at PND7 to female vulnerability at PND35 demonstrates that developmental toxicant effects cannot be understood from single timepoint assessments. The stability of molecular changes from PND28 to PND35, despite evolving behavioral phenotypes (though different tests at each timepoint prevent direct longitudinal comparison), indicates that early molecular alterations establish trajectories that manifest differently as development proceeds. An important consideration is that most statistically significant effects occurred at the 6.0 mg/kg/day dose, which exceeds environmentally relevant human exposures by approximately 10-fold. However, the molecular changes observed at lower doses (0.1-1.0 mg/kg/day) may represent early adverse outcome pathway events that, while not producing overt behavioral changes in controlled laboratory conditions, could increase vulnerability to additional stressors in real-world settings.

Non-Monotonic Dose-Response Patterns

The consistent observation of non-monotonic dose responses across multiple endpoints challenges traditional toxicological paradigms. Female social memory deficits at low and medium but not high doses, the inverted U-shaped DIO1 response in females, and the threshold effects for male vocalizations all deviate from linear dose-response assumptions. These patterns have critical implications for risk assessment, as they indicate that low doses relevant to human exposure may produce effects distinct from those predicted by high-dose studies.

7.2 Limitations and Considerations

Several limitations must be acknowledged when interpreting these findings. The descriptive nature of the correlation analyses identifies associations but cannot establish causation. While we observe extensive correlations between molecular features and behavioral outcomes, experimental manipulation would be required to prove causal relationships. The substantial individual variation observed, particularly in thyroid hormone responses and behavioral metrics, suggests that genetic background or early life experiences may modify susceptibility to PCB effects.

Species differences in xenobiotic metabolism must be considered when extrapolating to humans. Mice metabolize PCBs more rapidly than humans, potentially underestimating chronic exposure effects. The specific congener profile of the Fox River Mixture, while environmentally relevant to Great Lakes populations, may not represent global PCB exposure patterns. Additionally, the dietary exposure route, while avoiding stress associated with gavage, may not fully replicate the complex exposure scenarios in human populations consuming contaminated fish.

Technical limitations of the omics approach also warrant consideration. The 16S rRNA sequencing provided genus and species-level resolution but not strain-level discrimination or functional capacity. The metabolomics captured major pathways but may have missed low abundance signaling molecules. The RNA sequencing reflected steady-state transcript levels but not post-transcriptional regulation or protein activity. Integration of these datasets, while revealing, represents a snapshot rather than dynamic processes.

7.3 Future Directions

Future investigations should establish causal relationships between the observed associations. Fecal microbiota transplantation (FMT) experiments could determine whether the

sex-specific microbiome alterations directly contribute to behavioral outcomes. Transplanting microbiota from PCB-exposed dams into germ-free recipients would test whether microbiome changes alone can recapitulate the behavioral phenotypes. Gnotobiotic models colonized with defined bacterial consortia could identify specific species responsible for behavioral effects.

Targeted metabolite supplementation studies could validate the functional importance of identified pathways. Administration of DOPA or thyroid hormone to PCB-exposed females might rescue social memory deficits. Conversely, blocking purine salvage pathways in males could test whether nucleotide metabolism contributes to their resilience. Cell-specific knockout models targeting hepatic DIO1 or intestinal barrier proteins would clarify tissue-specific contributions to the integrated phenotype.

Longitudinal imaging and physiological monitoring could capture dynamic processes missed by endpoint analyses. Repeated sampling of the same animals for metabolomics and hormone measurements would reveal individual trajectories rather than population averages. Advanced imaging techniques could visualize gut barrier function, hepatic metabolism, and neural activity in real-time during development. Immunohistochemical validation of key findings, including tight junction proteins, microglial activation markers, and thyroid hormone receptors, would strengthen molecular observations.

7.4 Public Health Implications

These findings have significant implications for environmental health policy and risk assessment. The sex-specific vulnerabilities identified indicate that current regulatory frameworks based primarily on male animal studies may inadequately protect female populations. The non-monotonic dose responses observed for multiple endpoints suggest that linear extrapolation from high-dose studies, the current regulatory standard, may miss or mischaracterize low-dose effects relevant to environmental exposures.

Environmental justice considerations arise from the continued exposure of vulnerable populations to PCBs through subsistence fishing and residence near contaminated sites. Indigenous communities and low-income populations depending on locally caught fish for nutrition face disproportionate exposure risks. The developmental effects observed here, occurring

at doses approaching human exposure levels, underscore the need for continued remediation efforts and fish consumption advisories.

The identification of early biomarkers, including microbiome signatures and metabolite profiles, could enable screening of at-risk populations before behavioral deficits manifest. The correlation between molecular alterations at PND28 and behavioral outcomes at PND35 suggests that early intervention might prevent or mitigate later effects. Development of sex-specific intervention strategies, potentially including probiotic supplementation or thyroid support, could benefit exposed populations.

7.5 Conclusions

This dissertation demonstrates that maternal exposure to environmentally relevant PCB mixtures causes complex, multi-system alterations in offspring development that differ fundamentally between males and females. The work reveals that environmental toxicants disrupt not just individual organs but integrated physiological networks, with effects cascading through the gut-liver-brain axis to influence behavior. The sex-specific patterns observed - from opposite thyroid responses to divergent network architectures - indicate that males and females employ different biological strategies to cope with developmental challenges.

The temporal dynamics uncovered here, with vulnerability windows shifting between sexes across development, emphasize that developmental toxicology must consider the entire developmental trajectory rather than isolated timepoints. The non-monotonic dose responses observed across multiple systems highlight the inadequacy of linear dose-response models for endocrine-disrupting chemicals. These patterns suggest that low-dose exposures relevant to human populations may produce unique effects not predicted by traditional toxicological approaches.

The biology systems employed here, integrating behavior, microbiome, metabolome, and transcriptome data, provides a more complete understanding of toxicant effects than any single measure alone. The extensive correlations identified between molecular features and behavioral outcomes suggest that early molecular signatures might predict later functional consequences. This predictive potential could enable early identification and intervention for at-risk populations.

Most importantly, this work establishes that sex must be considered as a primary biological variable in environmental health research. The fundamental differences observed between males

and females - not merely in magnitude but in responses - indicate that single-sex studies provide an incomplete and potentially misleading picture of environmental health risks. Understanding these sex-specific mechanisms is essential for developing targeted interventions and protective policies.

The persistent nature of the molecular alterations observed, maintaining from weaning through adolescence, suggests that early life PCB exposure creates lasting biological changes. Whether these alterations persist into adulthood and influence disease susceptibility remains an important question for future investigation. The public health significance of these findings extends beyond PCBs to other persistent organic pollutants and endocrine-disrupting chemicals that may act through similar mechanisms.

In conclusion, this dissertation advances our understanding of how developmental exposure to environmental contaminants affects the complex interplay between gut microbiota, hepatic metabolism, the thyroid, and neurobehavioral outcomes. The findings support a paradigm shift in environmental health assessment from single-organ toxicology to integrated systems biology, from single-sex studies to sex-specific investigations, and from linear dose-response models to recognition of non-monotonic effects. As we face continued challenges from legacy contaminants and emerging chemicals, this systems-level, sex-aware approach will be essential for protecting human health across the lifespan.

References

Bal-Price, A., Crofton, K. M., Sachana, M., Shafer, T. J., Behl, M., Forsby, A., et al. (2015). Putative adverse outcome pathways relevant to neurotoxicity. *Critical Reviews in Toxicology*, *45*(1), 83-91. https://doi.org/10.3109/10408444.2014.981331

Benjamini, Y., & Hochberg, Y. (1995). Controlling the false discovery rate: A practical and powerful approach to multiple testing. *Journal of the Royal Statistical Society: Series B*, *57*(1), 289-300.

Bernal, J. (2007). Thyroid hormone receptors in brain development and function. *Nature Clinical Practice Endocrinology & Metabolism*, *3*(3), 249-259.

Bianco, A. C., Salvatore, D., Gereben, B., Berry, M. J., & Larsen, P. R. (2002). Biochemistry, cellular and molecular biology, and physiological roles of the iodothyronine selenodeiodinases. *Endocrine Reviews*, *23*(1), 38-89.

Boelen, A., Kwakkel, J., & Fliers, E. (2011). Beyond low plasma T3: Local thyroid hormone metabolism during inflammation and infection. *Endocrine Reviews*, *32*(5), 670-693.

Bokulich, N. A., Chung, J., Battaglia, T., et al. (2013). Antibiotics, birth mode, and diet shape microbiome maturation during early life. *Science Translational Medicine*, *5*(193), 193ra91.

Branchi, I., Santucci, D., & Alleva, E. (2001). Ultrasonic vocalisation emitted by infant rodents: A tool for assessment of neurobehavioural development. *Behavioural Brain Research*, *125*(1-2), 49-56.

Brielmaier, J., Matteson, P. G., Silverman, J. L., et al. (2012). Autism-relevant social abnormalities and cognitive deficits in engrailed-2 knockout mice. *PLoS One*, *7*(7), e40914.

Centers for Disease Control and Prevention (CDC). (2023). *Fourth national report on human exposure to environmental chemicals, updated tables*. U.S. Department of Health and Human Services.

Cheng, S. L., Li, X., Lehmler, H. J., Phillips, B., Shen, D., & Cui, J. Y. (2018). Gut microbiota modulates interactions between polychlorinated biphenyls and bile acid homeostasis. *Toxicological Sciences*, *166*(2), 269-287.

Chevallier, C., Kohls, G., Troiani, V., Brodkin, E. S., & Schultz, R. T. (2012). The social motivation theory of autism. *Trends in Cognitive Sciences*, *16*(4), 231-239.

Choi, Y. J., Seelbach, M. J., Pu, H., et al. (2010). Polychlorinated biphenyls disrupt intestinal integrity via NADPH oxidase-induced alterations of tight junction protein expression. *Environmental Health Perspectives*, *118*(7), 976-981.

Christensen, K. Y., Thompson, B. A., Werner, M., et al. (2016). Levels of persistent contaminants in relation to fish consumption among older male anglers in Wisconsin. *International Journal of Hygiene and Environmental Health*, *219*(2), 184-194.

Clayton, J. A., & Collins, F. S. (2014). Policy: NIH to balance sex in cell and animal studies. *Nature*, *509*(7500), 282-283.

Cohen, J. (1988). *Statistical power analysis for the behavioral sciences* (2nd ed.). Lawrence Erlbaum Associates.

Crofton, K. M., Craft, E. S., Hedge, J. M., et al. (2000). Thyroid-hormone-disrupting chemicals: Evidence for dose-dependent additivity or synergism. *Environmental Health Perspectives*, *113*(11), 1549-1554.

Cryan, J. F., O'Riordan, K. J., Cowan, C. S. M., et al. (2019). The microbiota-gut-brain axis. *Physiological Reviews*, *99*(4), 1877-2013.

Curran, C. P., Vorhees, C. V., Williams, M. T., et al. (2011). In utero and lactational exposure to a complex mixture of polychlorinated biphenyls: Toxicity in pups dependent on the Cyp1a2 and Ahr genotypes. *Toxicological Sciences*, *119*(1), 189-208.

Environmental Protection Agency (EPA). (2023). *Fox River cleanup progress report*. U.S. Environmental Protection Agency Region 5.

Grandjean, P., & Landrigan, P. J. (2014). Neurobehavioural effects of developmental toxicity. *Lancet Neurology*, *13*(3), 330-338.

Hart, S. N., Cui, Y., Klaassen, C. D., & Zhong, X. B. (2009). Three patterns of cytochrome P450 gene expression during liver maturation in mice. *Drug Metabolism and Disposition*, *37*(1), 116-121.

Hazenberg, M. P., de Herder, W. W., & Visser, T. J. (1988). Hydrolysis of iodothyronine conjugates by intestinal bacteria. *FEMS Microbiology Reviews*, *4*(1), 9-16.

Imamoglu, I., & Christensen, E. R. (2002). PCB sources, transformations, and contributions in recent Fox River, Wisconsin sediments determined from receptor modeling. *Water Research*, *36*(14), 3449-3462.

Jacobson, J. L., & Jacobson, S. W. (1996). Intellectual impairment in children exposed to polychlorinated biphenyls in utero. *New England Journal of Medicine*, *335*(11), 783-789.

Kaya, D., Imamoglu, I., Sanin, F. D., & Sowers, K. R. (2018). A comparative evaluation of anaerobic dechlorination of PCB-118 and Aroclor 1254 in sediment microcosms from three PCB-impacted environments. *Journal of Hazardous Materials*, *341*, 328-335.

Keil, K. P., Sethi, S., & Lein, P. J. (2019). Sex-dependent effects of 2,2′,3,5′,6-pentachlorobiphenyl on dendritic arborization of primary mouse neurons. *Toxicological Sciences*, *168*(1), 95-109.

Klocke, C., & Lein, P. J. (2020). Evidence implicating non-dioxin-like congeners as the key mediators of polychlorinated biphenyl (PCB) developmental neurotoxicity. *International Journal of Molecular Sciences*, *21*(3), 1013.

Klocke, C., Sethi, S., & Lein, P. J. (2020). The developmental neurotoxicity of legacy vs. contemporary polychlorinated biphenyls (PCBs): Similarities and differences. *Environmental Science and Pollution Research International*, *27*(9), 8885-8896.

Knezevic, J., Starchl, C., Tmava Berisha, A., & Amrein, K. (2020). Thyroid-gut-axis: How does the microbiota influence thyroid function? *Nutrients*, *12*(6), 1769.

Koh, W. X., Hornbuckle, K. C., Marek, R. F., Wang, K., & Thorne, P. S. (2016). Hydroxylated polychlorinated biphenyls in human sera from adolescents and their mothers living in two U.S. Midwestern communities. *Chemosphere*, *147*, 389-395.

Kostyniak, P. J., Hansen, L. G., Widholm, J. J., et al. (2005). Formulation and characterization of an experimental PCB mixture designed to mimic human exposure from contaminated fish. *Toxicological Sciences*, *88*(2), 400-411.

Kraeuter, A. K., Guest, P. C., & Sarnyai, Z. (2019). The Y-maze for assessment of spatial working and reference memory in mice. *Methods in Molecular Biology*, *1916*, 105-111.

Krishnan, D., Cromwell, H. C., & Meserve, L. (2014). Effects of polychlorinated biphenyl (PCB) exposure on response perseveration and ultrasonic vocalization emission in rat during development. *Endocrine Disruptors*, *2*(1), e969608.

Li, X., Wang, K., Suh, Y. J., Lehmler, H. J., & Cui, J. Y. (2024). Significant metabolic alterations in mouse dams exposed to an environmental mixture of polychlorinated biphenyls (PCBs) during gestation and lactation: Insights into PCB and metabolite profiles. *Environmental Toxicology and Pharmacology*, *111*, 104567.

Li, X., Lim, J. J., Wang, K., et al. (2022). The disposition of polychlorinated biphenyls (PCBs) differs between germ-free and conventional mice. *Environmental Toxicology and Pharmacology*, *92*, 103854.

Lim, J. J., Li, X., Lehmler, H. J., Wang, D., Gu, H., & Cui, J. Y. (2020). Gut microbiome critically impacts PCB-induced changes in metabolic fingerprints and the hepatic transcriptome in mice. *Toxicological Sciences*, *177*(1), 168-187.

Lord, C., Cook, E. H., Leventhal, B. L., & Amaral, D. G. (2000). Autism spectrum disorders. *Neuron*, *28*(2), 355-363.

Love, M. I., Huber, W., & Anders, S. (2014). Moderated estimation of fold change and dispersion for RNA-seq data with DESeq2. *Genome Biology*, *15*(12), 550.

Lyall, K., Croen, L. A., Sjödin, A., et al. (2017). Polychlorinated biphenyl and organochlorine pesticide concentrations in maternal mid-pregnancy serum samples: Association with autism spectrum disorder and intellectual disability. *Environmental Health Perspectives*, *125*(3), 474-480.

Marassi, M. P., Fortunato, R. S., da Silva, A. C., et al. (2007). Sexual dimorphism in thyroid function and type 1 iodothyronine deiodinase activity in pre-pubertal and adult rats. *Journal of Endocrinology*, *192*(1), 121-130.

Marek, R. F., Thorne, P. S., DeWall, J., & Hornbuckle, K. C. (2014). Variability in PCB and OH-PCB serum levels in children and their mothers in urban and rural U.S. communities. *Environmental Science & Technology*, *48*(22), 13459-13467.

Martin, L., & Klaassen, C. D. (2010). Differential effects of polychlorinated biphenyl congeners on serum thyroid hormone levels in rats. *Toxicological Sciences*, *117*(1), 36-44.

Mayer, E. A., Nance, K., & Chen, S. (2022). The gut-brain axis. *Annual Review of Medicine*, *73*, 439-453.

McCarthy, M. M., Nugent, B. M., & Lenz, K. M. (2018). Neuroimmunology and neuroepigenetics in the establishment of sex differences in the brain. *Nature Reviews Neuroscience*, *19*(9), 521-534.

Mehri, F., Bashirian, S., Khazaei, S., & Jenabi, E. (2021). Association between pesticide and polychlorinated biphenyl exposure during pregnancy and autism spectrum disorder among children: A meta-analysis. *Clinical and Experimental Pediatrics*, *64*(6), 286-292.

Morse, D. C., Wehler, E. K., Wesseling, W., Koeman, J. H., & Brouwer, A. (1996). Alterations in rat brain thyroid hormone status following pre- and postnatal exposure to polychlorinated biphenyls (Aroclor 1254). *Toxicology and Applied Pharmacology*, *136*(2), 269-279.

Org, E., Mehrabian, M., Parks, B. W., et al. (2016). Sex differences and hormonal effects on gut microbiota composition in mice. *Gut Microbes*, *7*(4), 313-322.

Patandin, S., Lanting, C. I., Mulder, P. G., et al. (1999). Effects of environmental exposure to polychlorinated biphenyls and dioxins on cognitive abilities in Dutch children at 42 months of age. *Journal of Pediatrics*, *134*(1), 33-41.

Pessah, I. N., Cherednichenko, G., & Lein, P. J. (2010). Minding the calcium store: Ryanodine receptor activation as a convergent mechanism of PCB toxicity. *Pharmacology & Therapeutics*, *125*(2), 260-285.

Qatanani, M., Zhang, J., & Moore, D. D. (2005). Role of the constitutive androstane receptor in xenobiotic-induced thyroid hormone metabolism. *Endocrinology*, *146*(3), 995-1002.

Rice, D., & Barone, S., Jr. (2000). Critical periods of vulnerability for the developing nervous system: Evidence from humans and animal models. *Environmental Health Perspectives*, *108*(Suppl 3), 511-533.

Ridlon, J. M., Kang, D. J., Hylemon, P. B., & Bajaj, J. S. (2014). Bile acids and the gut microbiome. *Current Opinion in Gastroenterology*, *30*(3), 332-338.

Rieger, M. A., & Dougherty, J. D. (2016). Analysis of within subjects variability in mouse ultrasonic vocalization: Pups exhibit inconsistent, state-like patterns of call production. *Frontiers in Behavioral Neuroscience*, *10*, 182.

Scattoni, M. L., Crawley, J., & Ricceri, L. (2009). Ultrasonic vocalizations: A tool for behavioural phenotyping of mouse models of neurodevelopmental disorders. *Neuroscience & Biobehavioral Reviews*, *33*(4), 508-515.

Schantz, S. L., Gardiner, J. C., Aguiar, A., et al. (2010). Contaminant profiles in Southeast Asian immigrants consuming fish from polluted waters in northeastern Wisconsin. *Environmental Research*, *110*(1), 33-39.

Schantz, S. L., Widholm, J. J., & Rice, D. C. (2003). Effects of PCB exposure on neuropsychological function in children. *Environmental Health Perspectives*, *111*(3), 357-576.

Sethi, S., Keil Stietz, K. P., Valenzuela, A. E., et al. (2021). Developmental exposure to a human-relevant polychlorinated biphenyl mixture causes behavioral phenotypes that vary by sex and genotype in juvenile mice expressing human mutations that modulate neuronal calcium. *Frontiers in Neuroscience*, *15*, 766826.

Sethi, S., Morgan, R. K., Feng, W., et al. (2019). Comparative analyses of the 12 most abundant PCB congeners detected in human maternal serum for activity at the thyroid hormone receptor and ryanodine receptor. *Environmental Science & Technology*, *53*(7), 3948-3958.

Sharon, G., Sampson, T. R., Geschwind, D. H., & Mazmanian, S. K. (2016). The central nervous system and the gut microbiome. *Cell*, *167*(4), 915-932.

Shin, N. R., Whon, T. W., & Bae, J. W. (2015). Proteobacteria: Microbial signature of dysbiosis in gut microbiota. *Trends in Biotechnology*, *33*(9), 496-503.

Silverman, J. L., Yang, M., Lord, C., & Crawley, J. N. (2010). Behavioural phenotyping assays for mouse models of autism. *Nature Reviews Neuroscience*, *11*(7), 490-502.

Sinha, R. A., Singh, B. K., & Yen, P. M. (2019). Thyroid hormone regulation of hepatic lipid and carbohydrate metabolism. *Trends in Endocrinology & Metabolism*, *25*(10), 538-545.

Spear, L. P. (2000). The adolescent brain and age-related behavioral manifestations. *Neuroscience & Biobehavioral Reviews*, *24*(4), 417-463.

Sprowles, J. L. N., Monaikul, S., Aguiar, A., et al. (2022). Associations of concurrent PCB and PBDE serum concentrations with executive functioning in adolescents. *Neurotoxicology and Teratology*, *92*, 107092.

Steenport, D. M., Anderson, H. A., Hanrahan, L. P., et al. (2000). Fish consumption habits and advisory awareness among Fox River anglers. *Wisconsin Medical Journal*, *99*(8), 43-46.

Tripathi, A., Debelius, J., Brenner, D. A., et al. (2018). The gut-liver axis and the intersection with the microbiome. *Nature Reviews Gastroenterology & Hepatology*, *15*(7), 397-411.

Vandenberg, L. N., Colborn, T., Hayes, T. B., et al. (2012). Hormones and endocrine-disrupting chemicals: Low-dose effects and nonmonotonic dose responses. *Endocrine Reviews*, *33*(3), 378-455.

Virili, C., Antonelli, A., Santaguida, M. G., Benvenga, S., & Centanni, M. (2018). Gastrointestinal malabsorption of thyroxine. *Endocrine Reviews*, *40*(1), 118-136.

Wahlang, B., Falkner, K. C., Gregory, B., et al. (2014). Human receptor activation by aroclor 1260, a polychlorinated biphenyl mixture. *Toxicological Sciences*, *140*(2), 283-297.

Wahlang, B., Jin, J., Beier, J. I., et al. (2019). Identifying sex differences arising from polychlorinated biphenyl exposures in toxicant-associated liver disease. *Food and Chemical Toxicology*, *129*, 64-76.

Watanabe, M., Houten, S. M., Mataki, C., et al. (2006). Bile acids induce energy expenditure by promoting intracellular thyroid hormone activation. *Nature*, *439*(7075), 484-489.

Willems, A. (2014). The family Comamonadaceae. In E. Rosenberg et al. (Eds.), *The prokaryotes* (pp. 777-851). Springer.

Wilson, R. J., Li, X., Chen, S., Lehmler, H. J., & Cui, J. Y. (2024). Developmental exposure to the Fox River PCB mixture modulates behavior in juvenile mice. *Neurotoxicology*, *103*, 146-161.

Wisconsin Department of Natural Resources (DNR). (2024). *Fox River PCB cleanup: 2024 progress report*. Wisconsin DNR.